INTEGRATION OF ACTUATORS AND SENSORS

INTO COMPOSITE STRUCTURES

by

Jonathan David Ehresman

A thesis submitted in partial fulfillment
of the requirements for the degree

of

Master of Science

in

Mechanical Engineering

MONTANA STATE UNIVERSITY
Bozeman, Montana

August 2009

©COPYRIGHT

by

Jonathan David Ehresman

2009

All Rights Reserved

APPROVAL

of a thesis submitted by

Jonathan David Ehresman

This thesis has been read by each member of the thesis committee and has been found to be satisfactory regarding content, English usage, format, citation, bibliographic style, and consistency, and is ready for submission to the Division of Graduate Education.

Dr. Doug Cairns

Approved for the Department Mechanical and Industrial Engineering

Dr. Chris Jenkins

Approved for the Division of Graduate Education

Dr. Carl A. Fox

STATEMENT OF PERMISSION TO USE

In presenting this thesis in partial fulfillment of the requirements for a master's degree at Montana State University, I agree that the Library shall make it available to borrowers under rules of the Library.

If I have indicated my intention to copyright this thesis by including a copyright notice page, copying is allowable only for scholarly purposes, consistent with "fair use" as prescribed in the U.S. Copyright Law. Requests for permission for extended quotation from or reproduction of this thesis in whole or in parts may be granted only by the copyright holder.

Jonathan David Ehresman

August 2009

ACKNOWLEDGMENTS

I would like to first thank my family for all of their years of support in my pursuit of higher education. Their understanding of what I was trying to accomplish and their backing of me in all things big and small allowed me to reach the place I am at right now in my life. The Bozeman Cutthroat rugby club for giving me a confidence I could not have achieved through any other means. The Sensi's at Ash's Okinawan Karate for their expert instruction on Isshinryu Karate. Karate has combined mental and physical discipline together like nothing I have ever experienced before. The crew at S.S.E.L. for letting me work on their satellite. J.C. Blockey for all of his work in getting the prototype blade to be functional. Tiok Agastra for his help in showing Nate and I how to properly make flat plates of coupon samples for our research, and for his help in any fiberglass questions we had. Nate Palmer for his tireless work ethic and drive to make the research as accurate and usable as possible. Dr. Cairns for guiding our research and driving the publishing of papers in AIAA journals, Sandia National Laboratory reports, and all the help he gave me in my pursuit of a Masters Degree. Dr. Mckittrick for reviewing my thesis and serving on my committee. Dr. Mandel for his help with my thesis committee and reviewing my thesis.

TABLE OF CONTENTS

TABLE OF CONTENTS-CONTINUED

TABLE OF CONTENTS-CONTINUED

LIST OF TABLES

Table Page

LIST OF FIGURES

Figure Page

LIST OF FIGURES-CONTINUED

Figure Page

LIST OF FIGURES-CONTINUED

Figure Page

LIST OF EQUATIONS

Equation Page

GLOSSARY

MFSG- Metal Foil Strain Gage

PVDF- Polyvinylidene Fluoride

FO- Fiber Optic

LVDT- Linear Variable Differential Transformer

LP- Linear Potentiometer

DAQ- Data Acquisition Unit

VS-VP- Variable Speed Variable Pitch

TCFD- Transitional Computational Fluid Dynamics

FBG- Fiber Bragg Gratings

FFP-Fiber Fabry-Perot

TDM- Time Division Multiplexing

WDM- Wave Division Multiplexing

RHS- Relative Humidity Sensor

TIG- Tungsten Inert Gas

VDC- Voltage Direct Current

AE- Acoustic Emission

NDT- Non-Destructive Testing

NDE- Non-Destructive Examination

ID- Inside Diameter

OD- Outside Diameter

PVC- Poly Vinyl Chloride

LIDAR- Light Detecting and Ranging

VARTM- Vacuum Assisted Resin Transfer Molding

ABSTRACT

The need for more efficient wind turbine blades is growing in our society. One step in accomplishing this task would be to make wind turbines blades into smart structures. A smart structure is one that incorporates sensors, complete control systems, and active control devices, in order to shed, or redistribute the load placed on the structure. For wind turbine blades this means changing the shape of the blade profile as it encounters different wind conditions. In order to have active control surfaces functioning on wind turbine blades, the existing blades would have to be retrofitted, and the new blades being manufactured would have to be redesigned. There are different control surfaces to consider: gurney flaps and false wall flaps are two that can perturb the boundary layer across the low pressure side of the wing. A flat plate and blade section test bed will be manufactured in order to gather empirical data from wind tunnel testing. For actuation of the control surface there are many choices: electrical, hydraulic, pneumatic, and electro-hydrostatic. These actuator types will be investigated under a set of criterion to determine the best one for turbine blade application. Sensors will be investigated with respect to their use in sensing strain, temperature, acceleration, humidity, and delamination. Sensors are also used for health monitoring. This helps engineers design under a damage tolerant philosophy as opposed to a safe life structure philosophy. These sensors will be placed into laminates and different surface treatments will be reviewed to find the best configuration for each sensor. The sensor will be cleaned with isopropyl alcohol, dipped in a 20% by mass solution of nitric acid, and submerged in a 20% by mass solution of nitric acid for 10 seconds. Detailed surface images will be taken of sensors with different surface treatments in order to better understand the bonding between the sensor and laminate. These images indicate that submerging the sensors into 20% by mass solution of nitric acid is the best surface treatment.

INTRODUCTION

The need for more efficient wind turbines is growing in our society. As increases in power output of wind turbines requires longer blades, the need for a blade level smart structure increases. A smart structure is one that incorporates sensors, complete control systems, and active control devices, in order to shed, or redistribute the loads placed on the structure. In order to make a wind turbine blade a smart structure, it is necessary to understand the blade's role in creating power. There are many factors which determine the power output of a wind turbine: air density, machine efficiencies, length of the blades, and wind velocities. Air density is related to temperature and atmospheric pressure. Machine efficiencies are a function of all the bearings, gear meshing, electrical systems, and movable parts in the turbine. The blade length is increasing as a result of higher power output needed from the turbines. And, the wind velocity needs to be from a constant direction in order to make the three blade rotor turbine work at its most efficient. Power output of a wind turbine has many contributing factors. The equation for power which can be drawn from moving fluid is given in equation 1.

$$P = \frac{1}{2} * \rho * C_{\mathrm{p}} * N * \pi * R^2 * V^3 \quad 1)$$

Equation 1. Power Output of Wind Turbine

Where P is wind turbines capacity, ρ is the air density, Cp is the coefficient of performance, N is the machines efficiency, R is the blade length, and V is the velocity of the wind. For the most part, everything on the right hand side of the equation can be controlled. Due to the value of wind velocity being cubed it is the largest contributing factor for power generation. Because of this fact, placement of the tower is extremely

important; especially when there are multiple wind turbines in one farm [1]. N is the mechanical and electrical efficiency, which is being constantly improved upon by ongoing research. The C_p is the Betz Limit of 0.59 [2]. Due to the amount of sensors in the gear box, bearings, and other parts of the nacelle, the blade of a wind turbine would benefit from additional health monitoring by sensors [3].

Active control surfaces are needed to change the shape of the blade as it rotates through the air. Their movement is the output of a smart structure. Gurney flaps and false wall flaps will be investigated with respect to retrofitting of current blades and manufacturing changes needed for new blade design. Many different actuators will be reviewed; cables, hydraulics, electric, pneumatic, and electro-hydrostatic actuators will be studied along with the complete system needed to support the actuator within a blade.

The complete systems, which are necessary to activate the active control surfaces, will be investigated. The control system, necessary sensors for the actuators, retrofitting of current blades, manufacturing of new blades, and blade maintenance will be investigated in order to find a viable solution to each of those issues.

Empirical testing is necessary for validation of transitional computational fluid dynamics. This requires a test bed that will work in a wind tunnel. The first test bed will be a flat plate design for validation of simpler calculations. The second test bed will be a section of blade with multiple rear flap mounting points in order to have a larger envelope of testing parameters.

Health monitoring in the case of wind turbine blades requires a variety of sensors, i.e. sensors for acquisition of strain, strain fields, gust loading, impending gust loading, temperature, humidity, acceleration, and delamination. These aspects of health

monitoring for a smart structure will be investigated in this paper. Sensing strain inside of fiberglass composites will be accomplished by imbedding some sensors into, and affixing some sensors onto fiberglass layups. The sensors that are being imbedded and investigated are Metal Foil Strain Gages (MFSG), Polyvinylidene Fluoride (PVDF), and Fiber Optics (FO). For gust loading, a pressure transducer will be investigated. For impending gust loading, a laser sensing RADAR system will be reviewed. Temperature will be sensed by a thermocouple, and FO. Humidity will be sensed by a relative humidity sensor. Acceleration will be sensed by a 3 axis accelerometer. Delamination of the composite layup will be monitored by an ultrasonic transducer. These health monitoring devices will be tested for their effectiveness. Specific attention will be paid to the MFSG and PVDF for their effectiveness in sensing strain. The FO will be extensively tested for their ability to allow signal ingress and egress from the laminate. A review will be presented of FO as a strain sensor and its capabilities as a medium for sensing temperature. The dependability, reliability, and accuracy of these sensors are paramount to the success of a smart structure.

The need for a coherent manufacturing process is paramount to success in the cases of wind turbine blades. Different manufacturing ideas will be investigated in order to find proper embedding techniques for each of the sensors involved.

The sensors will be investigated with different surface treatments; cleaning with isopropyl alcohol, dipping into 20% by mass solution of nitric acid, and submerging in a 20% solution of nitric acid for ten seconds. Detailed surface images will be taken of sensors with different surface treatments in order to better understand the bonding between the sensor and laminate.

Turning Wind Turbine Blades into Smart Structures

Smart structures are complex. In the case of wind turbine blades there is a need for sensors, a control system, actuators, and active control surfaces. Placing control surfaces into wind turbine blades is not a trivial task. Heavy modification of presently deployed blades will be needed. For new blades, complete redesign would be needed in order to make the active control surfaces and complete support systems necessary.

Active Control Surfaces

Due to the large variations in wind speed, wind profiles, needs of the rotors, and gearboxes, it is not possible to achieve a satisfactory operating performance covering all possible operating conditions with a single style of blade [2]. Large surface areas are exposed. The increased force increases the weight. Active control surfaces perturb the airflow around a given airfoil; generally they change the angle of attack for the wing or blade causing lift in a desired direction. Active control surfaces have been around as long as humans have tried to gain lift from the wind, and they are prevalent in harvesting power from the wind. In order to best understand the control surfaces that could be used in wind turbine blades, it is necessary to review the history and types of control surfaces in powered flight. In the first manned powered flight the Wright Flyer 1 had lateral control which was achieved by warping the entire wing [4]. Active control surfaces have been on nearly every manned flying machine since the dawn of the airborne age. Even before heavier-than-air flight was achieved, a means of control was necessary. Alberto Santos-Dumont designed, built, and flew the first practical dirigible balloons [5]. He achieved this control by affixing a lightweight motor/propeller combination and rudder

system to his dirigibles. In this endeavor Santos-Dumont was able to loft around Paris to any destination, this required a great deal of control on the part of the dirigible and also a ladder. In his heavier-than-air aircraft Santos-Dumont was the first to employ active control surfaces, which were the precursor to ailerons. Numerous control schemes have been tried over the years, with varying results. The successful schemes have culminated into a series of control surfaces that can typically be found on modern airplanes. Flaps fully deployed on a modern aircraft can be seen in Figure 1.

Figure 1. Flaps deployed on Commercial Aircraft [1]

The study of the control surfaces in aircraft will yield information necessary in the success of applying control surfaces to wind turbine blades. The control surfaces of modern aircraft can be put into two categories: passive and active. The winglets at the end of the blade are passive, in that they are stationary, and cannot be altered in flight. All the other flaps, slats, ailerons and spoilers are deployable and therefore active control surfaces. The nominal wing span of a Boeing 747-400 is 64.4 meters and with an interior

cabin width of 6.1 meters this means that an individual wings length is about 29 meters. A 747 can actually fit inside the area swept by the blades of a large turbine as can be seen in Figure 2.

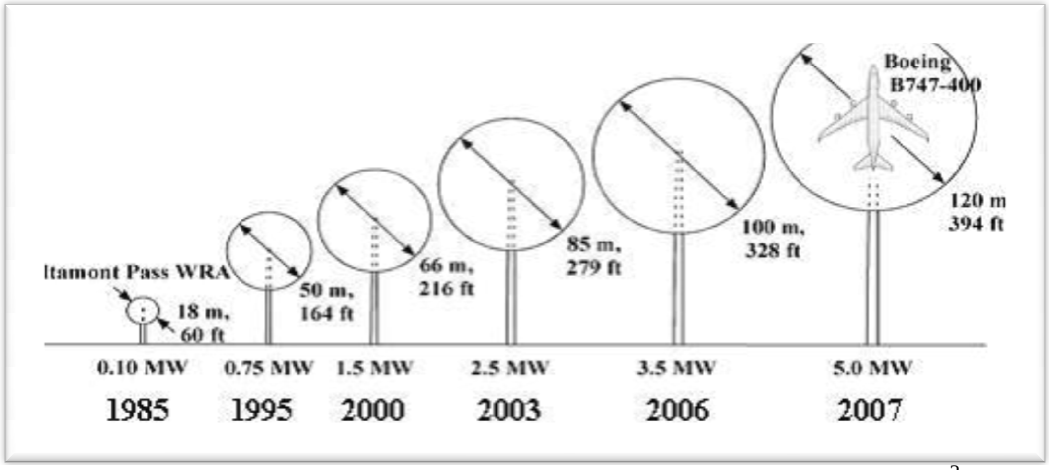

Figure 2. 747 Compared to a 5 MW Wind Turbine Cross Section [3][2]

Today's large wind turbine blades are longer than the wings of large commercial aircraft. The majority of actuators in today's commercial aircraft are hydraulically powered. Although some, like the Airbus A380's control surfaces, have electro-hydrostatic actuators as a backup to their primary hydraulic system [6]. The actuators and control surfaces in wind turbines will have to stand up to very high loads. The control needed on a commercial aircraft is one that is born of necessity. The plane has to lift off from the ground, fly smoothly, turn safely, and land in a reasonable fashion. A wind turbine blade has to fly through varying wind conditions, and travel through many millions of loading cycles between periods of maintenance. Active control surfaces and making the system a smart structure would increase the effectiveness of a wind turbine blade in varying wind conditions. A commercial aircraft has multiple control surfaces for the multiple conditions in which it must perform well. The maintenance periods for

aircraft are dictated by ground air ground cycles, and flight hours. The inspection and maintenance for a single turbine is done in some cases every 6 months [7]. With the increase in mechanical systems housed in the blades, the maintenance periods would have to be updated and increased in frequency.

Control Surfaces for Integration in Wind Turbine Blades

There are many different types of control surfaces that could be integrated into a wind turbine blade; ailerons, low speed flaps, slats, spoilers, and gurney flaps. Initially control surfaces of airplane wings were modeled after bird wings. Wilber Wright made detailed observations of a pigeon's wings in flight.

> "The thought came that possibly it had adjusted the tips of its wings about a lateral transverse axis so as to present one tip at a positive angle and the other at a negative angle, thus, for the moment, turn itself into an animated windmill. That when its body had revolved on a longitudinal axis as far as it wished, it reversed the process and started to turn the other way. Thus the balance was controlled by using dynamic reactions of the air instead of shifting weight [4]."

This flexing of a birds wing can be equated to the passive stall control on today's wind turbine blades. Bend-twist coupling gives the potential for a few percentages of energy yield improvement for constant-speed pitch control turbines and improves starting torque by 10% [8]. Passive stall control has been around for decades. The need for active control and fast acting control surfaces is paramount to success. Different kinds of control surfaces will be investigated including Gurney flaps, and false wall gurney flaps.

Gurney Flaps

The Gurney flap has been around for decades. The first patent on this device was obtained by Edward Zaparka in 1931 [9]. The simple flap that was mounted on a hinge

on the tail end of the airfoil had the ability to be deployed in order to increase the lift on the airfoil. A gurney flap can be seen in Figure 3

Figure 3. Gurney Flap Used on a 1971 Race Car[3]

The implementation of Gurney flaps is useful anywhere there needs to be an increase in lift associated with a reduction of drag. Dan Gurney first implemented the flap on an Indy race car driven by Bobby Unser and achieved the desirable results of more down force needed for the car [10]. The Gurney flap secret was shared with Robert Liebeck who worked for McDonnell Douglas Corp. His wind tunnel tests and numerical analysis showed that the flaps increased lift and decreased drag on the airfoil [11]. The results were presented at the AIAA 9th Fluid and Plasma Dynamics Conference in July 1976. Liebeck was not able to patent the Gurney flap due to an existing patent by Zaparka.

The Gurney flap has been proven to be very effective; the small flap can be located on the suction side of the wing in order to increase lift or on the pressure side in order to decrease lift on the airfoil. The flaps height, its distance from the end of the airfoil, and the flap mounting angle has a great deal of influence on the effectiveness of the flap.

Flap Configurations

The height of the flap is given as a percentage length of the cord of the airfoil. Liebeck predicted a flap height of 2% would work best, above that height a significant amount of drag would be introduced. Distance from the end of the airfoil and the angle that the flap is mounted to the blade can be tailored to the specific application [11]. More in depth information can be found in related publications [12].

False Wall Flap

The false wall flap is a method of boundary layer separation that can be easily achieved. The mechanical parts are simple; all that is needed is a pipe with a series of holes drilled along its length and a source of high pressured gas, and the necessary valves and hoses to transport the pressurized gas to the holes. Either a compressed air tank or the combustion of hydrogen gas can be used as a high pressure source. The same parameters of flap height distance from the end of the airfoil, and flap angle can be controlled through proper selection of hardware and manufacturing of the blade. The construction of this is simple in its design, and manufacturing is greatly simplified due to the small number of parts that would have to be deployed into the blade.

ACTUATOR INFORMATION

Actuator Types

Actuators are as varied as the wings and blades they are integrated into. They must be robust enough to withstand changes in forces during deployment, and while being deployed. Actuators in commercial airplane wings do not have to be very fast acting, on the order of tens of seconds. But in a wind turbine blade the actuators have to be extremely fast, on the order of half a second. This speed is needed to mitigate the forces from gust loading. Each of the main types when applied to wind turbines will be examined for its pros, cons, complexity, cost, force generated, speed, and weight. The information will be gathered in a table and analyzed. The majority of the prices that are quoted are from McMasterCarr and reflect 2009 prices [13].

Cables

The first actuators were wire cables pulled by the pilot and connected directly to the warping wings [4]. This cable control system is still used today in many light aircraft. Yaw control for many light aircraft is achieved through foot pedals that connect to steel cables that traverse the length of the plane and are connected to the tail rudder. This is also true for the ailerons and tail flaps on modern light aircraft including the Beach 99's and Beach 1900's. The warping of the wings under load can be done using the fiberglass itself with aero-elastic tailoring. This outcome is being accomplished by a change in the stacking sequence [8]. This results in a bend twist coupling of the structure.

Pros: Lightweight, inexpensive.

Cons: Not an actual actuator, just a method of force re-direction. The actuator that pulled on the cables would have to be mounted inside the wing.

Complexity: The complexity inherent in a cable system is due to the redirection of forces. First the cables need to be pulled by an actuator and then that force can be redirected through tension in the cables. For discrete control, there needs to be either two cables running to each attachment point, or a cable coupled with a spring. The system needs expert tuning to be set up correctly and constant maintenance in order to function properly.

Cost: This cost is an estimation of what it would take to outfit 3 blades with just the cables, cable ends, and pulleys. Stainless steel 1x19x1/4" wire rope costs $1.84 per foot, with an estimated 50 ft in each blade would add $276. Zinc plated pulleys that are 3" in diameter and made for ¼" rope cost $11.44 per pulley. It is estimated that there will be 4 needed per blade, resulting in a new added cost of $138. Cable ends in the form of eye fittings for ¼" cable are $26.29 at 4 per blade that makes for $316, summing to a total cost of $730.

Force: The 304 stainless steel cable has a breaking strength of 8,200 lbs, and that particular type of steel has a modulus of 28,600 ksi. If the force that is needed to be transferred through the cables is higher than the cables can comfortably hold, then redundant cables or larger cables are necessary.

Speed: Speed associated with cables is governed by the speed of the actuator to which the cables are attached.

Weight: The cables weigh very little 0.17 lbs/ft, with 150 ft of wire rope making for 25.5 lbs, a dozen pulleys and cable ends the whole cable linkage would weigh ~40 lbs.

Hydraulics

Hydraulic actuators have an extremely high power density. Power is needed in the form of electricity to spin a hydraulic pump, which turn moves hydraulic fluid through lines where that energy is translated into linear motion through a ram. That ram would be attached to a control surface that will act upon the air flowing on the outside of the blade. This infrastructure to deliver hydraulic power is very heavy due to its robust nature. In commercial aircraft hydraulics operate at very high pressures, 3000 psi in most cases and 5000 psi in the new Airbus A380. This high pressure saves weight while providing the necessary power to the control surfaces [6]. Great care must be given to the placement of the components of this type of system into rotor hub and wings in order to keep the rotor balanced.

Pros: high power density.

Cons: bulky, expensive.

Complexity: The complexity inherent in a hydraulic system like this one is associated with the pump, switching, and fluid reservoir housed in the center hub. The mounting of the hydraulic lines would have to account for the pitch control of the blades. Each blade would need a single actuator, a corresponding accumulator, a dedicated solenoid control valve, and the necessary hydraulic lines to function properly. The placement of the actuator will have to correspond with the necessary travel required. There would have to be just one pump and one reservoir tank for the entire system.

Cost: A 2” linear hydraulic actuator with 12” of travel will cost $341 each, making for a total of $1023. ½” hydraulic hoses cost $3.64 per foot and with 50 ft for each blade it comes to $546. The accumulators would have to be the diaphragm type which can be mounted in any orientation. The price for a 1 gallon capacity accumulator is $377 making a total price $1131. The reservoir and pump will need to be able to be mounted in any position due to the rotor hub constantly turning. An all-in-one hydraulic power unit with a 10 gallon capacity and 3 hp motor costs $2192. The solenoid control valves which need to be attached between the pump-accumulators and actuators run $167 each making for a total price of $501. This makes for an estimated total of $9269 for each 3 blade system.

Force: 1000 psi from the pump can be converted into 3,141 lbs of pushing force by the 2” diameter linear actuator. This force converts to 13972 Newtons. Applied in the proper location this is more than enough force to properly deploy and hold the control surface of the blade.

Speed: The speed inherent in a hydraulic system is dictated by the flow of the pump, in this case 2.7 gallons per minute at 1750 psi. This flow rate into a 2” diameter actuator would cause it to open fully in 3.62 seconds. A higher flow rate, smaller diameter actuator, or any number of things could make that number smaller. These systems are not known for being very fast acting.

Weight: The actuator weighs ~40 lbs for a total of 120 lbs. The lines weigh in at roughly1 lb/ft for a total of 150 lbs. hydraulic oil is 6.8 lbs/gallon making the total weight 68 lbs. The pump and reservoir tank weigh ~65 lbs, and the accumulators are 7 lbs each, making 21 lbs total. This makes for an estimated total of 424 lbs. or 193 kg.

Electric

Electric screw type actuators provide fast actuation, but require precise controls to achieve that actuation. A device that would be placed in a wind turbine blade would have to be very powerful in order to deploy the control surfaces reliably. The most reliable type of linear actuator for position repeatability is the ball screw linear actuator. That is why this type of linear actuator is used in Computer Numerically Controlled (CNC) machines [14].

Pros: No alternating from electricity to motion, very exact, lightweight.

Cons: Not very fast acting.

Complexity: The complexity inherent in a purely electrical system is present in the solid state relays needed for the system to be very fast acting. The control system will need to be center mounted in the hub and individual wires (two lines per actuator) will have to be run to each actuator. These lines will have to account for the pitch control of the blades.

Cost: There is a need for multiple solid state relays for each actuator, 4 per actuator should suffice. 12 relays that can handle 10 Amps cost $14.20 apiece, this makes for a total of $171. The lines to the actuators should be made of wire that can be flexed multiple times without damage. The wire should be 12 AWG and it costs $1.52 per foot for 150 ft make for $228. The ball screw actuators needed would be the same kind used in CNC systems. A ball screw jack and motor that can push with a force of 4000 lbs and travel 12” costs $815 for a total price of $2445.

Force: Force can be tailored for the specific application; electric linear actuators can range from 5 - 40,000 lbs. This broad range lends itself to optimization for the wind

energy industry. A ball screw type actuator can put out 4000 lbs of force which converts to 17793 Newtons. Generally the speed decreases as the force increases but this can be countermanded by the use of a more powerful and quicker turning motor.

Speed: The 4000 lbs of push from the ball screw actuator travels ¼" per revolution, and a gear ratio of 6:1, a motor spinning at 1750 rpm can propel a 12" ball screw to its full extension in 1.21 seconds. Faster results can be achieved using a faster motor, since this time far exceeds the 500 mS.

Weight: The actuators and motors weigh ~40 lbs each for a total of 120 lbs. The solid state relays and wire weigh a total of 4 lbs. making for a total of 124 lbs or 56.2 kg. This lightweight configuration is well suited for this application.

Pneumatic

Pneumatic actuators are both fast and powerful, although not very accurate when it comes to deployment. The infrastructure is very similar to that of hydraulics, although the power density is not as high. There is a need for a pump, control valves, and lines that go to each actuator. This system is lightweight when compared to a hydraulic system. The main reason for this is that the working fluid is air and not oil, the pressures are not as high, the reservoir tank will just hold pressurized air, and that air will be drawn from the atmosphere, and the lines do not need to handle the same amount of pressure that is present in a fluid based system.

Pros: Fast acting, Lighter weight

Cons: Not very powerful due to the relatively low pressures.

Complexity: Many of the same complexities that face the hydraulic system also face the pneumatic system. There is a need for a pump, reservoir tank, solenoid powered

valves, pressure lines out to the actuators, and the actuators themselves. The lines will have to account for the pitch control of the blades. The pump and reservoir tank can just be a simple air compressor with a tank; these can generally be mounted in any orientation. On these air compressors it is necessary to empty the system of water periodically, an autonomous relief valve will have to be set up to keep the system from building up to much condensation.

Cost: An 80 gallon reservoir tank attached to an electric motor that can output 17.2 cubic ft per minute will cost $2046. ½" hose that can hold up to 170 psi cost $46 per 50 ft for a total of $138. The solenoids for this are $60 for one actuator for a $180 total. The solenoids will have to control air pressure on both sides of the actuator ram for precise control. The actuators have a 3" bore and cost $160 apiece, totaling $480 for a set of three. The estimated total for the entire set is $2844.

Force: With a working pressure of 100 psi the 3" diameter actuator will output 662 lbs of force or 2944 newtons. With control on both the output and input side of the actuator rod, precision can be achieved.

Speed: With the pump having an output of 17.2 cfm, a 3" diameter rod could be deployed to 12 inches in 0.171 seconds

Weight: The actuators are aluminum cases with steel rods. They weigh approximately 8 lbs each for a 24 lb total. The hoses weigh a ¼ lb per foot making for a 37.5 lb total for 50 ft. The solenoids and valves are mostly aluminum and weigh 4 lbs each for a 12 lb total. The big ticket item is the compressor and tank, the 80 gallon compressor with pump weighs in at 185 lbs. The total weight would come to approximately 258.5 lbs. or 117 kg.

Electro-Hydrostatic

Electo-Hydrostatic actuators perhaps offer the best of both worlds when it comes to weight savings, reliability, and performance. This system has wires carrying electricity to actuators that have enclosed hydraulic systems internal to each actuator. So each actuator houses the pump, fluid, and ram of a hydraulic system but not the lines and reserve tank associated with a full blown hydraulic system. Since each actuator is fully enclosed the system can be very fast acting and very accurate [15].

Pros: Very powerful.

Cons: Expensive.

Complexity: The electro-hydrostatic system would have the benefits of the power of a hydraulic system without the added weight. The complexity would be the same as a purely electric system with a different actuator.

Cost: The same components would be used at the back end of the system. There is a need for multiple solid state relays for each actuator, 4 per actuator should suffice. 12 relays that can handle 10 Amps cost $14.20 apiece, this makes for a $171 total. The wire should be 12 AWG and it costs $1.52 per foot for 150 ft make for $228. The 4,200 lbf actuators are around $1600 apiece making for $4800 for a set of three. The total system cost with these estimations is $5,200.

Force: The Moog 52 HP dual tandem electro-hydrostatic actuator has a stall force of 42,000 lbf. Not all of this force will be needed, $1/10^{th}$ of this force will suffice, and 4200 lbf is equivalent to 18683 newtons. The placement of the actuator will have to be carefully determined due to the actuator having only a total throw of 7-8”.

Speed: The maximum no load rate of travel is 8.2 in/sec so the actuator can be deployed in .95 seconds. This time can be shortened by the use of less stoke from the actuator.

Weight: The electro-hydraulic actuators are heavy, with a weight of near 65 lbs each, they are the heaviest actuators of this study. The total estimated weight for the entire system is 200 lbs. or 90.7 kg.

Table 1. Quantitative Data for Actuators

Quantitative table				
	Hydraulics	Electric	Pneumatic	Electo-Hydrostatic
Pro's	High power density	No change in energy form, very exact, lightweight	Fast acting	Powerful
Con's	Bulky, expensive	not very fast	Not very powerful	Expensive
Cost (Total Dollars)	$9269	$2850	$2844	$5200
Authority (N)	13972	17793	2944	18683
Speed (seconds)	3.62	1.21	0.171	0.95
Weight (Total Kg)	193	56.2	117	90.7

Table 1 illustrates the sometimes dramatic differences between the different options for actuators. Each of these systems can be optimized for use in blades as they have been optimized for serving the machines and systems of which they are already a part of. The rankings for the table were easy to do in some categories, for price and weight everything for a whole system was just summed up. For force on the pneumatic piston the area of the rod was multiplied by the air pressure available. The calculation of the speed of the pneumatic piston can be seen in Equation 2.

$$\left(\frac{17.2ft^3}{min} * \frac{1min}{60\,sec} * \frac{1728\,in^3}{1ft^3} * \frac{1}{\pi * 1.5in^2} * \frac{1}{12in}\right)^{-1} = 0.171\,sec \qquad 2)$$

Equation 2. Speed of actuation for pneumatic cylinder

The information in Table 2 is the ranking of these actuators. The ranking is done from 1 to 4 with 1 being the best in that category.

Table 2. Ranking of Actuators

	Hydraulics	Electric	Pneumatic	Electo-Hydrostatic
Cost (Total Dollars)	4	2	1	3
Authority (Lbs)	3	2	4	1
Speed (seconds)	4	3	1	2
Weight (Total Lbs)	4	1	3	2
Total Score	15	8	9	8

As can be seen by this ranking of these systems the electric and electro-hydrostatic systems have scored the same. These systems will have to be studied more in-depth and optimized for each wind turbine blade application.

INTEGRATION OF ACTUATORS INTO WIND TURBINE BLADES

In any control system a feedback loop is necessary in order to achieve accurate deployment. This feedback loop would consist of a linear sensor, a linear potentiometer, or linear variable differential transformer (LVDT). This measurement device would have to be parallel to the actuator and attached in such a manner that accurate measurement of the deployed surface position. This sensor would feed into the control circuit. The system would take in signals from many sensors, run them through an algorithm, and then output a controlled response to the actuators. These actuators would be connected to control surfaces that would be deployed in wind turbine blades. Linear variable differential transformers; and linear potentiometer sensors will have to be investigated in order to find the best fit for the working environment inside of a wind turbine blade.

Linear Variable Differential Transformer

The LVDT is a method of tracking position in one dimension. The system runs off of AC power and is characterized by three coils set in the movable armature, which is wrapped around cylindrical ferromagnetic core. The center coil is the primary coil, and the two outer coils are the secondary coils. An alternating current is driven through the primary coil, causing a voltage to be induced in the each of the secondary coils proportional to its mutual inductance with the primary coil. As the core moves, these mutual inductances change, causing the voltage induced in the secondary's to change. The output voltage is the difference between these two secondary coils. When the core is displaced in one direction the voltage in one of the secondary coil increases as the other decreases, causing the output voltage to increase from zero to maximum. This voltage is

in phase with the input voltage. When the core moves in the other direction its phase is opposite of the primary coil. The magnitude of the output voltage is proportional to the distance moved by the core [16]. Some of the positive aspects of LVDT as pertains to wind turbine blade application is that it is solid and robust, and has high signal to noise ratio and low impedance. Some of its detractions are that a series of amplifiers and voltage meters are needed to process the input signal. This would increase the complexity and parts needed to make this sensor viable in any application. Also the LVDT sensor is more expensive and more sensitive to electrical noise than the linear potentiometer.

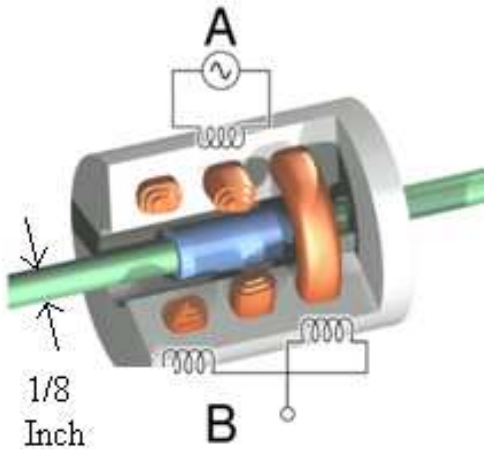

Figure 4. The Inside of a LVDT Sensor[4]

Linear Potentiometers

Linear potentiometers (LP) are very simple devices. They consist of a resistive material and generally 3 wires. Two wires are on either end of a resistor and the third wire is attached to the movable armature that slides along the resistive device. This device can be used as a voltage divider, or simply as a variable resistor. In both configurations, the armature's position directly relates to the resistive value between the appropriate wires. These potentiometers can be very accurate and robust in their design.

Although the nature of the armature sliding along the resistive material make for a device that has a finite working life, and provides for an ever present contact resistance between these two materials. Due to the low cost and resistance to interference from external electrical noise, the linear potentiometer is a better choice for a distance sensor in a wind turbine blade.

Complete System Requirements

The active control surface systems will be fairly extensive. Take the example of using electro-hydrostatic actuators and gurney flaps for a system. Electric power will be needed constantly to run this system. This power can be provided from the nacelle and travel along slip rings in the rotor hub to the interior of the hub and blades. This power will have to be regulated and distributed to the actuators and to the data acquisition (DAQ) software.

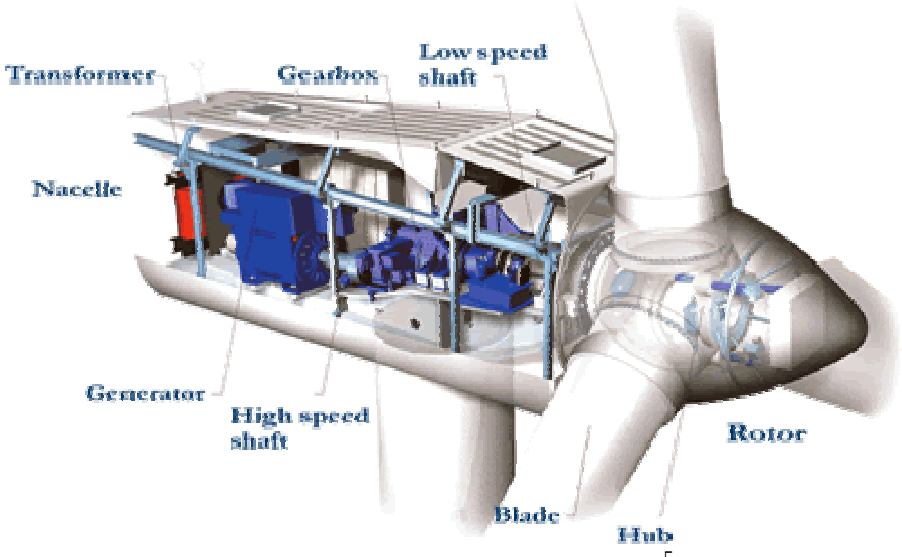

Figure 5. Parts of a Wind Turbine[5]

Control System

The control system for the electro-hydrostatic actuators would not consist of many parts. There would have to be an electronic control box which would house the high voltage input from the nacelle and the high voltage output to the actuators. This box would consist of relays, some normal, some solid state, in order to achieve the necessary control the design requires. The relays, DAQ control computer, and sensors, would run on low voltage power that is stepped down from the high voltage power provided by the nacelle. The sensors, as discussed earlier, would feed into the DAQ control computer and an active control loop would be in place to best change the shape of the wing in response to variable loading conditions.

The control system would be best housed in the rotor hub for multiple reasons. If there are asymmetric discrepancies in the layout of the control system with respect to the axis of rotation the effect will not be dramatic. This is due to the relatively small size of the control system in relation to the size of the rotating hub, and the small distance to the center of rotation. The blades on pitch controlled turbines rotates in relation to the rotor hub. This rotation is as high as 60° [17]. This is a design feature of the blades that the plumbing of lines to the necessary sensors and actuators will have to be built around.

For other systems such as electronic screw type actuators, hydraulic, and pneumatic systems the same sort of design requirements are in place. For the hydraulic actuation systems there is a need for some sort of reservoir tank. For the hydraulic and pneumatic systems an electric pump is needed to increase pressure for the system. These tanks and pumps would be mounted inside of the rotor hub. Process control often requires the simultaneous use of electronic and pneumatic instruments. For example, in many

cases it is advantageous to effect the measurement electronically but control it pneumatically [18].

Variable Speed Variable Pitch

With the addition of a deployable gurney flap to the blades of a wind turbine, the turbine will have a variable speed and variable pitch (VS-VP) rotor configuration. The variable pitch is obtained slowly by rotation of the blades at their base, and quickly by the gurney flaps being deployed within 500 milliseconds. With the aim of using simple controllers, the generator torque and pitch angle of VS-VP wind turbines are often controlled separately. In low wind speeds, wind turbines are operated at variable speed and fixed pitch in order to capture as much energy as possible. In high wind speeds the pitch angle is adjusted to limit the captured power at its rated value whereas the generator torque characteristic often remains unchanged [19].

Retrofitting of Present Wind Turbine Blades

There is a need for retrofitting of blades with active control surfaces which are presently deployed in the field. With tens of thousands of turbines currently in operation the benefit is substantial.

Figure 6. Wind Farm[6]

Turbine blades which are presently in service are very large, mostly static structures. LM Glasfiber is manufacturing a 61.5 meter blade for the 5 MW turbine prototypes near Brunsbüttel in North Germany. These blades weigh less than 18 tons, and are the largest blades currently being manufactured [20].

There are many steps that would have to be taken in order to outfit the majority of wind turbine blades with an active control system. First and foremost would have to be the choice of system to implement. The system would have to be effective, and require minor modifications to the blade. Minor modifications to the blades are necessary in order to maintain the current strength of the blades. The false wall system would fit very well into this category. A series of simple yet time consuming steps would have to take place in order for the retrofitting procedure to work and be safe.

Steps for Retrofitting Existing Blades

These procedures are centered on the retrofitting of a false wall system into an existing blade.

- Step one: Take the turbine out of commission and detach the rotor hub/blades from the tower and place it on the ground.
- Step Two: Unbolt the blades from the rotor hub and place them in a form onsite with the trailing edge pointed down.
- Step Three: Place in the pipe along the trailing edge. This step will have to be done very carefully due to the close quarters inside the blade. Tooling would have to be used to lay the pipe in the correct place and to epoxy the pipe into place. The pipe should have no holes drilled in it at this stage of the process due to the imperfect nature of this process.
- Step Four: Take an image with acoustic emission or x-ray of the trailing edge of the blade. This is to gather a specific location on the epoxied pipe. The pipe itself can be PVC or some other polymer, metal should be avoided due to corrosion and differing coefficients of thermal expansion. The amount of epoxy will have to be regulated as to not add to much weight to the blades, also the blades themselves will have to be rebalanced after this process.
- Step Five: Drill holes at appropriate locations through the blade, the epoxy that is holding the pipe in place, and the pipe itself. De-burring of the holes must be done on the inside and outside of these holes.

- Step Six: Install the compressor, reservoir tank, and control system into the rotor hub.
- Step Seven: Stab the blades back into the rotor hub and hook up the hoses in the blades to the control system in the rotor hub.
- Step Eight: Test the system whilst still on the ground and make sure its functioning properly.
- Step Nine: Fly the rotor hub/blades back into the air and onto the tower.
- Step Ten: Test the system while it is installed on the tower.

These are the steps for retrofitting an existing blade with Gurney flaps with electrical linear actuators. Due to the large amount of material to be removed and the significant amount of modification needed of the blade, retrofitting blades with gurney flaps is not recommended. Images of this process can be seen in Appendix A.

- Step One: Take the turbine out of commission and detach the rotor hub/blades from the tower and place it on the ground.
- Step Two: Unhook the blades from the rotor hub and place them in a form onsite with the low pressure side facing up.
- Step Three: Using a chalk line and pattern mark out on the blade surface the material to be removed.
- Step Four: With a worm drive skill saw and appropriate diamond coated cutting wheel remove the marked material. Be sure to use a mixture of lubricant such as water and a slow cutting speed like 10 in/min in order to keep the temperature of the blade to a reasonable level and not burn the material being cut. Thicker sections will have to be cut at a slower feed rate,

like 4 in/min for 2 inch thick sections. This cutting will have to be done to within an accuracy of 0.25 inch's

- Step Five: Once the material is removed a reinforcing shear web will have to be installed. This shear web will span from the top of the low pressure side to the inside of the high pressure side. This shear web will have to be epoxied into place.
- Step Six: The mounting points for the hardware will have to be installed. Using a predetermined pattern mark the locations of mounting points and drill through the material. A hole through the added shear web will have to be cut, this hole will have to line up with the rest of the mounting hardware to within $1/8^{th}$ of an inch.
- Step Seven: The mounting points will have to be countersunk and backfilled in order to maintain the blades profile. The mounting points should be fit tightly and multiple checks should be made to ensure proper alignment and square in relation to the other mounting points.
- Step Eight: When the mounting points are secure and the shear web is cured the hardware can be installed. If manufacturing up to this point has been done with sufficient quality the hardware instillation should be a smooth operation. The electronic linear actuators, flap, and electrical lines should fit relatively easily within the design of the retrofitted blade.
- Step Nine: Install the necessary relays and hardware into the rotor hub.
- Step Ten: Stab the blades back into the rotor hub and hook up the actuator's electrical lines in the blades to the control system in the rotor hub.

- Step Eleven: Test the system whilst still on the ground and make sure its functioning properly.
- Step Twelve: Fly the rotor hub/blades back into the air and onto the tower.
- Step Thirteen: Test the system while it is installed on the tower.

Design and Construction of New Turbine Blades

If gurney flaps are to be placed in new wind turbine blade construction, significant design changes need to be made to the blade. The tail end of the cord will have to be notched out and allowances made for the flap and actuator mounting points.

Figure 7. Gurney Flap Installed in Wing[7]

New molds will have to be made, but the manufacturing process will be the same as with current blades. Fittings and wear surfaces for the actuator, control surface, and electrical/pneumatic/hydraulic lines inside the blade will have to be taken into account. This will be in the form of holes in certain locations and possible heavy duty plastic or

metal fittings formed into the blades during construction. The implications of these control surfaces on the noise output of the turbines will have to be investigated. Furthermore, the hub, the rotor, and the tower may act as loud-speaker transmitting the machinery noise and radiating from it [21].

Steps for New Construction

The following are steps to implement control surfaces in new manufacturing of wind turbine blades. This Process will be centered on the use of electrical actuators.

- Step One: Layout all necessary ply's in their proper location in the newly designed molds.
- Step Two: Embed sensors in proper locations throughout the manufacturing process in the correct locations and correct orientations.
- Step Three: Embed mounting points for hardware and points for securing lines from the sensors and for the actuators on the inside of the blade. It is vital that all of these points be mounted in their proper locations within specified tolerances. Those tolerances should not exceed ± 0.125 inches.
- Step Four: Secure all material under a vacuum bag. Make sure the lead wires from the sensors are housed in a second vacuum bag.
- Step Five: Use vacuum assisted resin transfer molding to inject resin into the layup.
- Step Six: Remove vacuum bag after curing, be sure not to damage the lead wires on the sensors.

- Step Seven: Epoxy the two pieces of the wing together along with the shear web using the standard procedure currently in place.
- Step Eight: Using the mounting points and tie downs, install the actuators, active control surfaces, electrical lines for the actuator, and secure all the actuator lines and lead wires from the sensors.
- Step Nine: Hook up sensors to DAQ and actuator wires to a control system and check to see that everything is working properly.
- Step Ten: Secure the wires for transport.

The actual decision to implement active controls will be driven by economics. The present cost of one kilowatt/hour of electricity from Northwestern Energy is 5.5 cents [22]. This is the bottom line number that wind turbines will have to compete against. Expensive capital costs include the re-engineering of new blades, and the retooling of the blade manufacturer's plants. The radical redesign will have to go through the same rounds of testing that the current blades have to go through. This design is governed by IEC 1400-1 and 1400-2 which details safety philosophy, quality assurance, and engineering integrity [23]. The increase in operating cost will come in the form of more frequent in service inspections [24]. The individual cost of components as well as the expertise to install those components also needs to be considered. Power can be obtained from the slip rings that power the pitch control of the blades. The slip rings on a GE 1.5MW turbine can transfer 65 amps at 600 volts [25]. Once the blades are stabbed into the rotor all of the circuitry and components will have to be hooked up and tested before the hub/blade assembly is hoisted up to the tower. Testing will have to be accomplished by hooking the system to a standalone power source and computer system

in order to check the functionality of the DAQ and active control surface system. A system like this would be mounted on its own truck. The costs for these extra qualifications, engineering, equipment and maintenance will have to be balanced against the increased power output and longer blade life achieved by the use of active control systems.

Maintenance of Complete Blades

These blades will have more moving parts, which requires regular maintenance and inspection. The periods between maintenance can be elongated with selection of proper materials for the contact points. Polyurethane for all bushings, wear plates attached to the surface of the blade for those contact areas. The best thing for maintenance is an elegant design; something that has very few moving parts, and is built in a robust fashion. The gurney flap will have to be robust enough to handle the weather, i.e., snow, rain, and freezing rain [26].

There are many different aspects that need to be considered in placing active control surfaces into wind turbine blades. Size, location, activation, effectiveness, control systems, and the conditions it would operate in would all have to be considered in design. The use of active control surfaces on wind turbine blades needs to be investigated further. There is a need for Transient Computational Fluid Dynamics (TCFD) calculations for a flat plate Gurney flap, flap imbedded into a section of a blade, and each containing a false wall Gurney flap. Expertise in atmospheric fluid dynamics, aerodynamics, and structural dynamics is essential for understanding the behavior of the system under fluctuating conditions of the wind regime [27]. The mass of these control surfaces has so far been

assumed to be rigidly attached to the actuator. Although this is a valid assumption for the majority of industrial applications, there are some cases in which an allowance for the elasticity for either the mass itself or the member attaching it to the actuator has to be made. Aircraft powered flying control surfaces are a typically modeled as an elastic system [28]. For empirical data, a flat plate test bed and a blade section test bed need to be manufactured and tested in a wind tunnel. A quote about Wilber Wright “Still impatient, he then began work on a much larger model, one that could be flown as a kite. At this stage, he knew, all the theorizing in the world was not worth ten minutes of experiment. And he wanted to submit his idea to the natural selection of the wind” [4].

The retrofit, design and maintenance of blades with active control surfaces is an endeavor that needs to be investigated further. To this end a series of experiments needs to be conducted on the subject of active control surfaces on blades. The testing ladder starts at the coupon level, goes to the elemental stage, then to the sub-components, then the full scale components [29]. The experiments for the gurney flap can be on the order of the sub-components. This is due to their ability to change configurations through actuation. A flat plate test bed will be manufactured in order to test the transitional portion of a gurney flap under conditions that are easy to model. This flat plate will also house a false wall flap for study. A blade section test bed will be manufactured to study the transitional portion of a Gurney flap in a real word scenario.

TEST BEDS

The flat plate and blade section test beds will be made in accordance with the design considerations which are going to be applied to full scale blades. The purpose of these test beds are to validate Transitional Computational Fluid Dynamic (TCFD) computations by placing the test beds in a wind tunnel. The test beds will serve as valuable empirical data source components. There are two primary design considerations for these test beds. The first primary design consideration is that the flap be deployed in under 500 milliseconds. The second primary design consideration is that the test bed will have to be mounted securely within a 1 meter square wind tunnel. The wires to the Data Acquisition System (DAQ) will be held within one loom. More than one type of Gurney flap should be incorporated into the flat test bed for better use of allocated wind tunnel time.

Manufactured Flat Plate Test Bed

For validation of TCFD calculations, it is advisable to start with a simple model. A flat plate test bed was constructed for this purpose. The manufacturing and assembly steps are outlined below.

- Step One: The bottom piece of 0.5” thick Al was drilled with through holes and that became the base of the flat plate test bed. The holes are counter bored with a 0.5” End Mill to a depth of 0.5 inches. Everything will mount to this plate.
- Step Two: The upright for the back of the actuator was manufactured from a solid piece of 0.5” thick aluminum. Tapped holes fit over through holes in the base

plate and through holes were drilled to fit the hole pattern on the back of the actuator.

- Step Three: The uprights for the connecting rods were manufactured next. The bases of these uprights were two tapped holes that fit with through holes in the base plate. The top of the holders has a through hole to allow the connecting rods to slide through.
- Step Four: The base for the Gurney flap was manufactured and the bottom of it contained tapped holes that lined up with holes in the base plate. The top of the holder was tapped for bolts to attach to the flap.
- Step Five: The Gurney flap is a piano hinge design. It is made from two strips of metal glued to two and a half hinges. The back side of one hinge was bolted to the base; the two pieces are held together with a hinge, and the front of the flap was connected to the connecting rods with half of a hinge.
- Step Six: The flap is connected to four connecting rods which have holes drilled and tapped into the back end of them. The front end of them contains a small hole which connects to half of the hinge that is attached to the flap. These four connecting rods are .25 inch thick steel bars which are bent to align the flap with the actuator. A horizontal bar attaches the actuator to the four connecting rods. This piece has five through holes drilled into it: four for the connecting rods and the fifth to attach to the actuator itself. This assembly can be seen in Figure 8.

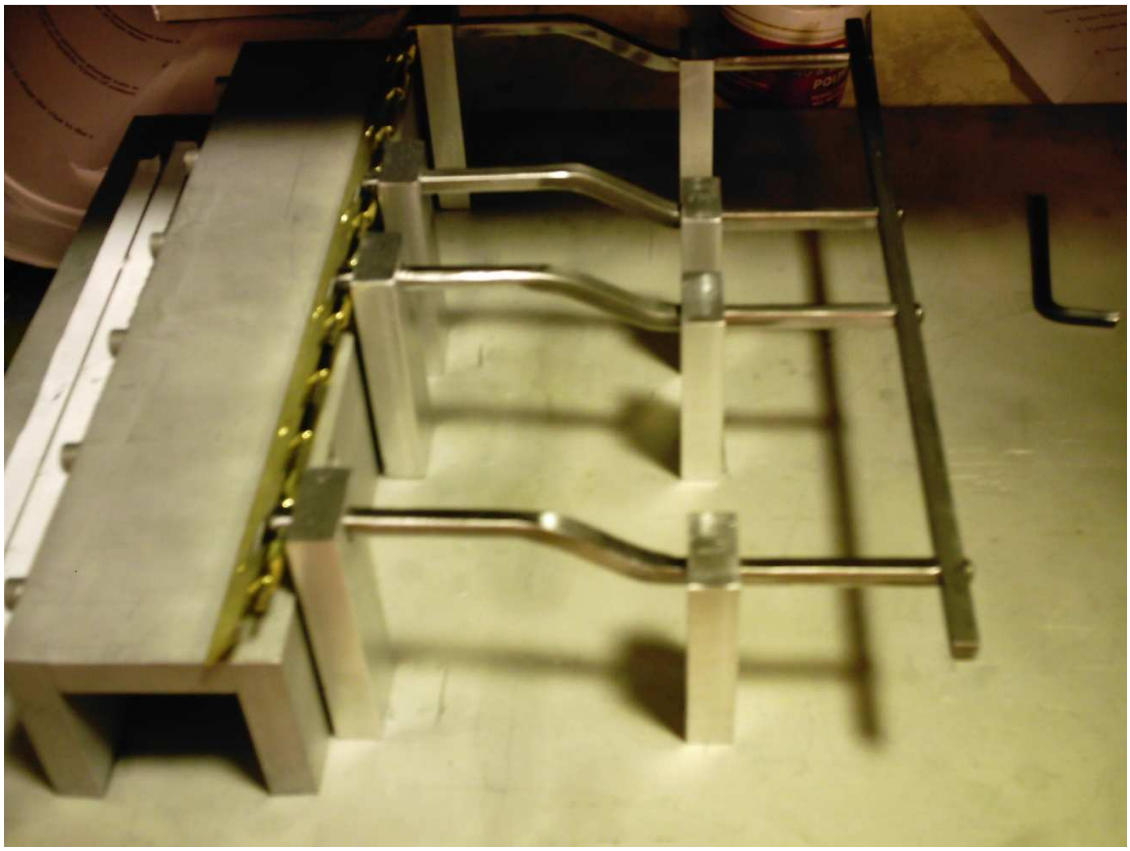

Figure 8. Gurney Flap Pushrod Assembly

- Step Seven: A small cylinder of aluminum was turned on the lathe to hold the linear potentiometer in place. The linear potentiometer was attached to two horizontal bars which were mounted to the base plate.
- Step Eight: The false wall flap manifold was manufactured. A 1” diameter steel pipe was drilled with 1/8” holes every 1” along its length. Two pieces of air hose was fit to the pipe and secured with hose clamps.
- Step Nine: The holders for the false wall pipe are manufactured and bolted to the base plate. They contain a hole that fits around the pipe, clamps it into place with two bolts, and is secured to the base plate.

- Step Ten: The stands for the top plate are manufactured by drilling and tapping holes in the bottoms of them for securing them to the base plate. Also holes are drilled and tapped on the top sides for securing the top plate down.
- Step Eleven: The top plate is a $1/8^{th}$ inch thick piece of aluminum, A slot is cut for the Gurney flap and air to be injected into the stream for the false wall flap.

The gurney flap was placed as close as possible to the flat upper surface of the test bed, without any protrusions into the flow along the top of the plate. The actuator is a fast acting screw type, which pushes with 70 lbs of force. Solid state relays were needed to meet the first primary design requirement of 500 mS actuation. The electronic actuator was the best choice for the test beds due to its fast acting design, repeatable, and reliable deployment, and simple control in the sense that all you need is electric power to activate. A fast acting fuse was also necessary due to the nature of trouble shooting the system, if any large current got past the initial automotive fuse the solid state relays would blow before the automotive fuse had a chance to react. A measurement of actual deployment length of the actuator was necessary inside of the test bed, so a linear potentiometer was installed parallel to the actuator for the most accurate results. This flat plate test bed is made from aluminum, steel and plastic, it measures 24.375x15.25x4 inches, and this is to meet the second primary design consideration of fitting into a wind tunnel. Also contained in the flat plate test bed is the false wall flap. This false wall flap consisted of a pressurized air tank and a fast acting valve that released the air into the false wall pipe. This is for better use of the wind tunnel as a TCFD validation tool. This setup can be seen in Figure 9. Drawings of the individual parts can be seen in Appendix B.

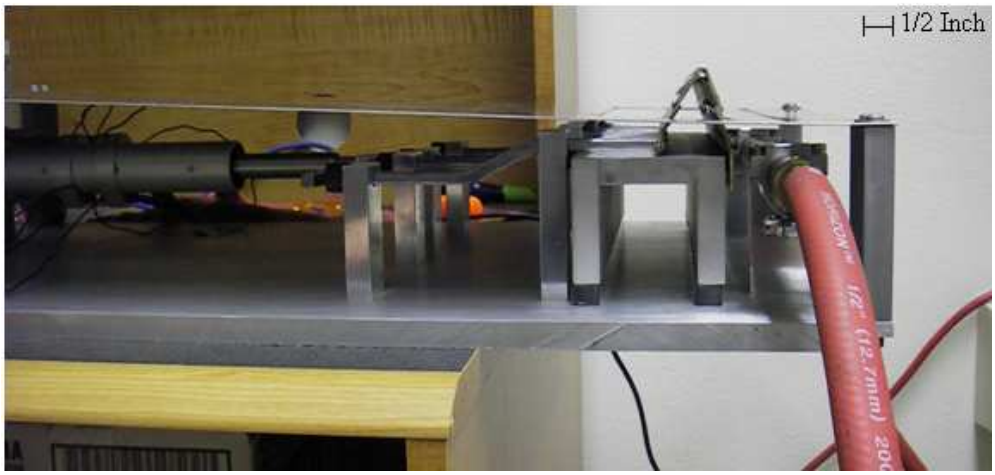

Figure 9. Flat Plate Test Bed[8]

Manufactured Blade Test Bed

The second test bed was a Gurney flap embedded into a section of wind turbine blade. The flap was installed on the low pressure side of the blade with a height equal to 10% of the cord length of the blade section as can be seen in Figure 12. This actuator is an Ultra Motion, 24 VDC, 'bug' series actuator. It was chosen for its high velocity capabilities while under load.

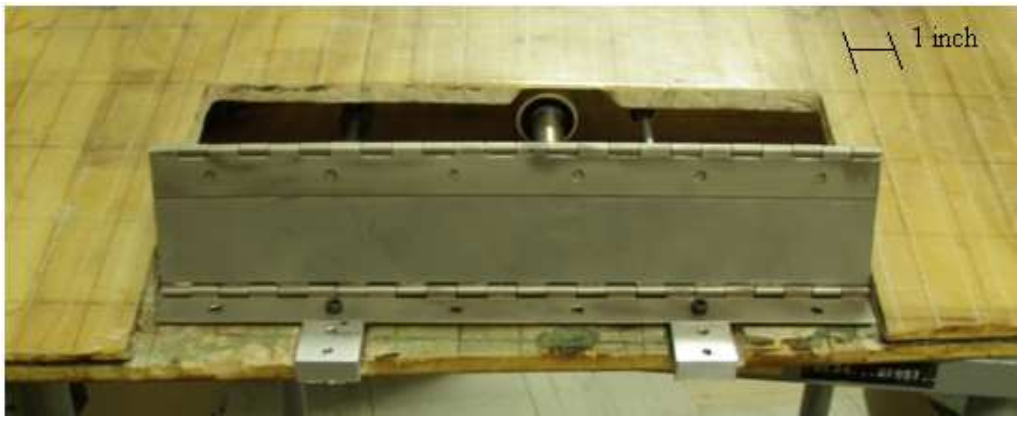

Figure 10. Gurney Flap installed in a Blade Section[9]

The steps to manufacture the blade test bed can be seen below.

- Step One: Take a 65 KW 9 meter blade and cut out a section that has a near 1:1 aspect ratio. This section is 24x26 inches. This is to address the second primary design consideration by being able to fit in a wind tunnel. Cutting the blade is accomplished by use of a circular saw. Proper personal protective equipment must be worn when cutting fiberglass; this equipment consist of dust masks, safety glasses, gloves, long pants, long sleeve shirts, and closed toed shoes. Smooth the edges of the fiberglass blade section with sandpaper.
- Step Two: Sketch out and remove all material on the suction side of the blade where the Gurney flap will reside. This is accomplished by the use of a Dremel tool.
- Step Three: Remove the material for the rear mounting points of the Gurney Flap. A flat head screwdriver is best for removing an exact amount of balsa wood from the inside of the blade. Drill the two holes through which the pieces of aluminum will be attached and sit flush with the inside of the blade.
- Step Four: The Gurney flap is made from strips of $1/16^{th}$ inch steel glued to two and a half hinges. The Gurney flap will have a height of roughly 10% of the cord length, making it 2.4~2.5 inches tall.
- Step Five: The backing plate for the actuator has through holes to mount to the actuator and holes on the sides of it for mounting to the aluminum suspender pieces that attach to the Aluminum webbing.
- Step Six: Aluminum suspending pieces are manufactured by drilling a series of through holes and tapped holes to mount the actuator to the webbing.

- Step Seven: A CLP-100 linear potentiometer (LP) from Celesco was mounted parallel to the actuator, along with a fluid filled dampener. These devices are held into place with aluminum pieces turned down on a lathe and held in place by bolts secured to the suspending pieces.
- Step Eight: The aluminum webbing that spans the height of the blade is made from 1/8th inch flat bars that are bent to conform to the inside of the blade. The pieces are lined up and then a total of eight holes are drilled through the blade and the webbing in order to hold it into place.
- Step Nine: 1/8th inch holes are drill on the suction side and the pressure side of the blade in order to mount the solid state H bridge relays to full fill the first primary goal of 500 ms actuation.

This test bed was also developed in order to gather empirical data for confirmation of TCFD analysis. Drawings for the machined parts can be seen in appendix C. This blade test bed is equipped to be placed in a mounting fixture inside of a wind tunnel due to the area inside the blade that is near the edges and without equipment as seen in Figure 11.

Figure 11. Area for Mounting into a Wind Tunnel[10]

The amount of material that would need to be removed to outfit the blades with the present configuration of gurney flaps is prohibitive. Far too much of the blade has to be removed in order to accommodate the Gurney flap as can be seen in Figure 12.

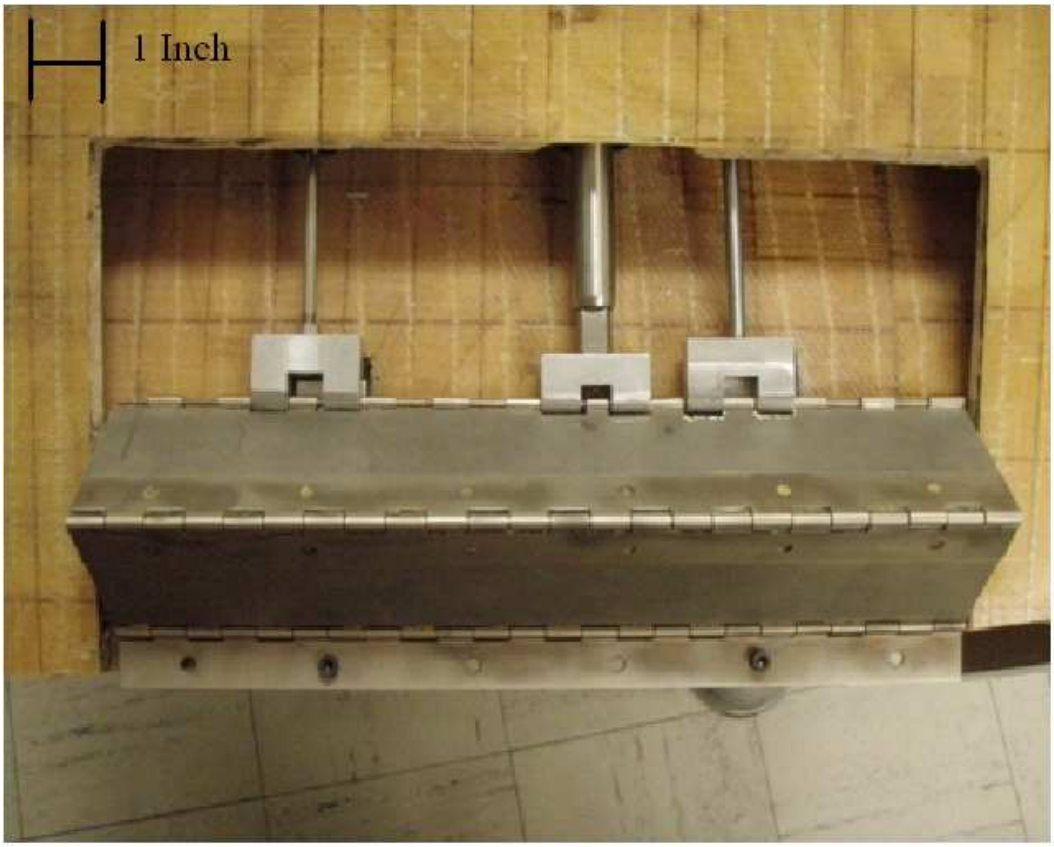

Figure 12. Large Amount of Material Removed for Gurney Flap[11]

The manufacturing of these components were all done with a Bridgeport mill and lathe. The individual components were kept very simple, rectangles with holes drilled and tapped in them. The simple individual components made for easy manufacturing and assembly, and were part of a simple overall design. The brackets that the rear of the Gurney flap is mounted too can be seen in Figure 13.

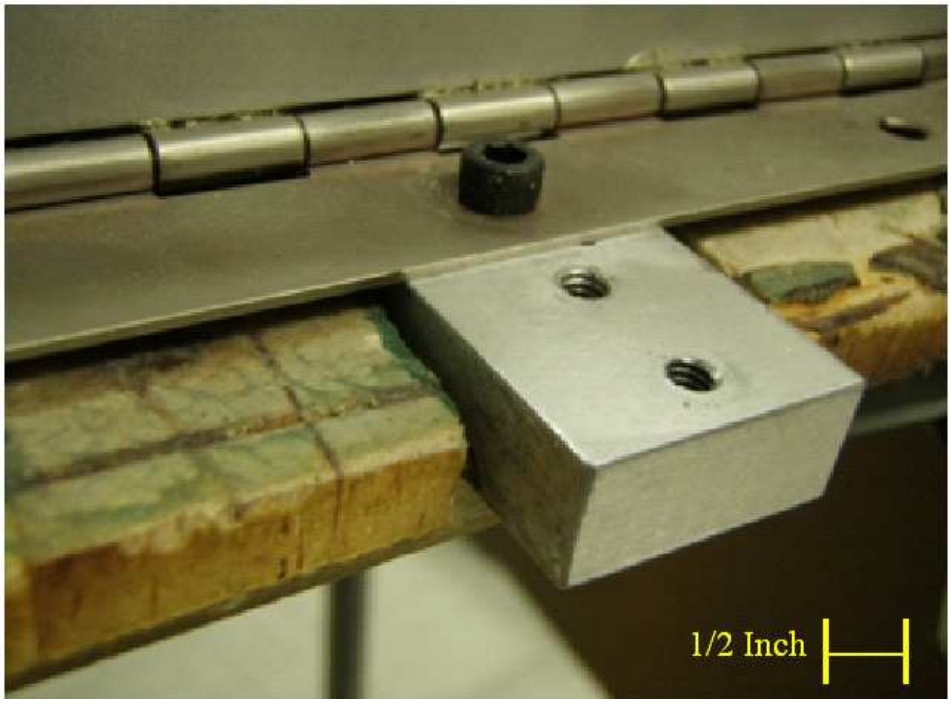

Figure 13. Rear Mounting Point for Flap[12]

The holes that secure the webbing into place were drilled while the piece was in place, through the fiberglass and the aluminum. The holes were counter sunk and once the screws and nuts were in place, the holes were filled in with epoxy and smoothed over to create a smooth outside surface for the blade, as can be seen in Figure 14.

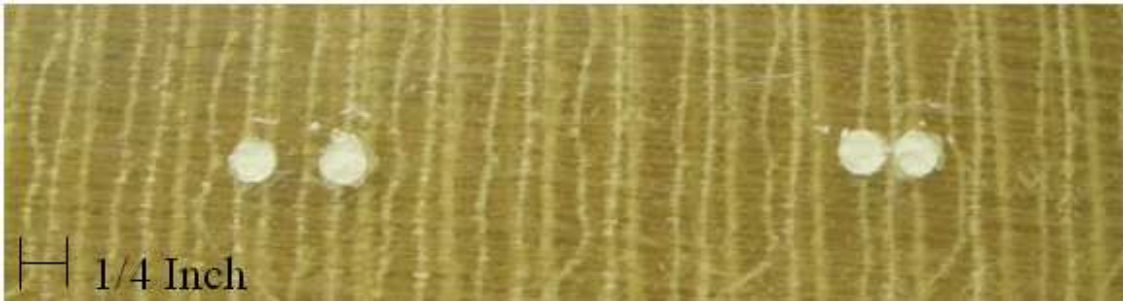

Figure 14. Recessed Holes Smoothed Over[13]

The hinges are gorilla glued in place to the steel that makes up the flap. The hardware was all standard fair that is obtainable from a hardware store. Screws, nuts, and bolts are all standard sizes and easily obtainable. This simple design philosophy needs to be incorporated into the full scale system in order to keep it manageable. A list of the manufactured test beds can be seen in Table 3.

Table 3. Test beds manufactured

Device Manufactured	Contents	Size LxWxH inches	Data Acquisition System
1 Flat Plate Test Bed	Gurney flap False wall flap	24.375x15.25x4	LabVIEW
1 Blade section test bed	Gurney flap	26x24x6	LabVIEW

Test Bed Conclusions

The flat plate and blade section test bed were both manufactured successfully, and fit within the primary deign considerations. Each of these test beds were hooked to a LabVIEW data acquisition software program. This program controlled the actuators movement in response to a pressure transducers input signal, as well as deployment of the active control surface to an exact position from input to the DAQ software. Tests were performed and software design iterations transformed these test beds to working proofs of concepts. Results from these tests and software iterations can be seen in related publications [12].

Acceptance of Modified Wind Turbines

Modified wind turbines will have to undergo the same rigorous acceptance criterion as normal wind turbines. The experience so far gathered indicates that environmentally friendly technologies such as wind may have environmental impact and may encounter acceptance difficulties from the population. The dimensions and importance of these are definitely lower than those of other conventional energy technologies but they are even capable of causing oppositions difficult to overcome [30]. Also the need for finding the acoustic emissions of the newly designed blades will have to be investigated. After the power curve, the sound power level has become the most important technical parameter today. The noise accreditation nowadays required for every wind energy project is based on the sound power level of the wind turbine [31]. The power output of these turbines will have to be more constant and provide smoother power quality than current blades. The fuel for turbines is the wind; when the wind blows the turbines are call on to provide power to the grid. Today the measurement and assessment of the power quality characteristics of grid-connected wind turbines is defined by IEC standard 61400-21 prepared by IEC Technical Committee 88 [32].

HEALTH MONITORING

In situ measurement is paramount to successful health monitoring. Sensor embedding is an effective method of solution in order to gather the internal forces present in a composite blade. The forces from the blades working in general, and larger forces that come mainly in the form of gust loading on the blades, are going to be catalogued over the life of these structures. This will aid future engineers in damage tolerant design for these blades, as opposed to the safe life design which is the current design philosophy. Safe life structures and Damage Tolerant Design will be reviewed to highlight the differences between the two philosophies. This section of the research focuses on embedding sensors into fiberglass layups in order to better facilitate health monitoring. The focus will be on MFSG, PVDF films, and fiber optics, all used for strain gauges. Also humidity, temperature, acceleration, tip deflection, delamination, gust loading, and impending gust loading will be addressed in order to provide a broad view of the loads and environmental conditions within which health monitoring of a blade will occur.

Safe Life Structures

Safe life is a design philosophy that was prevalent for decades, and is still prevalent in many applications, including the wind turbine industry. The idea behind it is that the product is made to works well for its entire design life, within certain loading limits. This is the philosophy that is governing in Wind Turbine Blade design [33]. Some other examples of things made with this philosophy in mind are: carabineers for rock climbing, automobile tires, rifles, Nalgene bottles, and most buildings. The rifle for

example is made to be used repeatedly, and with proper cleaning and minimal inspection, it will function properly for decades [34]. In some cases this is the best option for simple products. Unfortunately, this causes products to be made that are not optimized. These products tend to be over designed, due to using the “worst case scenario” as the design parameter.

With the addition of health monitoring sensors the loads these blades will be seeing in the actual field will be better understood. This information can be used to transition from a safe life design philosophy to a more optimizing damage tolerant design philosophy.

The perennial and on-going challenge in airframe structural design is simultaneously to satisfy three major competing and disparate requirements in one optimum solution. They are, (1) to provide maximum inherent safety, (2) to achieve superior structural performance in terms of weight and durability and (3) deliver an airframe with minimum realistic costs of production and long-term ownership by the operator. They must always be mutually and efficiently satisfied to bring real value to the flying public, our only reason for existence [35]. For its use in wind turbines all of these same requirements can be directly applied to blades.

Damage Tolerant Design

Damage tolerant design is a philosophy of optimization and periodic maintenance. Damage tolerant structures are made to perform well after some damage has been incurred. This design philosophy also calls for smaller periods of time between maintenance so damage can be observed and tracked before it becomes catastrophic. Also the maintenance can be condition based maintenance as opposed to timed, or run till

failure maintenance. Condition based monitoring must be used in conjunction with properly trained personal in order to best achieve the benefits of damage tolerant design. Airplanes, cars, buildings that are earthquake resistant, and most military vehicles are designed under the guise of damage tolerant design. This design philosophy has a place in systems which are placed in a harsh environment. Wind turbine blades operate in a variety of harsh conditions, rain, snow, and freezing sleet. Being placed in remote areas, or out at sea, they are hard to inspect, so a damage-tolerant design philosophy is best used [36]. A good example of damage tolerant design is the A-10 warthog, pictured in Figure 15 is an A-10 Warthog with the 332nd Air Expeditionary Wing from Pope Air Force base N.C. shot up over Baghdad, and landed safely.

Figure 15. A-10 Warthog which Landed Safely[14]

SENSORS

Three Sensors to be Investigated

The sensors that are the focus of the research are Metal Foil Strain Gages (MFSG), Polyvinylidene Fluoride (PVDF) and Fiber Optics (FO). MFSG's were chosen due to their ubiquity, ease of use, and inexpensive nature. PVDF's were chosen due to their unique quality of not having to be powered in order to be active as a sensor. Fiber Optic sensors were chosen due to their versatility, and ability to sense strain of an entire field. Each of these sensors has its own embedding methods. This is due to different avenues of data transmission and therefore different types of data acquisition equipment are required. The different sensors and their particular embedding procedures during manufacturing will be investigated, along with their different data acquisition needs and effectiveness.

Metal Foil Strain Gage

The Metal Foil Strain Gage (MFSG) is a classic method of sensing strain. The metal foil consists of a series of small lines of conductor laid down back and forth in a series of parallel lines with only two endpoints to which the leads are connected. The long thin wire has some resistance to it. When the foil is affixed to a material and that material undergoes some displacement the foil becomes longer as a result. This longer foil has a greater resistance. The change in resistance has been correlated very well with a change in displacement or strain.

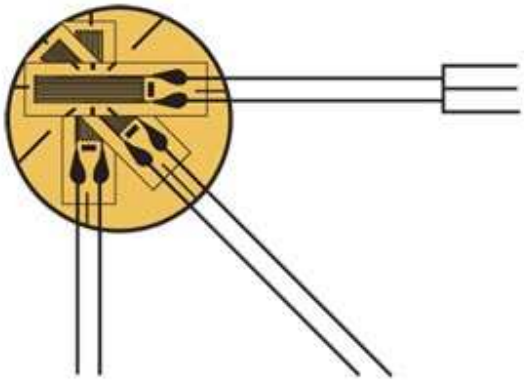

Figure 16. Triaxial MFSG Rosette[15]

The triple strain gage rosette seen in Figure 16 can provide a complete 2D strain picture for the coupon section it is attached to. Knowledge of strain in a specific location can be used on areas of interest, such as ply drops and other stress risers [37].

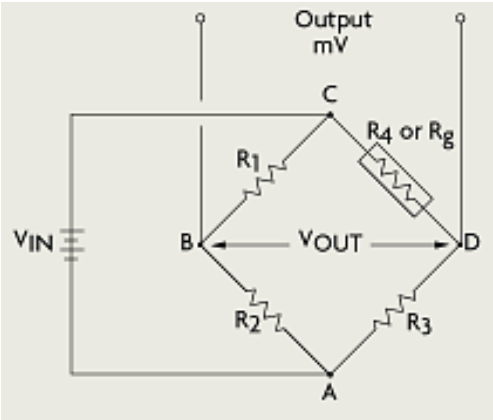

Figure 17. Wheatstone Bridge Circuit for MFSG[16]

For three individual MFSG affixed in the configuration as seen in Figure 16 one circuit is needed for each strain gage, so for the triple strain gage 3 different circuits are needed. The circuit is a Wheatstone bridge as can be seen in Figure 17, which provides a differential voltage that is directly related to the strain sensed by the MFSG. The change

is voltage is related to the change in resistance. This voltage change equation can be seen in Equation 3. The V_{in} is the voltage provided by the DAQ. R_1, R_2 and R_3 are all resistors whose values are the same as the gage resistance values. V_{out} is the voltage that is measured by the DAQ, this change in voltage is linearly related to strain.

$$V_{out} = V_{in} * \left[\frac{R_3}{R_3+R_G} - \frac{R_2}{R_1+R_2}\right] \quad 3)$$

Equation 3. Voltage out for Wheatstone Bridge Circuit

Polyvinylidene Fluoride

PVDF is a relatively thin sheet consisting of long repeating monomer chains. These chains act as a piezoelectric material, deflection causes a voltage to be produced across the copper lead wires of the sensor. There are many benefits to using the PVDF sensor; it is thin, which makes it able to fit into tight spots. The sensor is active in nature, producing a charge or voltage output in response to a mechanical perturbation. While piezo ceramics such as PZT, $BaTi0_3$, and quartz are also active, PVDF has significant advantages in terms of cost; its high elastic compliance makes it well suited for composite materials [38]. One major drawback of PVDF's is that the film is well suited for dynamic response and due to the method of discharging, is not well suited for quasi-static loads.

Fiber Optics

Fiber Optics can measure strain, strain field, and temperature. The technology exist for the practical application of the measurement of shear strain, transverse strain gradients as well as axial strain with the use of multiaxis fiber grating sensors. These sensors have a definite place in aerospace and civil structures [39].

The first research into the guided transmission of light was done is 1870 by John Tyndall. He directed a beam of sunlight into a path of water flowing from a pale. The light followed a zigzag pattern inside the curved path of the water. This was a clear representation of internal reflection to “bend” light along a curved path. The illustration of this experiment can be seen in Figure 18.

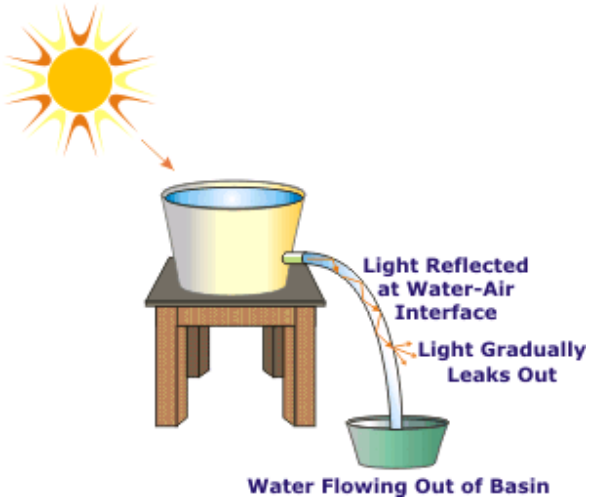

Figure 18. Internal Reflection Demonstration[17]

Research in the mid 1950’s culminated in the advancement of cladding on the exterior of the fiber’s core to permit complete internal reflection. The cable we used for our research was a single mode, data transfer cable. General Fiber Optic construction can be seen in Figure 19.

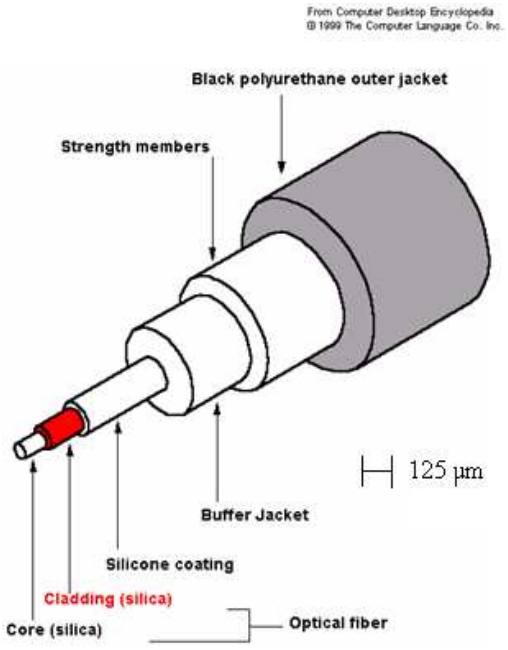

Figure 19. General Fiber Optic Construction[40][18]

Fiber Bragg Grating

Fiber Bragg gratings are sections of the fiber which contain glass that has been modified to have a different index of refraction at specified intervals [41]. The length of these intervals is directly related to the wavelength that is used in the FO [42]. All Fiber Bragg gratings have one thing in common; their lengths are all one-half of the modal wavelength within the fiber core. The wavelength of the ultraviolet light is 244 nm which corresponds to one half of 488 nm, the wavelength of the blue Argon laser line used to produce the "*Hill gratings*." The two overlapping ultraviolet light beams interfere producing a periodic interference pattern that writes a corresponding periodic index grating in the core of the optical fiber. The method called the transverse holographic technique is possible because the fiber cladding is transparent to the ultraviolet light

whereas the fiber core is highly absorbent to the ultraviolet light. A schematic of this can be seen in Figure 20.

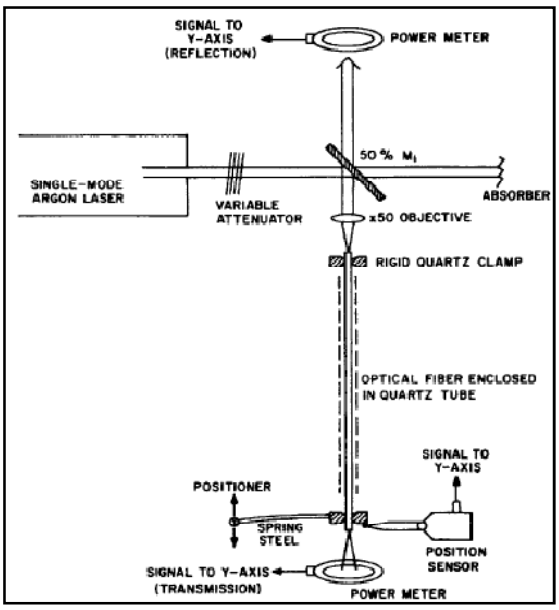

Figure 20. Schematic of Original Bragg Grating Writing Apparatus [19]

There are other methods of imprinting FBG into a FO. A simple one includes the two beam interferometer arrangement for side-writing fiber Bragg gratings. This method allows for the writings of gratings using a single exciter light pulse.

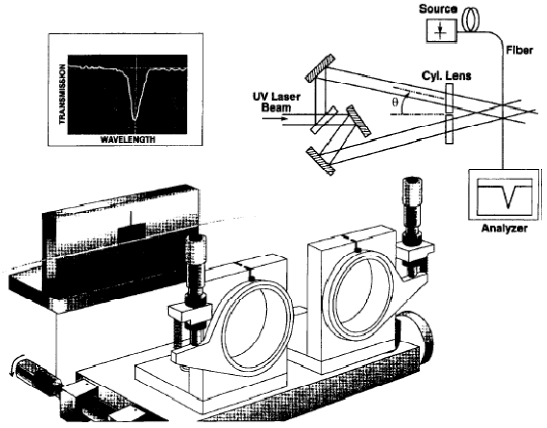

Figure 21. Two Beam Interferometer Arrangements for Side Writing FBG using the Holographic Technique[20]

The most popular method of writing FBG into a FO is the phase mask technique. This method of fabrication for FBG greatly reduces the manufacturing processes, allowing for a low per grating cost, and still produces gratings with high performance [42]. Another benefit of the Phase Mask Technique is the ability to tailor the profile of the indexed modulation, this process is called apodization. This technique can be extended to fabrication of chirped or aperiodic fiber gratings. Chirping means varying the grating period along the length of the grating in order to broaden its spectral response. Aperiodic or chirped gratings are desirable for making dispersion compensators.

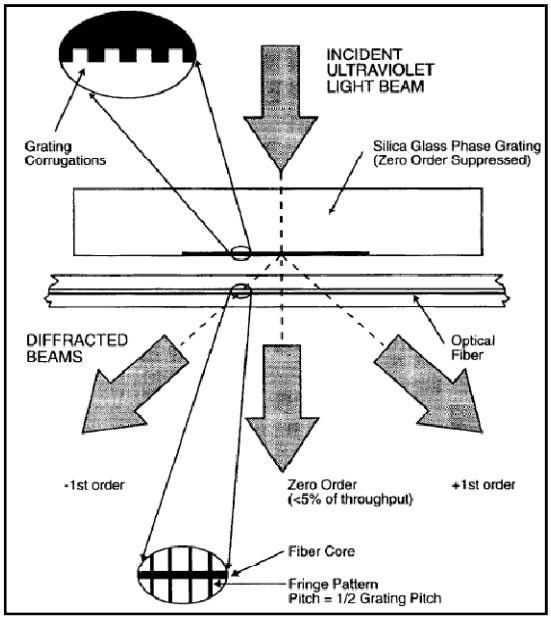

Figure 22. Phase Mask Technique[21]

Fiber Bragg Gratings allow for many different kinds of sensors; the most popular are temperature and strain. All of the sensors are based upon the idea of the FO being expanded and the change in length between the gratings is recorded by an interrogator. A FO with FBG can be used at a sensor for pressure, shear forces, 2D and 3D force measurements [43].

Strain Sensing Methods For Fiber Optics

In one method for obtaining strain from a fiber optic with a fiber Fabry-Perot (FFP) filter as a demodulator for FBG sensors. The system can be operated either in a closed-loop tracking mode for use with a single sensor element or in a scanning mode for use with multiple sensors. In the latter case a derivative form of signal detection is used to permit higher resolution to strain-induced shifts in the Bragg wavelengths of the sensor elements. This Fabry-Perot filter is for detecting the wavelength shift of fiber Bragg grating sensor or network [44].

Interrogators

For getting the necessary information from a FO with FBG an interrogator is needed. There are two general types of interrogators, Time-Division Multiplexing (TDM) and Wavelength-Division Multiplexing (WDM).

Time-Division Multiplexing: A TDM system utilizes a simple, pulsed, broad band light source in conjunction with low reflectivity gratings, sometimes less than 5% [45], each of which is written with the same grating period [46]. The TDM interrogator can achieve sample rates of 1kHz and handle 100 different sensors on a single FO strand, it is also a solid state device making it more robust for less than ideal conditions. A disadvantage of the TDM is that 1 meter of bare FO is needed between each sensor. TDM is also susceptible to cross-talk, which is interference between two returned signals and can be detrimental to the reliability of the returned signal.

Wavelength-Division Multiplexing: WDM is the most common type of interrogation technique. This system either uses a broadband light source with a spectrometer or a tunable swept-wavelength light source with photoelectric detectors [47]. WDM interrogators require that each FBG have a different grating period to operate properly. As the swept light source passes through the range of wavelengths, the wavelength of the light passing down the optical fiber is always known. When the wavelength passing down the optical fiber coincides with the Bragg wavelength of FBG, the light is reflected back up the fiber, to photo detectors. [47] The WDM system does not require the 1 meter separation between gratings sections, Also cross-talk is not a concern. The WDM system with the tuned swept-wavelength laser source is a delicate piece of equipment, which are more sensitive to harsh environments than a solid state system.

Currently the sample rate of WDM is lower than that of TDM. The sizes of the WDM system and power requirements are larger than that of the TDM system. The WDM is about the size of a desktop computer and the TDM system can be as small as a VHS tape [12]. With the vibration, harsh environmental concerns, and long design life, TDM is a viable method for interrogation in a wind turbine application.

Cost and Implementation of Fiber Optic System

Fiber Optic systems to be used as strain sensors would require many components. The fiber optics itself would have to contain fiber Bragg gratings. These FO would need to be hooked to an interrogator. They would have to be sheathed in order for the FO to survive the journey from inside the laminate, across the pitch control joint, to the interrogator mounted at the center of the hub. All three blades would have their

respective FO plugged into one interrogator. This interrogator would have to be hooked to a DAQ. An os1200 fiber optic with polyimide coating has 5 fiber Bragg gratings over its length and can operate at a frequency of 1526-1566 nm. A Fiber optic that is 1 meter in length and contains Fiber Bragg gratings sent by Sandia National Labs has a cost of 375$. An optical sensing interrogator sm130 field module which can handle 4 optical channels and operate in the 1510-1590 nm range starts at $20,000. The software to obtain the data from optical sensors is called ENLIGHT. ENLIGHT provides the basic functions of interrogator configuration, wavelength data acquisition, saving and visualization, and a host of other features. This software is estimated at a price of $600. For an estimated total of $30,000 for one interrogator with all four of the optical channels being used, the blades having 8 meters of sensors each along with an extra sensor not imbedded to be used for environmental offsets and the software to obtain the data. The most difficult part of the implementation of a FO system is the embedment of sensors, which will be covered in depth in the sensor integration portion.

Humidity

Relative humidity inside the rotor hub assembly. Humidity has a negative effect on the performance of composite materials under strain [48]. Knowing the relative humidity inside the blade over its lifetime will give engineers a more complete picture of the environmental conditions under which these blades operate.

Affixing humidity sensors to the inside surface of the blades and monitoring them with a DAQ system is a relatively simple undertaking. The relative humidity sensor (RHS) can be affixed to the inner blade surface much as a strain sensor would be. The blade surface would be cleaned with Isopropyl alcohol and let air dry. Then the sensor

would be affixed using an aerospace epoxy such as HySol, a substance commonly known as smurf glue. Sensors such as the TDK CHS-UPS exist which only need a ground wire, 5 VDC input, and a voltage output wire in order to operate effectively. The voltage output is a direct conversion to relative humidity in this type of sensor and can easily be read by any DAQ system, negating extraneous unnecessary circuitry.

Temperature

The temperature inside the rotor hub assembly should not be that different from the temperature outside. But the range in temperatures that the blades and rotor assembly are subjected to will be necessary for the engineers to know in order to better design the blades.

Thermocouples are the simplest way to measure temperature using a DAQ system. Two dissimilar wires are TIG welded together. That point is where the temperature measurement will take place. Due to the thermoelectric effect when a conductor is subject to a temperature gradient, a current is created [49]. A reference node is needed that is at a known temperature, in current DAQ systems this is done with simple circuitry. This is known as cold junction compensation [50]. In most modern DAQ systems there exists a cold junction compensator circuit. The relationship between temperature and voltage is non-linear and is described by this equation

$$\Delta T = \sum_{n=0}^{N} a_n v^n \qquad 4)$$

Equation 4. Relationship between Temperature and Voltage

Often times in a digital DAQ this equation will be part of the programming within that system. ΔT is the change in temperature, a_n are the coefficients and are given for n

from zero to between five and nine [50]. The voltage out is V^n and the values for n are coefficients which are specific to the thermocouple.

Thermocouples can be placed either on the inside the blades or on the exterior of the structure in many locations in order to get an idea of the temperatures that these structures operate under. With information from temperature probes on the interior and exterior of the blade an internal temperature gradient can be calculated. The inclusion of a thermocouple imbedded within a laminate would be a flaw in the laminate. This flaw is unnecessary due to this information being obtainable by other means. Temperature can also be sensed by a FO. A FO placed inside the rotor hub blade assembly but not embedded within a blade would function well as a temperature sensor by expanding and contracting with the internal temperature.

Acceleration

Accelerometers can be used to monitor gust frequency in blades presently deployed in the field. As a tool for comparison if a control surface was engaged on those same blades, the acceleration peaks from before and after the deployment could be compared and used as a metric to see if the control surfaces have a positive effect on the blade deflections. The accelerations felt within a blade as it flexes will vary with blade length.

Accelerometers are conventional and ubiquitous for this application. There are simple circuit based 3 axis accelerometers. The acceleration at the tip of a typical 35 meter blade should be covered by a ±20g accelerometer. A good accelerometer for this industrial application is the PCB 3713D1FE20G/025AY which measures ±20g's, has a

sensitivity of ± 5%, and +5 to 30 VDC excitation. This sensor is robust enough to withstand the instillation into the blades.

Tip Deflection

Measuring tip deflection directly has many advantages. Knowing how close the blades presently get to the tower coupled with wind speed at that time would be a great benefit in predicting and preventing tower strikes.

There are many methods to doing this. One such method is the deployment of accelerometers at the tips of the blades [37]. Sandia National labs outfitted a 9 meter TX-100 blade with a host of sensors and fatigue loaded the blade to test those sensors for performance in the realm of flaw detection. Accelerometers were successfully used in determining the tip deflection of the blade.

Delamination

Delamination of the fiberglass laminate is a separation of the individual layers of fiberglass, brought on by a breakdown in the laminate matrix.

By 20-30 years of operation (typically the expected lifetime of wind turbines), the cumulative number of fatigue cycles for wind turbine blades lies in the range of 10^8 to 10^9. This extreme accumulation of fatigue cycles with such a large amplitude range is unequaled by practically any other mechanical or structural system [21].

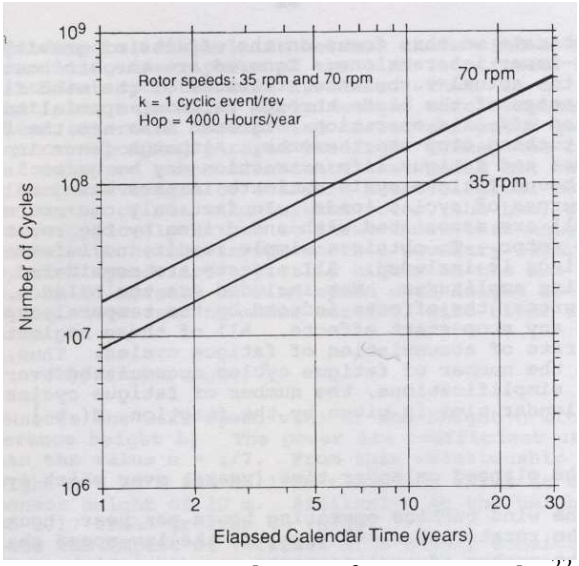

Figure 23. Accumulation of Fatigue Cycles[22]

There are many different forces that can act upon a blade in order to cause delamination. There are certain sections of the blade where it is more prone to delamination than others: ply terminations, skin-stiffener intersections, and sandwich ply terminations [51].

Delamination can be sensed by ultrasonic transducer probes that would have to be placed in contact with the blade. The effectiveness of ultrasonic transducers is displayed in a test done on a full scale blade. The testing parameters are outlined in their own words below.

> "The width of the scanned zones was 0.5m and covering the area over the main spar. Only the compression side of the blade (see Figure 24) was investigated by means of the ultra sonic tests. The tested areas had a length of 3.6m, 3.6m and 6m. This covered section 1, section 2 and section 3 as given in figure 1. A mobile scanning system, with two transducers, was mounted on the blade with suckers. The resolution/steps of the scans was 2.5mm. The ultra sonic waves are transmitted to the blade through water and the reflections from inter-faces like skin to glue, glue to main spar were measured. If any delaminations or lack of glue is in the zone, reflections will also been seen from these. In the figure below the result of such a scanning of the blade sections 3 are shown [52]."

i1: Skin/glue
In this area a red color indicates bad cohesion between skin laminate and epoxy or missing epoxy.

g1: Sandwich
Transition from red to yellow/green color indicates borders of the foam towards trailing edge.

g2: Sandwich
Transition from red to yellow/green color indicates borders of the foam towards leading edge.

c1: Tranducer signal not good
This area could not evaluated

o1: Area with damping
Blue color indicates high damping in skin or main spar laminate, which could be caused by porosities

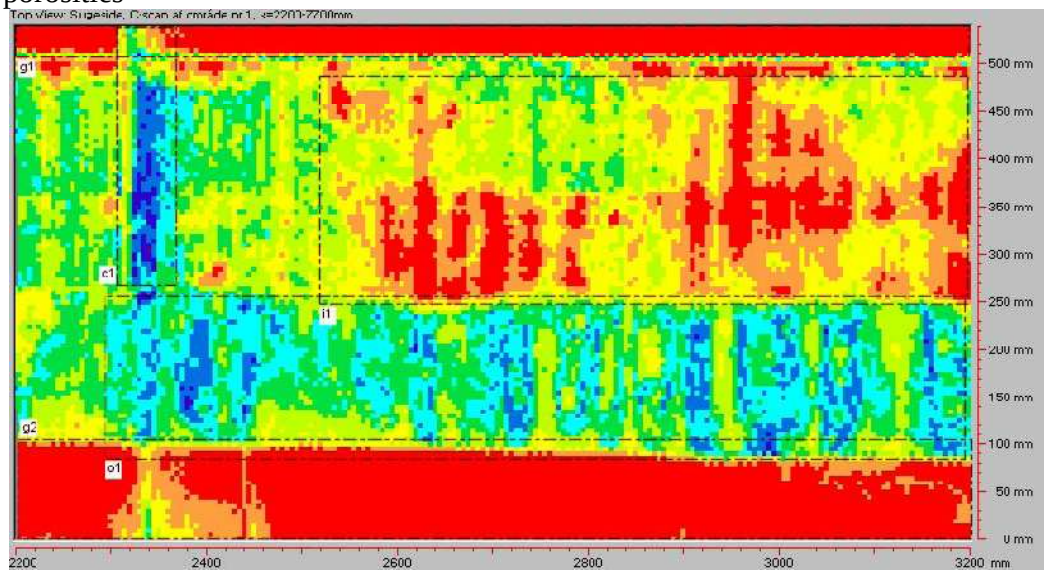

Figure 24. Results of Ultrasonic Transducer Testing[23]

This test is on a 25m (V52) blade, supplied by Vestas. This test, albeit in a laboratory environment shows the effectiveness of the ultrasonic transducer to sense flaws inherent in the blade. This specific blade had been tested to the static design load, and design fatigue loads which are similar to a 20 year lifetime. Due to these heavy loads

placed on the blade, the ultrasonic test was performed to investigate if any damage was present.

Acoustic Emission

Acoustic Emission (AE) is a simple microphone device that would be mounted to the internal surface of the blade. The merits of this type of sensor are not necessary for a smart structure due to the fact that the flaw propagation that they sense is irreversible. However the AE sensors have the distinct characteristic of recording valuable data about the type of failures a blade undergoes.

This microphone would listen for internal cracks caused by delamination and crack propagation [52]. The AE sensors coupled with other types of sensors can be used to correlate the strength of a load and the type of (if any) damage that occurred during, along with the location of the event over the lifetime of the blade [37]. Acoustic Emission is something that works very well in the laboratory setting due to its sensitive nature, but not well in a field setting due to that same sensitive nature.

Shearography

The ability to Non-destructively examine the ply's throughout a thick section of laminate. This method of non-destructive examination can be done without surface preperation. This sort of non-destructive examination is robust enough for use as a field inspection tool.

Shearography is a technology that uses heat, pressure, or vibration to excite a material. From that excitation a technique called interferometrics is used to measure microscopic surface deformations caused by internal flaws within the structure [53].

Currently there exists an ASTM standard E2581 which defines how to inspect composites with shearography. DANTEC dynamics makes a portable shearogrophy NDT inspection unit. This unit Q-810 is one that uses pressure in the form of a vacuum to hold itself to the inspection surface and excite the material being inspected. The inspection rate is 300mm x 200mm in 10 seconds [54]. Figure 25 is a picture of the results of a shearography test.

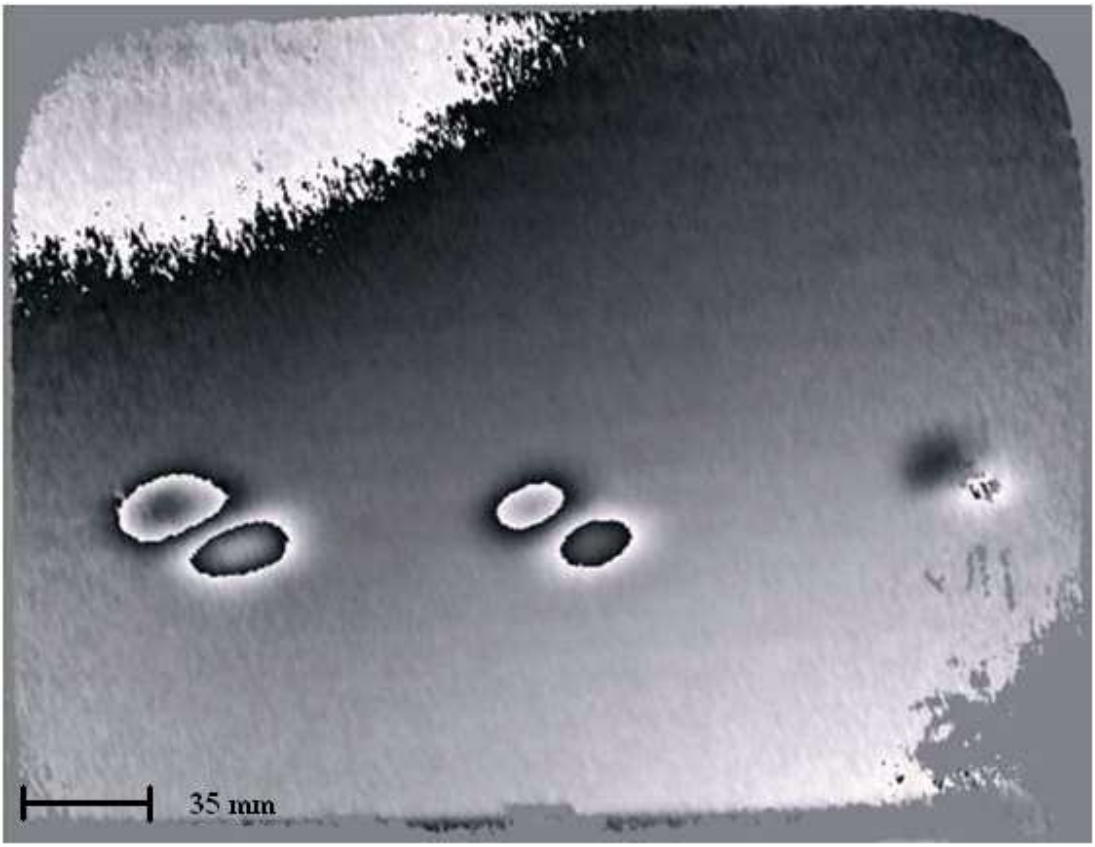

Figure 25. Shearography Image of Defects in a Composite Material[24]

EMBEDDING OF SENSORS

The MFSG, PVDF, and FO were all imbedded into a series of layups. This series can be seen in Tables 4-9. Each layup had the trio of sensors imbedded into it: initially everything was under the vacuum bag and this step provided a good seal and fiber volume fraction on the order of .42~.45. This also led to an indenting of the samples from the lead wires, and to an inability to get signal in and out of the sensors. Lead wires from each of the sensors were drawn through the top part of the layup, peel ply and flow media but left inside the vacuum bag. The drawbacks were that the wires were encrusted with resin every time a laminate was shot. The encrusted wires made for difficult handling and potential sources of breakage for the wire.

For ease of use, the wires should not be encrusted with resin. The solution was to draw the copper wires, and FO, through the top ply in the layup, the peel ply, flow media, and vacuum bag, and then it was to be sealed by applying tacky tape around the slit in the vacuum bag. This worked well for the PVDF and MFSG due to the robust nature of the PVC covered copper lead wires. This process was continued until the last 3 laminates. On these laminates a secondary vacuum bag was placed around the entire bank of sensors that were ingressing and egressing through the first vacuum bag. This created an area that was mostly free of resin and a very good vacuum seal. The PVC coated copper wire stood up well to the steps needed to extract sample coupons from the laminate. These steps include: removal of the vacuum bag, prying the laminate off of the mold, peeling off the peel ply and flow media, and cutting the samples out of the laminate using the diamond wheel saw. The wires all egressed out of the top of the laminate, so removal of the bottom side of peel ply and flow media was simple compared to removal of the peel

ply and flow media from the top of the laminate. The resin encrusted peel ply and flow media from the top of the laminate was removed by peeling it off and cutting it into sections in order to keep it away from the PVC wires that were coming through the top of the laminate. This extraction was made easier when rectangles measuring approximately 1” by 0.5” were cut into the peel ply and flow media and placed around the ingress and egress points of the sensors.

Steps for Embedding MFSG and PVDF Sensors

The following is a review of the steps to successfully embed sensors into fiberglass laminates.

- Step One: Clean samples with isopropyl alcohol.
- Step Two: Submerge sensor in 20% by weight solution of Nitric acid for ten seconds.

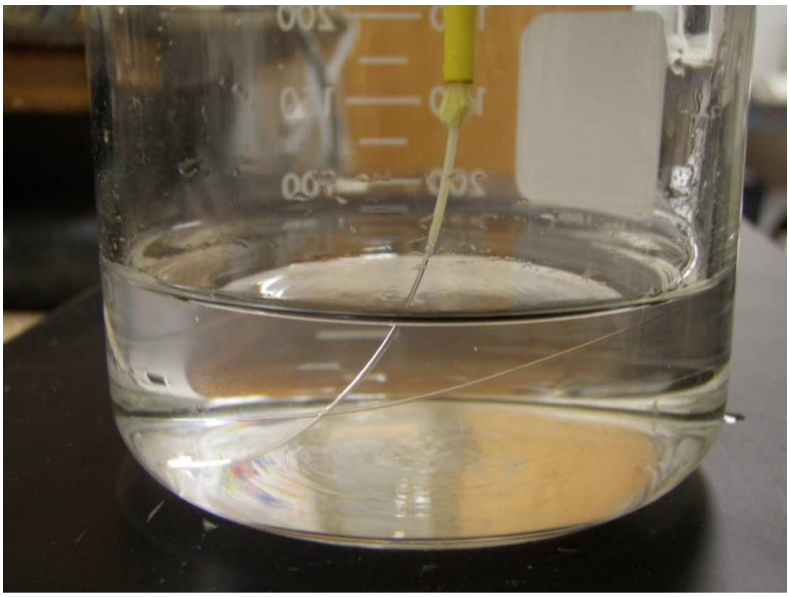

Figure 26. Fiber Optic Submerged in 20% by Weight Nitric Acid Solution[25]

- Step Three: Wash with water and let air dry.

- Step Four: Mark on laminate where the sensor will be affixed and keep sensor in place with spray adhesive. Take great car as to get the sensor in the proper orientation.

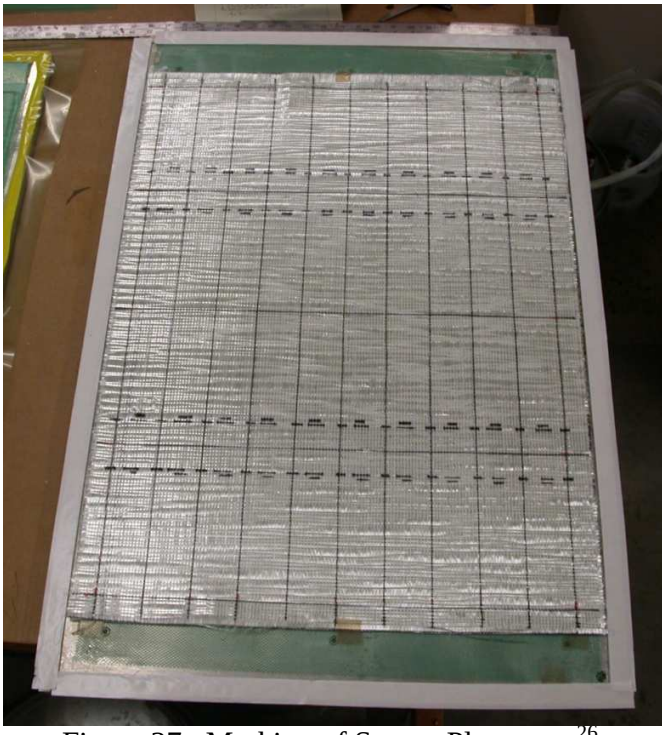

Figure 27. Marking of Sensor Placement[26]

- Step Five: Feed led wires through ply's above the sensor surface, take care not to damage the tows in the ply.
- Step Six: Cut ~1" by ~0.5" rectangles in the flow media and peel ply that the led wires will go through. Feed the wires through these rectangles.

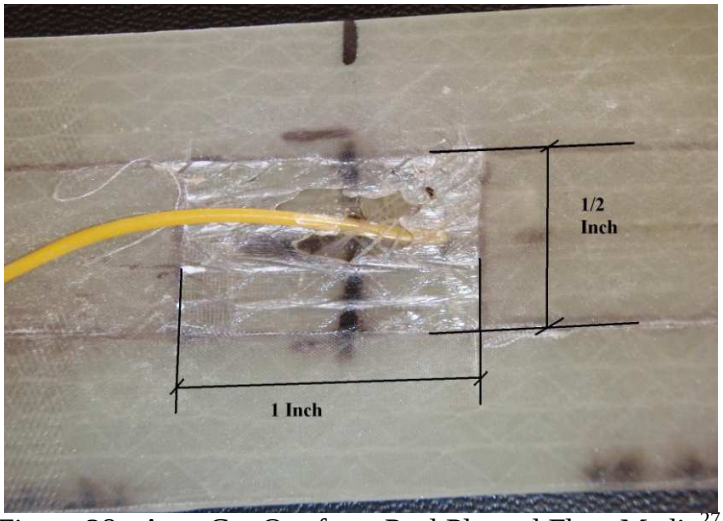

Figure 28. Area Cut Out from Peel Ply and Flow Media[27]

- Step Seven: Cut slits in the vacuum bag and feed the wires though those slits.
- Step Eight: Seal the slits with tacky tape.

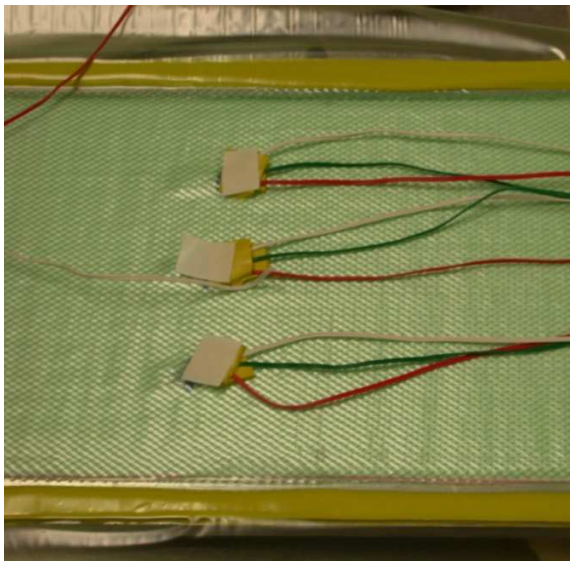

Figure 29. Sealing Slits in Vacuum Bag with Tacky Tape[28]

- Step Nine: Enclose the slit and extra lead wire in a second vacuum bag.

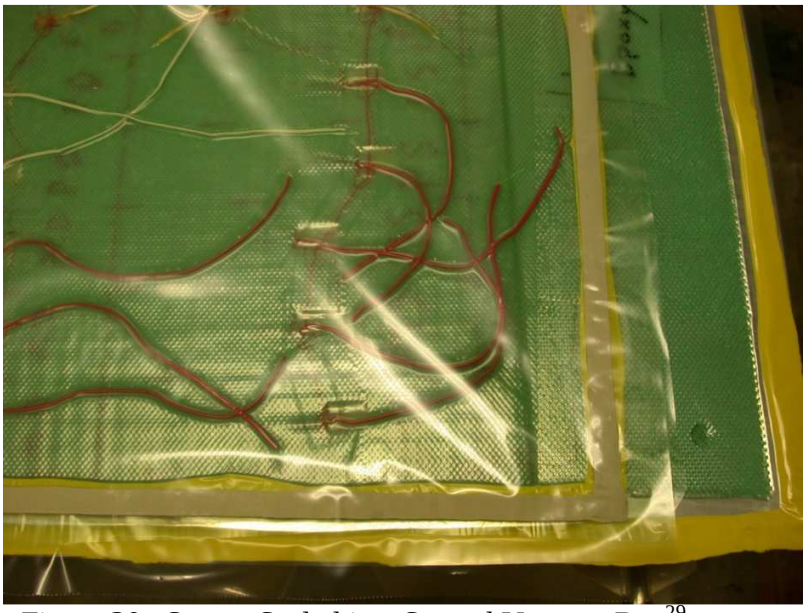

Figure 30. Sensor Sealed in a Second Vacuum Bag[29]

Signal Ingress and Egress From the Laminate

Fiber Optics are made from glass and therefore are brittle materials. If a FO is bent past its minimum bend radius flaws appear in the form of cracks transverse to the axial direction of the FO core. This generally occurs near the ingress and egress points of the FO sensor. Different styles of bringing the FO through the laminate will be investigated.

Fiber Optic Ingress and Egress Process

The FO ingress and egress process went through many design changes; initially the bare FO was run through the gauntlet of layers only to discover that every ingress and egress point was destroyed during laminate extraction. Then it was decided that a small metal tube was to be placed around the FO and was to travel through the layup, peel ply, flow media, and vacuum bag. This proved to work marginally better.

Figure 31. Aluminum Tube used as Fiber Optic Protector[30]

Next PVC coating from copper wire whose ID was close to the OD of the FO was split and placed around the FO providing a robust and flexible sheathing. The splitting of the sheathing provided too many openings for failure of the vacuum seal so the change was made to full PVC sheathing. Long pieces of PVC coating were stripped off and placed around the FO, through the bag, flow media, peel ply and top half of the laminate. Currently this is the best way of getting FO and their signals in and out of these layups. Also a one inch square around the ingress and egress points in the peel ply and flow media were cut out which made for much easier laminate extraction. This did create a larger resin rich area around the extraction points than what was already there from the FO inclusion.

The flaws inadvertently included in the FO can be seen in Figure 32 which shows the flaws as visible light, using a feature called the visual fault indicator included on the OWL Zoom II detector. The faults can be seen in the radius the FO traverses in order to get to the gage length of the sensor.

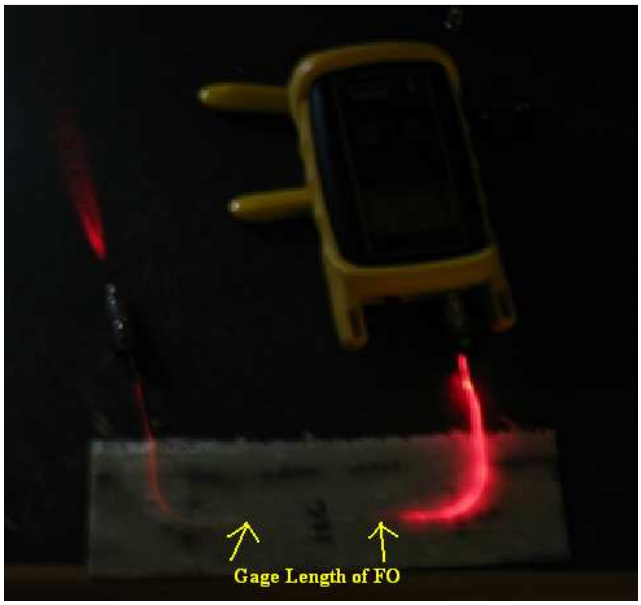

Figure 32. Visual Fault Indicator[31]

There were two methods of signal ingress and egress from the two ply laminates. The first was a FO with a PVC sheath which covered everything except the gage length and very end of the FO. This sheath was then laid between the two plies and exited the side of the laminate. This can be seen in Figure 33.

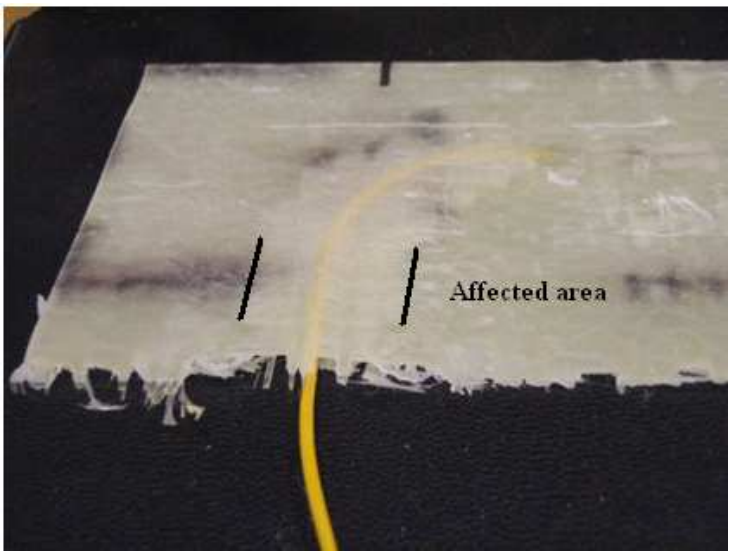

Figure 33. Side Ingress of FO[32]

As can be seen in Figure 33 the area affected by the FO sheathing is approximately ¼” on each side of the sheathing. In Figure 34 the second method of ingress and egress can be seen. The sheathing can be seen to exit the laminate through the top ply and the length of the sheath inside the material is significantly smaller than that of the side ingress and egress method.

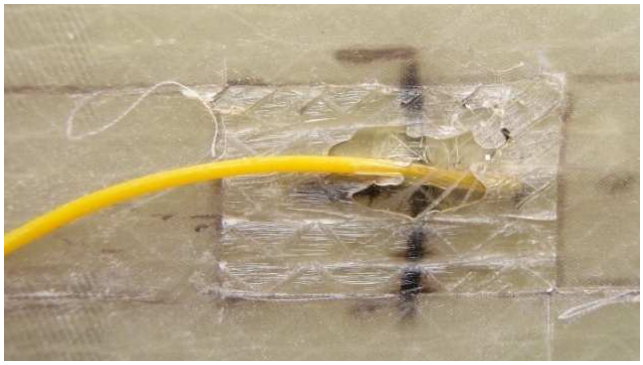

Figure 34. Ingress and Egress through Top Ply[33]

Steps for Embedding Fiber Optics Into Laminate

These steps are for embedding FO into a Blade. They will be focused on new blades being manufactured.

- Step One: Clean gauge length of sensor with isopropyl alcohol. Make sure there is enough FO to make multiple splices if necessary.
- Step Two: Submerge sensor in 20% by weight solution of Nitric acid for ten seconds.
- Step Three: At the proper spot in the layup raster the FO back and forth in the proper location and in the proper direction. Keep the FO in place with spray glue.

- Step Four: Thread a piece of protective PVC coating everywhere except the gauge length and connector end of the sensor.

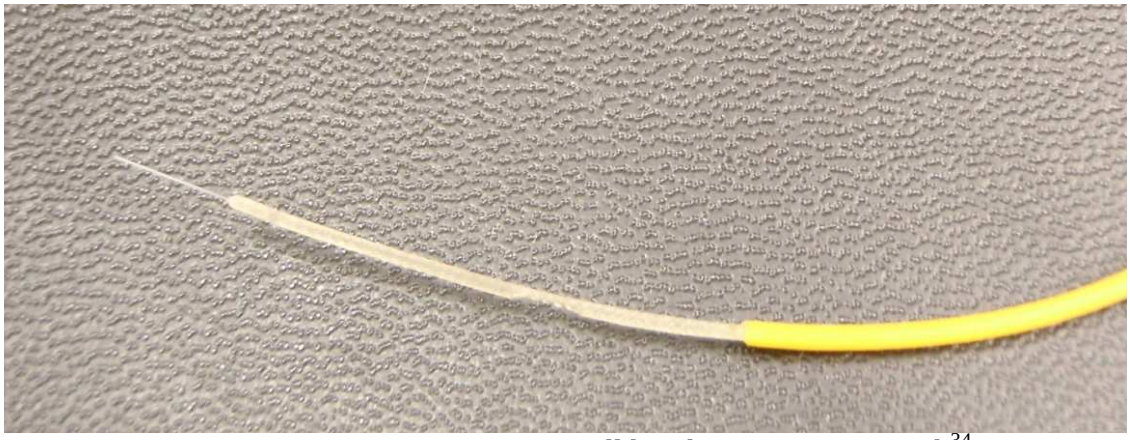

Figure 35. PVC Coating Covering all but the Connector Length[34]

- Step Five: As the laminate is being completed be sure to thread the FO along with its protective sheath through each layer. Make sure never to exceed the minimum bend radius of the FO.

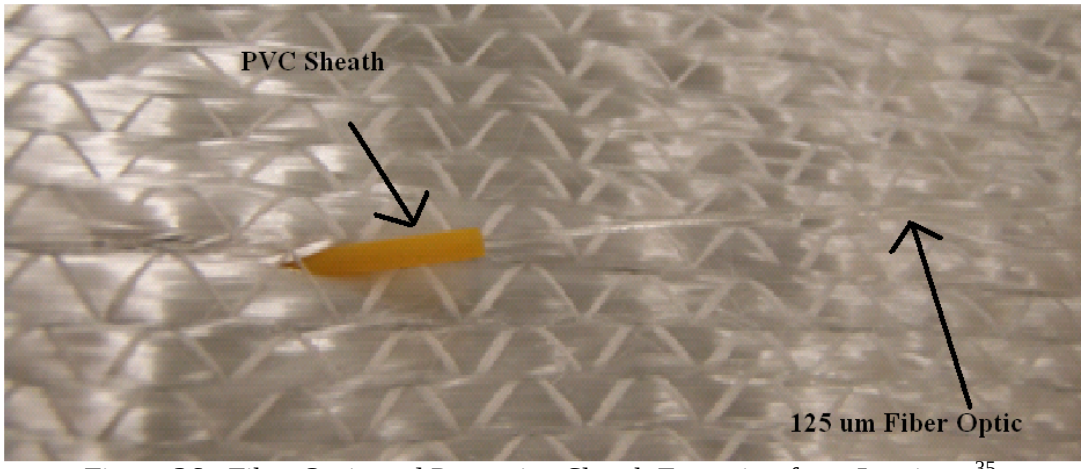

Figure 36. Fiber Optic and Protective Sheath Egressing from Laminate[35]

- Step Six: Protect the extra FO and PVC protective sheath in its own secondary vacuum bag before resin transfer molding has begun.

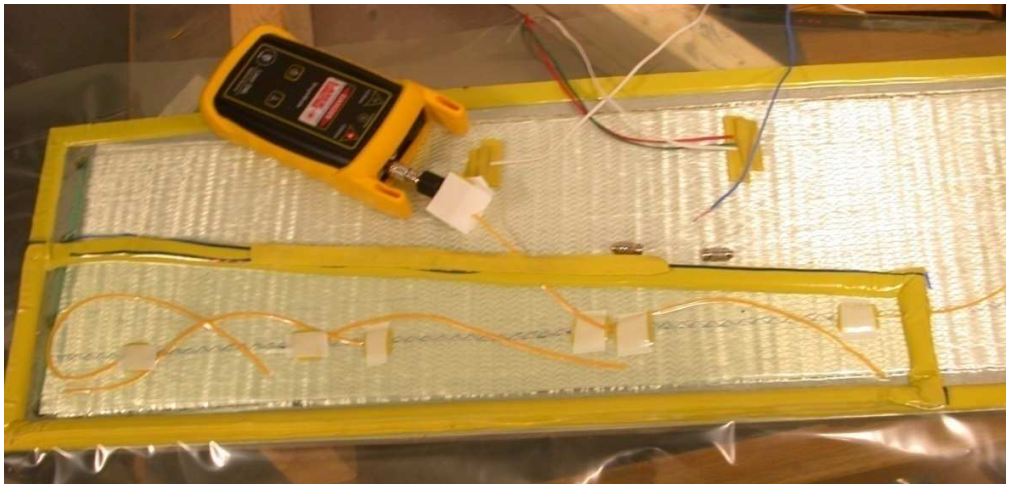

Figure 37. Second Vacuum Bag over Fiber Optics[36]

- Step Seven: After curing, extract the laminate carefully being sure not to exceed the minimum bend radius of the FO.
- Step Eight: Affix the proper end to the FO and secure it for transport.

Figure 38. Fiber Optic with Mechanical Ends Attached[37]

A list of the laminates that were created can be seen in Table 4-9. A brief description of each laminates resin, sensor contents, surface treatment, and purpose accompanies the date of manufacturing. These plates were cut into 2x8 inch coupons for tensile tests, and 1.5x7 inch samples for double cantilever beam mode 1 testing. These tests were performed to evaluate the manufacturing techniques and sensor conditioning steps previously outlined.

Table 4. Flat Plates 1-5 Manufactured to Date

Laminate	Date	Matrix	Sensor embedded	Surface treatment	Purpose
1	3/25/2008	Epoxy (Prime 20L)	Acrylate Fiber Optics w/ and w/o polymer jacket	none	become familiar with the steps needed to embed sensors
2	4/1/2008	Epoxy (Prime 20L)	none	none	epoxy control samples
3	4/3/2008	Vinylester (Fibre glast 1110 series)	none	none	vinylester control samples
4	4/14/2008	Epoxy (Prime 20L)	3 axis Strain gages, PVDF, Thermister, Thermocouple, acrylate Fiber optic	none	explore signal retrieval from sensors embedded in epoxy laminate
5	4/23/2008	Vinylester (Fibre glast 1110 series)	3 axis strain gages, PVDF, Thermocouple, Fiber optic	none	explore signal retrieval from sensors embedded in vinylester laminate

Table 5. Flat Plates 6-10 Manufactured to Date

Laminate	Date	Matrix	Sensor embedded	Surface treatment	Purpose
6	6/30/2008	Epoxy (Prime 20L)	3 Axis Strain Gage, PVDF, Acrylate Fiber Optics	Surface treated w/ emry cloth & cleaned with Acetone	Concentrate on three sensors. Start to explore surface treatment options in epoxy laminates
7	7/28/2008	Vinylester (Fibre glast 1110 series)	3 Axis Strain Gage, PVDF, Acrylate Fiber Optics	Surface treated w/ emry cloth & cleaned with Acetone	Concentrate on three sensors. Start to explore surface treatment options in vinylester laminates
8	8/4/2008	Epoxy (Prime 20L)	3 Axis Strain Gage, PVDF, Acrylate Fiber Optics	Surface treated w/ Nitric Acid and cleaned w/ Isopropyl Alcohol	Create Test plate to evaluate surface treatment options in epoxy laminate
9	8/28/2008	Vinylester (Fibre glast 1110 series)	3 Axis Strain Gage, PVDF, Acrylate Fiber Optics	Surface treated w/ Nitric Acid and cleaned w/ Isopropyl Alcohol	Create Test plate to evaluate surface treatment options in vinylester laminate, start to retrieve signal from fiber optics
10	9/12/2008	Vinylester (Fibre glast 1110 series)	3 Axis Strain Gage, PVDF, Acrylate Fiber Optics	Surface treated w/ Nitric Acid and cleaned w/ Isopropyl Alcohol	Replace laminate 9 because of manufacturing defects , initial try at fiber optic reinforcement (AL capillary tubes), collection of signal strength over time

Table 6. Flat Plates 11-15 Manufactured to Date

Laminate	Date	Matrix	Sensor embedded	Surface treatment	Purpose
11	9/26/2008	Epoxy (Prime 20L)	Acrylate Fiber Optic	Surface treated w/ Nitric Acid and cleaned w/ Isopropyl Alcohol	Second laminate used to evaluate fiber optic reinforcement techniques (Al capillary tubes) collection of signal strength over time
12	10/3/2008	Epoxy (Prime 20L)	Acrylate Fiber Optic	Surface treated w/ Nitric Acid and cleaned w/ Isopropyl Alcohol	Laminate to test second fiber optic reinforcement technique (wire jacketing), collection of signal strength over time
13	10/10/2008	Epoxy (Prime 20L)	Acrylate Fiber Optic	Surface treated w/ Nitric Acid and cleaned w/ Isopropyl Alcohol	Laminate to test fiber optic reinforcement technique with new technique of jacket collection, collection of signal strength over time
14	10/16/2008	Epoxy (Prime 20L)	Acrylate Fiber Optic	Surface treated w/ Nitric Acid and cleaned w/ Isopropyl Alcohol	Laminate to further test fiber optic reinforcement technique with new technique of jacket collection, collection of signal strength over time
15	11/11/2008	Epoxy (Prime 20L)	3 Axis Strain Gage, PVDF, Acrylate Fiber Optics	Surface treated w/ Nitric Acid and cleaned w/ Isopropyl Alcohol	Fiber Optic Signal strength test with optic reinforcement as well as initial attempts at creating G1c test coupons

Table 7. Flat Plates 16-20 Manufactured to Date

Laminate	Date	Matrix	Sensor embedded	Surface treatment	Purpose
16	11/26/2008	Vinylester (Fibre glast 1110 series)	3 Axis Strain Gage, PVDF, Acrylate Fiber Optics	Surface treated w/ Nitric Acid and cleaned w/ Isopropyl Alcohol	Mode 1 crack propagation testing (G1c testing)
17	11/25/2008	Epoxy (Prime 20L)	3 Axis Strain Gage, PVDF, Acrylate Fiber Optics	Surface treated w/ Nitric Acid and cleaned w/ Isopropyl Alcohol	Mode 1 crack propagation testing (G1c testing)
18	1/22/2009	Epoxy (Prime 20L)	Acrylate Fiber Optic	Surface treated w/ Nitric Acid and cleaned w/ Isopropyl Alcohol	Fiber Optic signal strength test with optic reinforcement
19	1/27/2009	Epoxy (Prime 20L)	Acrylate Fiber Optic	Surface treated w/ Nitric Acid and cleaned w/ Isopropyl Alcohol	Fiber Optic signal strength test with optic reinforcement
20	2/3/2009	Vinylester (Fibre glast 1110 series)	Acrylate Fiber Optic	Surface treated w/ Nitric Acid and cleaned w/ Isopropyl Alcohol	Fiber Optic signal strength test with optic reinforcement

Table 8. Flat Plates 21-25 Manufactured to Date

Laminate	Date	Matrix	Sensor embedded	Surface treatment	Purpose
21	2/6/2009	Vinylester (Fibre glast 1110 series)	Acrylate Fiber Optic	Surface treated w/ Nitric Acid and cleaned w/ Isopropyl Alcohol	Fiber Optic signal strength test with optic reinforcement
22	2/12/2009	Vinylester (Fibre glast 1110 series)	Acrylate Fiber Optic	Surface treated w/ Nitric Acid and cleaned w/ Isopropyl Alcohol	Fiber Optic signal strength test with optic reinforcement
23	2/12/2009	Epoxy (Prime 20L)	1axis Strain Gages ,PVDF, Polyimide Fiber Optics	Surface treated w/ Nitric Acid and cleaned w/ Isopropyl Alcohol	Manufacturing of additional tensile testing coupons with embedded sensors.
24	2/20/2009	Vinylester (Fibre glast 1110 series)	1 axis Strain Gages, PVDF, Acrylate Fiber Optics	Surface treated w/ Nitric Acid and cleaned w/ Isopropyl Alcohol	Manufacturing of additional tensile testing coupons with embedded sensors.
25	2/24/2009	Vinylester (Fibre glast 1110 series)	1 axis Strain Gages, PVDF, Acrylate Fiber Optics, Polyimide Fiber Optics	Surface treated w/ Nitric Acid and cleaned w/ Isopropyl Alcohol	Manufactured for additional G1c test coupons

Table 9. Flat Plates 26-29 Manufactured to Date

Laminate	Date	Matrix	Sensor embedded	Surface treatment	Purpose
26	2/26/009	Epoxy (Prime 20LV)	1 axis Strain gages, PVDF, Acrylat Fiber Optics, Polyimide Fiber Optics	Surface treated w/ Nitric Acid and cleaned w/ Isopropyl Alcohol	Manufactured for additional G1c test coupons
27	5/11/2009	Epoxy (Prime 20LV)	no sensors	no surface treatments	compare fracture toughness of new resin batch with older batch
28	5/13/2009	Epoxy (Prime 20LV)	1 axis Strain gages, PVDF, Acrylat Fiber Optics, Polyimide Fiber Optics	Surface treated w/ Nitric Acid and cleaned w/ Isopropyl Alcohol	Manufacturing of additional tensile testing coupons with embedded sensors.
29	6/12/2009	Vinylester (Fibre glast 1110 series)	1 axis Strain gages, PVDF, Acrylat Fiber Optics, Polyimide Fiber Optics	Surface treated w/ Nitric Acid and cleaned w/ Isopropyl Alcohol	Manufacturing of additional tensile testing coupons with embedded sensors.

Conclusions on Sensor Manufacturing

The iterations that the manufacturing underwent in the course of producing these plates and protecting signal ingress and egress can be seen in the purpose column of Table 3. One manufacturing step that was not outlined in the table was the addition of the second vacuum bag around the ingress and egress points of the sensor leads, this was done on laminate 13 and all subsequent laminates. The plates were manufactured successfully and the coupons were subsequently tested and the results of the test can be seen in related publications [59].

Gust Loading

Gust loading can be sensed in many different ways. Accelerometers, pressure transducers, piezoelectric sensors, and anemometers are all used as sensors for gust loading on a wind. Pressure transducers and anemometers will be reviewed with respect to sensing a gust load.

Pressure Transducers

There are a variety of pressure transducers on the market today. The most common type is a strain-gage based transducer. The conversion of pressure into an electrical signal is achieved by the physical deformation of strain gages which are bonded into the diaphragm of the pressure transducer and wired into a Wheatstone bridge configuration [55]. Another popular method for transduction is applications of piezoelectric materials like quartz. The ceramic material would contact the flowing air

current. As the flow of gas, in this case air, increases so does the load on the piezoelectric material. This in turn increases the voltage output at a linear rate by the ceramic.

Anemometers

This is the classic method of sensing wind velocities. The most prevalent form of this is the cup anemometer, which consists of three cups equal spaced from a vertical rotating axis. The spacing of 120º makes for more even torque through varying wind speeds. As the wind speed increases the rotational velocity of the vertical axis increases, this increase is linear up to a point and must be accounted for by an anemometer correction factor.

Figure 39. Three Cup Anemometer[38]

These methods of sensing gust loading have their individual positive qualities but they all have one glaring drawback. All of these sensors sense the gust at their individual locations. The gust of wind has to arrive and impart some load on the structure, or sensor, before any of them register a load or react to the wind speed. This delay between the arrival of a gust of wind and the sensing of a gust of wind seems counterproductive with respect to mitigating gust loading on the structure. If the load is on the structure and then

the structure reacts to the load it is too late to mitigate that load already present in the blade.

Impending Gust Loading

The ability of a smart structure to sense the loads placed on it has been demonstrated to be of paramount significance. To take that idea of sensing one step further and to actually be able to predict the loading that would be placed on the structure would be ideal. The technology exists in the form of Doppler LIDAR to do this. High resolution profiles of mean and turbulent statistics of the wind field upstream of a wind farm can be produced using a scanning Doppler LIDAR [56].

Figure 40. LIDAR Remote Measurement of Wind Profiles[39]

Light Detection and Ranging (LIDAR) can be used to monitor wind speeds up to 800 meters high with the station sitting on the ground [56]. The implications of being able to sense wind velocities at a range of even 100 meters upstream of the wind turbine are far reaching. The turbine could change its shape for the impending gust loadings and be ready when those gusts arrive. The blades would not have to be subject to unknown forces; those forces could be quantified through research, accounted for through proper programming of the control systems interaction with the LIDAR sensor, and mitigated through proper deployment of control surfaces housed in the blades themselves.

The use of LIDAR would be helpful for gust loadings as far as active control surfaces are concerned. More useful for the wind industry are accurate meteorological reports that would accurately be able to predict wind velocity and direction 30 to 45 minutes ahead of schedule. This would aid in smooth incorporation of wind turbines into the nations grid system.

Sandia National Labs Blade Study

Each of these sensors must be researched and their individual merits proven. As a proof of concept many of these sensors were embedded into a blade which was manufactured in Warren Rhode Island at the facilities of TPI aerospace under the guise of Sandia National Laboratories. MFSG, accelerometers, thermocouples, and FO with fiber Bragg gratings were all embedded or affixed to the inside of this blade. The FO with fiber Bragg gratings were designed to measure temperature and strain, the host of other sensors to be redundant and used as a benchmark in some cases; and as a source for correction factors in other cases.

Figure 41. Sensors Affixed to the Inside of a Blade[40]

Figure 41 shows the sensors affixed to the inside of the Sandia blade. The two metal cubes are three axis accelerometers with coaxial cable as data transfer conduit. Two are mounted into the blade for redundancy. As can be seen in this photo, the blade is packed full of sensors, the FO which were bonded to the inside of the blade contained a layer of foam around them in order to preserve them for extraction after the blades useful life was reached. This does not make for the best adherence to the inside of the blade structure and therefore not great strain sensing capabilities. The reason this was done was to have the ability to extract the FO for future use due to its expense and its containing of Fiber Bragg gratings. The sensors that were embedded into the flat laminates were to coincide with research that came from Sandia's blade. Embedding of MFSG, PVDF, and FO were also to be a proof of concept for the Sandia blade. The issues that were addressed concerning signal ingress and egress were to be shared with Sandia. Potentially these ideas could be used in an industrial sensor implementation situation.

FIBERGLASS LAYUPS

Initially metal foil strain gauges (MFSG), PVDF strips, and Fiber Optics (FO) were embedded into a 2 ply layup of saertek-14 fabric. The ply's consisted of 0º dominated toes stitched together with nylon, and a thin amount of 90º stitched in also. The stacking sequence for the layup was [0,90,90,0]. This made for a symmetric laminate that was easy to cut up into sample pieces. The samples were roughly 2" wide and were cut on a diamond wheel saw. The process of infusing resin was done with a vacuum assisted resin transfer mold (VARTM). The mold stacking sequence was a hard aluminum mold on the bottom, peel ply, flow media, the stacking sequence of the layup, another set of peel ply, flow media, and a nylon vacuum bag on top. This process was to mimic what is done in industry during blade manufacturing.

Resin

The resin was pulled through the stacking sequence in a matter of minutes due to the small layups that were being infused. There were two distinct types of resin that were used, the first being Prime-20 epoxy and the second being vinyl ester with an MEKP activator. These resins are commonly used in industry, and that is the reason they were chosen for this application. The polyester resin which is also very common was not investigated in this particular study. The prime-20 is mixed 100:26 by weight and the vinyl ester is mixed with a ratio of 1.25% by volume.

Bonding of sensor surface to the composite

A series of modifications were to be tested for improving bonding on the surfaces of each of the sensors. There were three different sensor sets that were tested. The first set was simply cleaned with isopropyl alcohol. The second set was dipped in a 20% by weight solution of nitric acid and then cleaned with isopropyl alcohol. The third set was submerged in a 20% by weight solution of nitric acid for 10 seconds and then cleaned with isopropyl alcohol. These sensors being embedded are viewed through the eyes of a Secondary Electron Microscope in order to gain a better view of the reaction of the surface treatments to the epoxy.

Secondary Electron Microscope (SEM)

The SEM is one of the tools used to investigate the bonding of the sensor surface to the fiberglass laminates. The samples were initially extracted from the laminate by the use of a diamond wheel; the samples were cut to about 1 cm square. Then were affixed into an aluminum holder and polished on a series of polishing wheels, all the way down to 0.05 microns. Initially the polished surface was cleaned with acetone but once it was realized that acetone ate away at some of the protective coatings of the sensors the cleanings were done with isopropyl alcohol. The effects can be seen in Figure 42 and Figure 43.

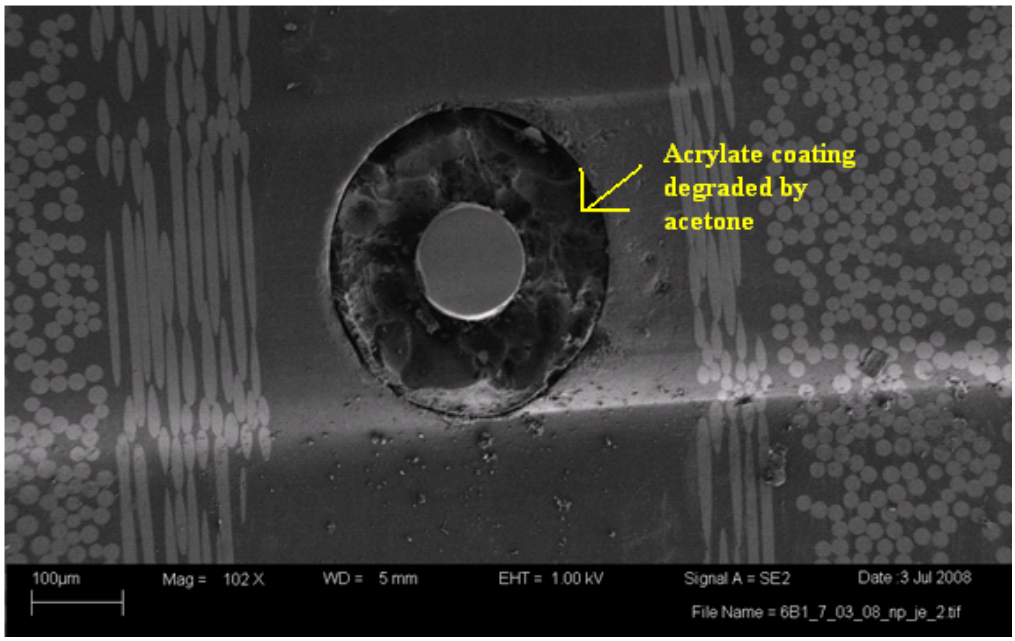

Figure 42. Fiber Optic Coating Degraded by Acetone[41]

Surfaces were then cleans with Isopropyl alcohol as to not degrade the acrylate coating of the Fiber Optic.

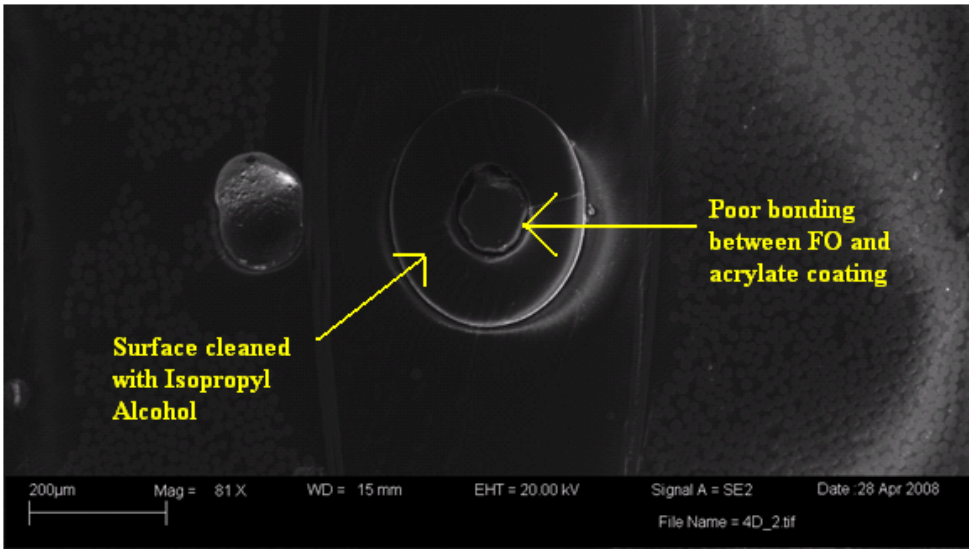

Figure 43. Fiber Optic cleaned with Isopropyl Alcohol[42]

The SEM images produced a lot of insight as to how the sensors bonded within the surfaces of the laminate. As seen in Figure 44 and Figure 43 the glass FO is not bonded well with the acrylate coating. This may be a product of the cutting and polishing process. The horizontal lines present in Figure 42 are caused by polishing. But even if this is the case it raises an interesting question. *When using FO as strain sensors; how well is the glass core and cladding bonded with the acrylate or polyimide coating that protects it?*

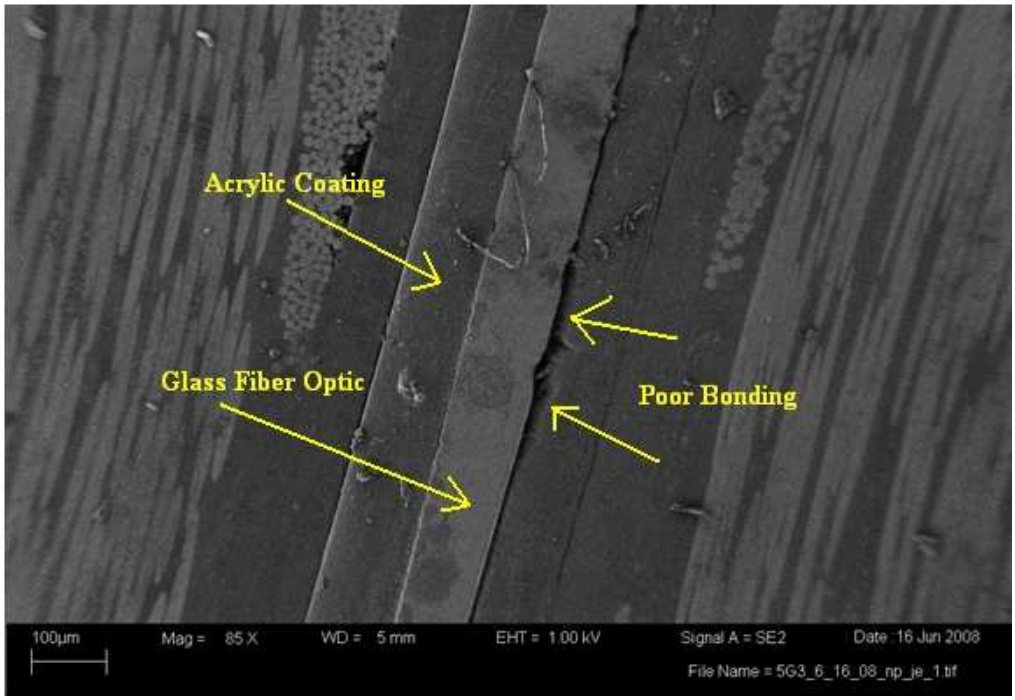

Figure 44. Fiber Optic with Acrylate Coating[43]

Similarly the PVDF films have an acrylate coating on one side of the film and nylon coating on the opposite side. The cleaning with acetone ate away at the acrylate coating on the PVDF, this coupled with the infusion of resin caused the silver ink to

"flow" from the PVDF. This lowers the reliability of the sensor since the silver ink forms the capacitive plates of the sensors. This ink flow can be seen in Figure 45.

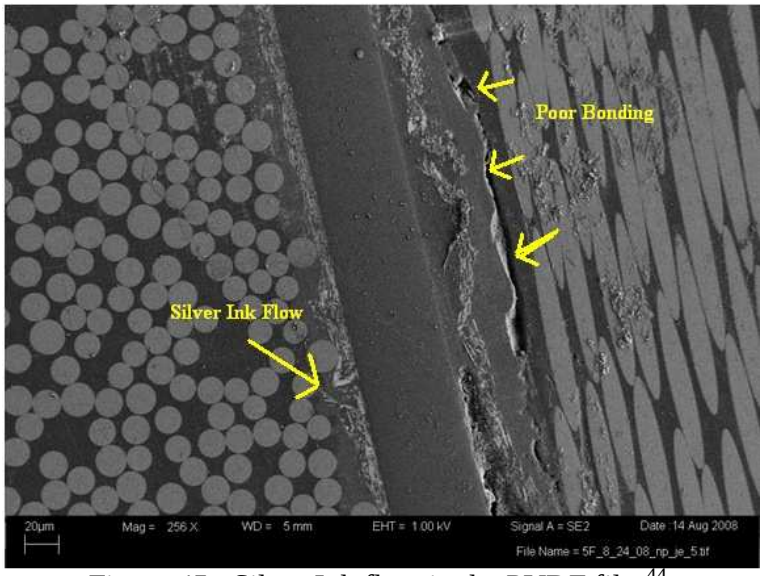

Figure 45. Silver Ink flow in the PVDF film[44]

The surface of the PVDF tells a similar story with regards to the surface treatment helping with bonding to the laminate. Figure 46 shows the surface of the PVDF sensor cleaned with isopropyl alcohol.

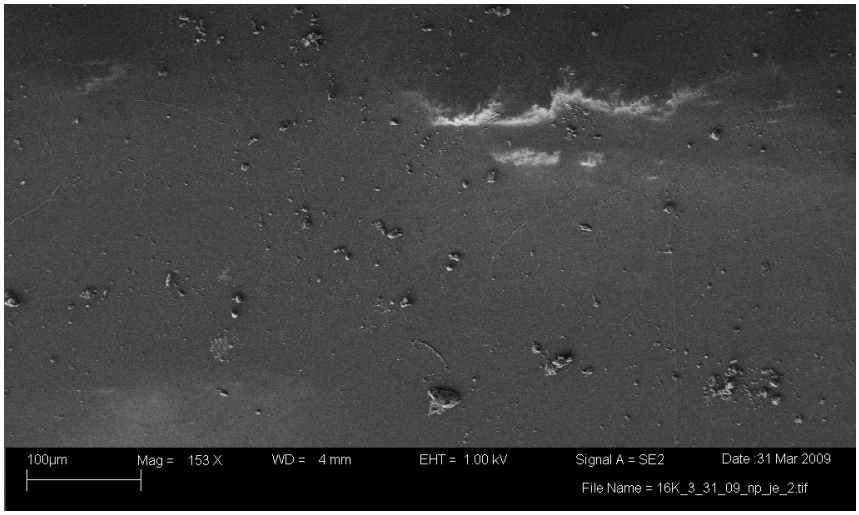

Figure 46. Poor Bonding of Epoxy to PVDF[45]

Figure 47 shows epoxy bonded well to the surface of the PVDF sensor which was submerged in Nitric Acid for ten seconds.

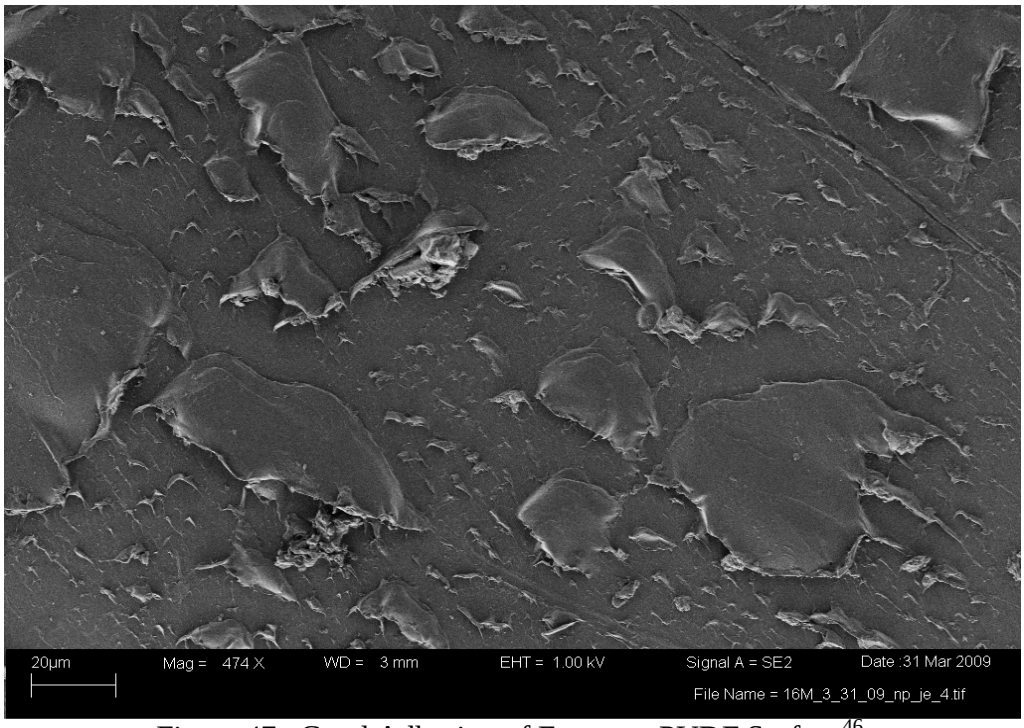

Figure 47. Good Adhesion of Epoxy to PVDF Surface[46]

The MFSG have a functionalized surface on one side that is made to be bonded onto a coupon. The opposite surface has no such surface treatment. Therefore when the sample is only cleaned with isopropyl alcohol the top surface does not bond well. This can be seen in Figure 48. This picture also brings up the issue of flaw initiation. A flaw initiation's volume does not matter in relation to the structures overall volume.

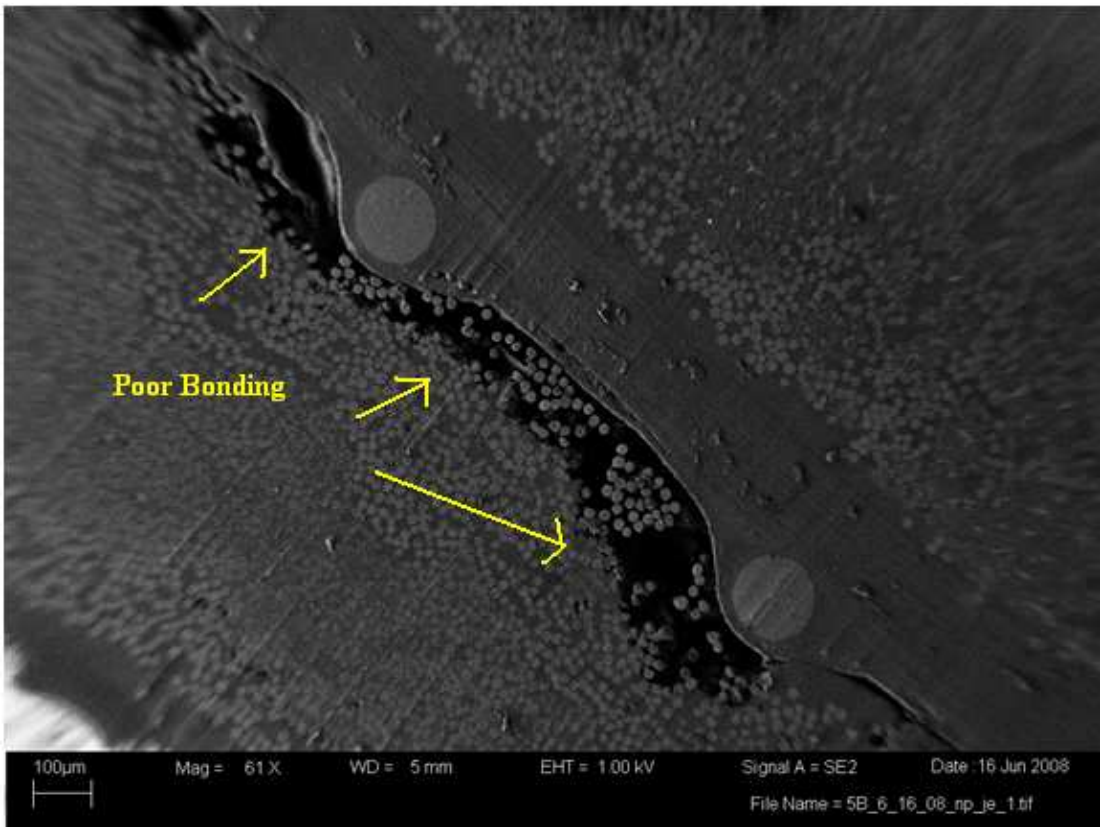

Figure 48. Poor bonding on surface of MFSG[47]

The view in Figure 49 is of an embedded MFSG which underwent the Nitric acid submerging process. As can be seen in the picture The MFSG sensor path can be seen along with the rough surface left by the resin. This demonstrates poor bonding between the top surface of the sensor and the fiberglass that was above the sensor.

The embedded MFSG in wind turbine blades would still be protected from lightening strikes due to the blades lightening protection systems which are installed by the blade manufacturers. This protection system, when working properly, would also protect the electronics and DAQ that would be present in the rotor and blades.

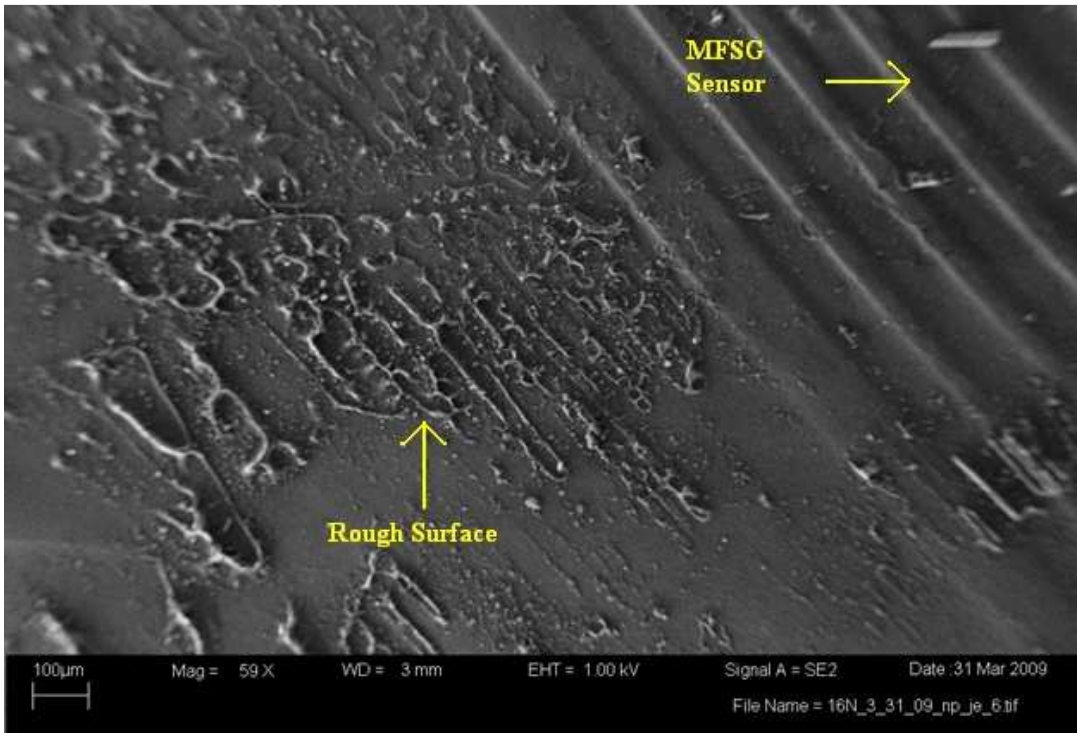

Figure 49. Embedded MFSG[48]

Figure 50 shows the 125 µm FO with an acrylate coating which underwent the nitric acid submersion process. The acrylate coating present on the outside of the FO is bonded well to the resin around it. This is evident in the fracture lines that propagate through the resin/acrylate boundary.

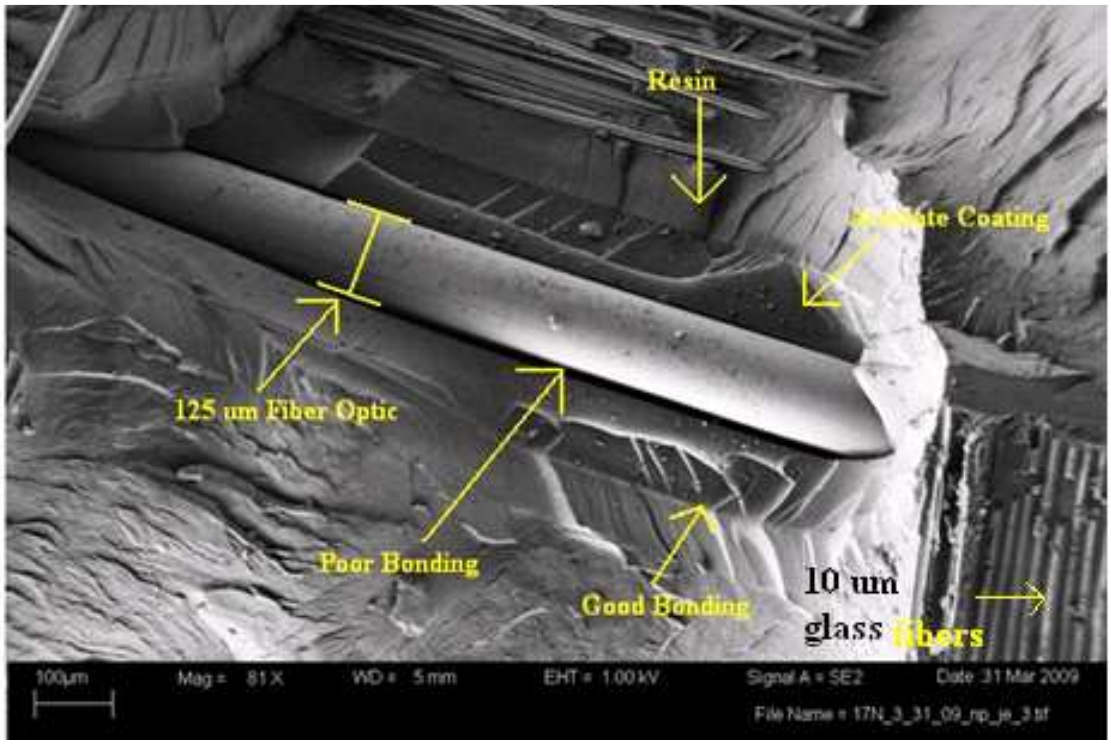

Figure 50. Embedded Fiber Optic[49]

The poor bonding evident in this photo is at the FO/acrylate surface. This brings up the issue of how well the strain through the fiberglass is transferred to the FO, and how sensitive are the FO in this configuration to field strains. Resolving this issue will take collaboration between the FO manufacturers and their end users.

CONCLUSIONS FOR HEALTH MONITORING

The sensors that were modified with submersion in the 20% nitric acid solution for ten seconds bonded better to the fiberglass laminate. Installation tips and practices are outlined in Tables 10. These practices are for new construction only.

Table 10. Conclusions for Sensor Embedding

Sensor	Cleaning Method	Sensor Surface conditioning	Instillation practices
Fiber Optics	Wash with Isopropyl alcohol	submerge in 20% by weight solution of nitric acid	Cover in PVC sheathing material everywhere except gage length of the sensor. Take care not to bend past minimum bend radius.
MFSG	Wash with Isopropyl alcohol	submerge in 20% by weight solution of nitric acid	Spray with tacky glue in order to keep the sensor in place while laying up the fiberglass. Make sure the lead wires inside the layup do not touch.
PVDF	Wash with Isopropyl alcohol	submerge in 20% by weight solution of nitric acid	Spray with tacky glue in order to keep the sensor in place while laying up the fiberglass. Inspect sensor for to much etching of the PVDF's exterior
Humidity	Wash with Isopropyl alcohol and let air dry	No conditioning needed	Affix to inside of blade with HySol
Temperature (Thermocouple)	Wash with Isopropyl Alcohol	submerge in 20% by weight solution of nitric acid	Affix to inside of blade with HySol
Accelerometers	Wash with Isopropyl alcohol and let air dry	No conditioning needed	Affix to inside of blade with HySol

PROJECT CONCLUSIONS

The test beds were manufactured successfully. Blade test bed needs few modifications to be placed in a wind tunnel for validation of TCFD calculations. False wall flaps are easy to manufacture and potentially provide the same benefit with less manufacturing costs and steps. The steps for retrofitting a blade with a false wall flap are discussed below.

- Take the turbine out of commission and detach the rotor hub/blades from the tower and place it on the ground.
- Unbolt the blades from the rotor hub and place them in a form onsite with the trailing edge pointed down.
- Place in the pipe along the trailing edge. This step will have to be done very carefully due to the close quarters inside the blade. Tooling would have to be used to lay the pipe in the correct place and to epoxy the pipe into place. The pipe should have no holes drilled in it at this stage of the process due to the imperfect nature of this process.
- Take an image with acoustic emission or x-ray of the trailing edge of the blade. This imagery is used to determine the specific location of the epoxied pipe. The pipe itself can be PVC or some other polymer, metal should be avoided due to corrosion and differing coefficients of thermal expansion. The amount of epoxy will have to be regulated as to not add to much weight to the blades, also the blades themselves will have to remained balanced after this process.
- Drill holes at appropriate locations through the blade, epoxy that is holding the pipe in place, and the pipe itself. De-burring of the holes must be done on the inside and outside.
- Install the compressor, reservoir tank, and control system into the rotor hub.
- Stab the blades back into the rotor hub and hook up the hoses in the blades to the control system in the rotor hub.

- Test the system whilst still on the ground and make sure its functioning properly.
- Fly the rotor hub/blades back into the air and onto the tower.
- Test the system while it is installed on the tower.

The steps for retrofitting a blade with a Gurney flap can be seen below. There is a large amount of material to be removed and modified. The modifications come in the form of supports which need to be epoxied back into place, and fitting of active control hardware. Due to all of the steps being outlined but not fully analyzed in terms of cost of labor and materials, the retrofitting of deployed blades with Gurney flaps needs to be investigated further but is presently not recommended.

- Take the turbine out of commission and detach the rotor hub/blades from the tower and place it on the ground.
- Unhook the blades from the rotor hub and place them in a form onsite with the low pressure side facing up.
- Using a chalk line and pattern mark out of the blade surface the material to be removed.
- With a worm drive saw and appropriate diamond coated cutting wheel remove the marked material. Be sure to use a mixture of lubricant such as water and a slow cutting speed like 10 in/min in order to keep the temperature of the blade to a reasonable level and not burn the material being cut. Thicker sections will have to be cut at a slower feed rate, like 4 in/min for 2 inch thick sections. This cutting will have to be done to within an accuracy of 0.25 inches
- Once the material is removed a reinforcing shear web will have to be installed. This shear web will span from the top of the low pressure side to the inside of the high pressure side. This shear web will have to be epoxied into place.
- The mounting points for the hardware will have to be installed. Using a predetermined pattern mark the locations of mounting points and drill through the material. A hole through the added shear web will have to be cut, this hole

will have to line up with the rest of the mounting hardware within 1/8th of an inch.

- The mounting points will have to be countersunk and backfilled in order to maintain the blades profile. The mounting points should be fit tightly and multiple checks should be made to ensure proper alignment and square in relation to the other mounting points.
- When the mounting points are secure and the shear web is cured the hardware can be installed. If manufacturing up to this point has been done with sufficient quality, the hardware installation should be a fairly smooth operation. The actuators, flap, and actuator lines should fit relatively easily within the design of the retrofitted blade.
- Install the necessary hardware into the rotor hub.
- Stab the blades back into the rotor hub and hook up the actuator lines in the blades to the control system in the rotor hub.
- Test the system while still on the ground and make sure it is functioning properly.
- Fly the rotor hub/blades back into the air and onto the tower.
- Test the system while it is installed on the tower.

The process for embedding sensors into fiberglass laminates has gone through many iterations and a viable solution for ingress and egress of fiber optics has been found in the laboratory setting. The steps for successfully embedding MFSG and PVDF sensors into a laminate can be seen below.

- Clean samples with isopropyl alcohol.
- Submerge sample in 20% by weight solution of Nitric acid for ten seconds.
- Wash with water and let air dry.

- Mark on laminate where the sensor will be affixed and keep sensor in place with spray adhesive. Take great care to get the sensor in the proper orientation.
- Feed lead wires through ply's above the sensor surface, take care not to damage the tows in the ply.
- Cut ~1" by ~0.5" rectangles in the flow media and peel ply that the led wires will go through. Feed the wires through these rectangles.
- Cut slits in the vacuum bag and feed the wires though those slits.
- Seal the slits with tacky tape.
- Enclose the slit and extra lead wire in a second vacuum bag.

The following is a review of how to embed a Fiber Optics into a blade undergoing new construction.

- Clean gauge length of sensor with isopropyl alcohol. Make sure there is enough FO to make multiple splices if necessary.
- At the proper spot in the layup raster the FO back and forth in the proper location and in the proper direction. Keep the FO in place with spray glue.
- Thread a piece of protective PVC coating everywhere except the gauge length of the sensor.
- As the laminate is being completed be sure to thread the FO along with its protective sheath through each layer. Make sure never to exceed the minimum bend radius of the FO.
- Protect the extra FO and PVC protective sheath in its own secondary vacuum bag before resin transfer molding has begun.
- After curing, extract the laminate carefully being sure not to exceed the minimum bend radius of the FO.
- Affix the proper end to the FO and secure it for transport.

FUTURE WORK

False wall flap from high pressured air or combusting hydrogen should be studied further. This false wall flap also needs to be tested in a wind tunnel in a flat plate configuration and blade test bed configuration. Both blade and flat plate test beds need to be placed in wind tunnels for validation of Transitional Computational Fluid Dynamics results through the transient region of deployment. The current blade test bed is 26” long by 24” wide; this would fit well into a wind tunnel that has a 1 meter square cross section. This would allow for ample room in mounting the blade section and observing the effects of the flap on the airstream during the transitional region of deployment with an active gurney flap.

Correlate the results of the TCFD and wind tunnel tests with a more in-depth economic analysis of the manufacturing plans and construction overhaul for outfitting the blades with Gurney flaps.

Fiber Optics with fiber Bragg gratings need to be investigated more thoroughly. Fatigue testing of coupons with sensors imbedded is necessary. These tests with FO and fatigue testing should be done with carbon laminates also. Test with polyester resin need to be done. Testing for G1C values will be necessary in order to quantify the perturbment of sensors on mode 2 delamination.

Study how well the FO are bonded to the acrylate and polyimide coatings that protect them.

REFERENCES CITED

1. Grady, S.A., et al. *Placement of Wind Turbines using Genetic Algorithms.* s.l. : Elsevier Ltd., 2004.

2. Hau, Erich. *Wind Turbines.* Krailling, Germany : Springer, 2006.

3. —. *Wind Turbine, Fundamentals, Application, Economics 2nd Edition.* Krailling Genrmany : Springer, 2006.

4. Walsh, John Evangelist. *One day at Kitty Hawk.* New york : Thomas Y. Crowell Company, 1975.

5. Hoffman, paul. *Wings of Madness: Alberto Santos-Dumont and the Invention of Flight.* s.l. : Hyperion, 2003.

6. *Hydraulics on-board the A380.* Gannon, MC. s.l. : Hydraulics & Pneumatics, 2005, Vol. 6.

7. Lobitz, Veers, Eisler, Laino, Migliore, Bir. *The use of Twist-Coupled blades to Enhance the Performance of Horizontial Axis Wind Turbines.* Albequerque : Sandia Report, 2001.

8. Zaparka. *Aircraft and control Thereof. 1893065* United States Patent office, January 1, 1935.

9. *Design of subsonic Airfoils for High Lift.* liebech, Robert H. s.l. : Journal of Aircraft, 1978, Vol. 8.

10. *Pitch-Controlled Variable-Speed Wind Turbine Generation.* Eduard, Muljadi and Butterfield, C.P. 1, s.l. : IEEE Transactions on Industrial Applications, 2001, Vol. 37.

11. Aizerman, M.A. *Pneumatic and Hydraulic Control System.* Oxford : Pergamon Press, 1968.

12. Bianchi, De Battista, Mantz. *Wind Turbine Control System.* London : Springer-Verlag, 2007.

13. Roulston, Kaplan, Hardenberg, Smith. *Using medium-range Weather Forecasts to Improve the value of Wind Energy Production.* London : Elsevier Science, 2002.

14. Walters, R.B. *Hydraulics and Electro-Hydraulic Control Systems.* New York : Elseviers Science Publishers LTD, 1991.

15. Corrado, F. Ratto, Giovanni, Solari. *Wind Energy and Landscape.* Rotterdam : A.A. Balkema, 1998.

16. Lubosny, Z. *Wind Turbine Operation in Electric Power Systems.* Gdansk, Poland : Springer, 2003.

17. *The Piezoelectricity of Polyvinyldene Fluoride.* Kawai, H. 6, Tokyo : Japanese Journal of applied Physics, 1969, Vol. 8.

18. Mandell, Cairns, Samborsky. *Fatigue of Composite Materials and Substructures for Wind Turbine Blades.* Bozeman, MT : Sandia Nat. Labs, 2002.

19. All, Jorgensen et. *Full Scale Testing of Wind Turbine Blade to Failure-Flapwise Loading.* Roskilde : National Laboratory, 2004.

20. *Scanning Doppler LIDAR Measurments for Wind Energy Applications.* Frehlich, R. Kelley. Fall Meeting : North American Geophysical Union, 2008.

21. Wagner, Bareib, Guidati. *Wind Turbine Noise.* Stuttgart, Germany : Springer, 1996.

22. *Photosensitivity in Optical Fiber Waveguides: Application to Reflection filter fabrication.* Hill, K.O., et al. s.l. : Applied Physics , 1978, Vol. 32.

23. *Fiber Bragg Grating Technology Fundamentals and Overview.* Hill, K.O. et. All. s.l. : Journal of Lightwave Technology, 1997.

24. Van Bussel, G.J.W. and Zaaijer, M.B. *Reliability, Availability and Maintenance aspects of Large-Scalse offshore wind farms.* Rottordam : Siegler, 2001.

25. Rumsey, Mark A. and Paquette, Joshua A. *Structural Health Monitoring of Wind Turbine Blades.* Albuquerque, NM : Sandia National Laboratories, 2008.

26. Rupali, et al. *Optics and Laser Technology.* s.l. : Elsevier, July 2008.

27. Kersay, A.D., Berkoff, T.A. and Morey, W.W. *Multiplexed Fiber Bragg Grating Strain Sensor System with a Fiber Fabry-Perot Wavelength Filter.* Washington D.C. : NRL, 1993.

28. Bogue, Robert. *UK Start-up poised to take the Fiber Optic Sensor Market by Storm.* s.l. : Sensor Review , 2005.

29. Doyle, Crispin. *Fiber Bragg Grating Sensors-An introduction to Bragg Gratings and Interrogation Techniques.* s.l. : Smart Fibres Ltd, 2003.

30. Kasap, Safa. *Thermoelectric Effects in Metals: Thermocouples.* s.l. : Web-Materials, 2001.

31. *The Theory and Properties of Thermocouple Elements.* Pollock, D.D. Philidelphia, PA : ASTM Special Technical Publication, 1971, Vol. 492.

32. A., Buck John. *Fundamentals of Fiber Optics.* Atlanta, Georgia : Wiley, 2004.

33. Cairns, Douglas Scott, Palmer, Nathan and Ehresman, Jon. *Low Cost Inspection for Improved Wind Turbine Blade Reliability.* Bozeman : AIAA, 2009.

34. *Wind Turbine Technology.* Rumsey, Mark. Bozeman, MT : Sandia National labs, 2007.

35. Lobitz, Don W. and Veers, Paul S. *Areolastic Behavior of Twist-coupled HAWT Blades.* Albuquerque : American Institute of Aeronautics and Astronautics, 1998.

36. Brien, Glenn C. *Control of CNC machine tools. 36447428* United States, June 7, 1995.

37. Navarro, Robert. *Performance of an Electro-Hydrostatic Actuator on the F-18 Systems Research Aircraft.* Edwards : NASA, 1997. NASA/TM-97-206224.

38. *System on Chip Signal Conditioner for LVDT sensors.* A., Drumea, et al. 1, Bucharest : Electronics System-Integration Technology Conference, 2006, Vol. 1. 1-4244-0552-1.

39. Unser, Bobby, Penske, Roger and Pease, Paul. *Winners are Driven.* St. Louis : Wiley, 1997.

40. Blockey, James Craig. *Feasibility in Developing Smart Structures.* Bozeman : Montana State University, 2008.

41. LM Glasfiber. lmglasfiber. *www.lmglasfiber.com.* [Online] LM Glasfiber, March 3, 2009. http://www.lmglasfiber.com/Products/Wing%20Overview/2000-5000/LM%2061.5.aspx.

42. *Effects of Moisture and Temperature ont he Tensile Strength of Composite Materials.* Shen, Chi-Hung and Springer, George S. 1, Ann Arbor : Journal of Composite Materials, 1977, Vol. 11.

43. Omega. WWW.omega.com. *http://www.omega.com/techref/press-trans.html.* [Online] Omega. [Cited: 3 13, 2009.] http://www.omega.com.

44. Steinchen, Wolfgang and Yang, Lianxiang. *Digital Shearography.* Bellingham Washington : SPIE Press, 1989.

45. Harrison, Robert, Hau, Erich and Snel, Herman. *Large Wind Turbines Design and Economics.* West Sussex : Wiley, 2000.

46. Energy, Northwestern. http://rates.northwesternenergy.com/residentialelectricrates.aspx. *Northwestern Energy.* [Online] July 8, 2009. http://rates.northwesternenergy.com.

47. AWEA. http://www.awea.org/standards/iec_stds.html#WG123. *American Wind Energy Association* . [Online] July 8th, 2009. http://www.awea.org.

48. MOOG. http://www.polysci.com. [Online] MOOG component group, July 8, 2009. http://www.polysci.com/docs/AC7008SlipRingDtS.pdf.

49. *Low Cost Inspection for Improved Blade Reliability.* Cairns, Dr. Doug. Bozeman : Montana State University, 2009.

50. Carr, McMaster. http://www.mcmaster.com. *http://www.mcmaster.com/#.* [Online] McMaster Carr, July 12, 2009.

51. Rambo, Robert D. *Gun Bore Cleaning System. 5815975* United States Patent, Oct. 6, 1998.

52. Mathew, Sathyajith. *Wind Energy Fundamentals, Resoutce Analysis and Economics.* Tavanur : Springer, 2006.

53. Kong, C., Bang, J. and Sugiyama, Y. *Structural Investigation of composite wind turbine blades considering various load cases and fatigue life.* Gwangju : elsevier, 2005.

54. Goeij, WC De, Van Tooren, MJL and Beukers, A. *Implimentation of bend-torsion coupling in the design of a wind-turbine rotor-blade.* New York : Elsevier, 1999.

55. Michael Mohaghegh. *Evolution of Structures Design Philosophy and Criteria.* Palm Springs, CA : AIAA, 2004. AIAA 1004-1785.

56. Udd, Eric, et al. *Multidimensional strain field measurments using fiber optic grating sensors.* Fairview : Blue Road Research, 2000.

57. Mark Rumsey. *Wind Energy Technology presentation.* [Power point presentation] Albuquerque, NM : Sandia National Laboratories, Sandia National Laboratories , 2007.

58. Dynamics, Dantec. http://www.dantecdynamics.com/. *http://www.dantecdynamics.com/Default.aspx?ID=673.* [Online] dantec dynamics, july 29, 2009. http://www.dantecdynamics.com/.

59. Palmer, Nathan. *Smart Composites Evaluation of Embedded Sensors in Composite Materials.* Bozeman : Montana State university, 2009.

LIST OF FIGURE REFERANCES

1. http://www.fear-of-flying.us/web_images/flaps-slats-747.jpg

2. Wind Turbine Technology. Rumsey, Mark. Bozeman, MT : Sandia National labs, 2007.

3. Blockey, James Craig. Feasibility in Developing Smart Structures. Bozeman : Montana State University, 2008.

4. Blockey, James Craig. Feasibility in Developing Smart Structures. Bozeman : Montana State University, 2008.

5. http://www.drysdalewindfarm.com/images/nacelle.gif

6. http://www.windpowerninja.com/wp-content/uploads/2009/02/texas-wind-farm.jpg

7. Image taken from solidworks file June 2009.

8. Image taken of flat plate test bed May 2007.

9. Image taken of blade test bed in August 2008.

10. Image taken of side of blade test bed in August 2008.

11. Image taken of top of Gurney flap in August 2008.

12. Image taken of rear mounting points in August 2008.

13. Image taken of smoothed over mounting holes in August 2008.

14. http://images.google.com/imgres?imgurl=http://www.aircraftresourcecenter.com/Stories1/001-100/0016_A-10-battle-damage/01.jpg&imgrefurl=http://www.aircraftresourcecenter.com/Stories1/001-100/0016_A-10-battle-damage/

15. http://www.omega.com/Pressure/images/ROSETTES_PREWIRED_STRAIN_KFG_l.jpg

16. http://images.google.com/imgres?imgurl=http://www.play-hookey.com/dc_theory/images/wheatstone_bridge.gif&imgrefurl=http://www.play-hookey.com/dc_theory/wheatstone_bridge.html&usg=__Q35NXFsicxVrOgrf3401O8qu6Yg=&h=200&w=200&sz=2&hl=en&start=8&tbnid=l-cPj1hmm5palM:&tbnh=104&tbnw=104&prev=/images%3Fq%3Dwheatstone%2Bbridge%26gbv%3D2%26ndsp%3D18%26hl%3Den%26sa%3DN

17. http://www.mrfiber.com/images/fiber-history-02.gif

18. http://images.google.com/imgres?imgurl=http://content.answers.com/main/content/img/CDE/CLADDING.GIF&imgrefurl=http://www.answers.com/topic/fiber-optics-glossary&usg=__7i_sxN8DWDzQsRs6x3FOTOYLwYQ=&h=567&w=447&sz=9&hl=en&start=2&tbnid=Ua-EqMNXJC4zfM:&tbnh=134&tbnw=106&prev=/images%3Fq%3Dcore%2Band%2Bcladding%26gbv%3D2%26hl%3Den%26sa%3DG

19. Fiber Bragg Grating Technology Fundamentals and Overview. Hill, K.O. et. All. s.l. : Journal of Lightwave Technology, 1997.

20. Fiber Bragg Grating Technology Fundamentals and Overview. Hill, K.O. et. All. s.l. : Journal of Lightwave Technology, 1997.

21. Fiber Bragg Grating Technology Fundamentals and Overview. Hill, K.O. et. All. s.l. : Journal of Lightwave Technology, 1997.

22. Wagner, Bareib, Guidati. Wind Turbine Noise. Stuttgart, Germany : Springer, 1996.

23. All, Jorgensen et. Full Scale Testing of Wind Turbine Blade to Failure-Flapwise Loading. Roskilde : National Laboratory, 2004.

24. Publication No.: PI-Q-810_09_01

25. Image of Fiber Optic Submerged in 20% nitric Acid solution taken August 2009

26. Image of sensor placement taken in February 2009

27. Image of Area Cut Out from Peel Ply and Flow Media taken January 2009

28. Image of slits sealed with tacky tape taken in January 2009

29. Image of second vacuum bag taken in July 2009.

30. Image of Aluminum protector tube taken in October 2008

31. Image of Fiber Optic with visual fault indicator taken in January 2009.

32. Image of side ingress of Fiber Optic signal and resulting perturbed laminate taken in January 2009.

33. Image of Fiber Optic signal ingress and egress through laminate taken in January 2009.

34. PVC covering all but the connector length taken in January 2009

35. Image of PVC sheath over Fiber Optic in laminate taken August 2009

36. Second Vacuum bag over Fiber Optics Image taken on October 2008

37. Image of Fiber Optic with Mechanical ends attached is taken in October 2008

38. http://www.xconomy.com/wordpress/wpcontent/images/2007/12/c3anemometer_640.jpg

39. http://www.onera.fr/news/images/2007-017-leosphere-lidar-eolienne2.jpg

40. Image of sensor blade Taken May 30 2008 by Mark Rumsey of Sandia National Labs.

41. Image of degraded acrylate coating taken June 3rd 2008.

42. Image of acrylate coating cleaned with isopropyl alcohol taken April 28th 2008

43. Image of Fiber Optic bonded poorly with acrylate coating taken on June 16th 2008

44. Image of PVDF film with silver ink flow taken on August 14th 2008

45. Image of poor bonding of epoxy to PVDF taken March 31st 2009

46. Image of good adhesion of epoxy to PVDF film taken March 31st 2009

47. Image of poor bonding to the surface of MFSG taken June 16th 2008

48. Image of embedded MFSG taken March 31st 2009

49. Image of Fiber Optic taken march 2009

APPENDICIES

APPENDIX A

RETROFIT OF EXISTING BLADES WITH GURNEY FLAPS

APPENDIX A

These pictures corresponding with retrofitting existing blades with Gurney Flaps are taken from a SolidWorks file.

- Step One: Take the turbine out of commission and detach the rotor hub/blades from the tower and place it on the ground.
- Step Two: Unhook the blades from the rotor hub and place them in a form onsite with the low pressure side facing up.
- Step Three: Using a chalk line and pattern mark out on the blade surface the material to be removed.
- Step Four: With a worm drive skill saw and appropriate diamond coated cutting wheel remove the marked material. Be sure to use a mixture of lubricant such as water and a slow cutting speed like 10 in/min in order to keep the temperature of the blade to a reasonable level and not burn the material being cut. Thicker sections will have to be cut at a slower feed rate, like 4 in/min for 2 inch thick sections. This cutting will have to be done to within an accuracy of 0.25 inch’s

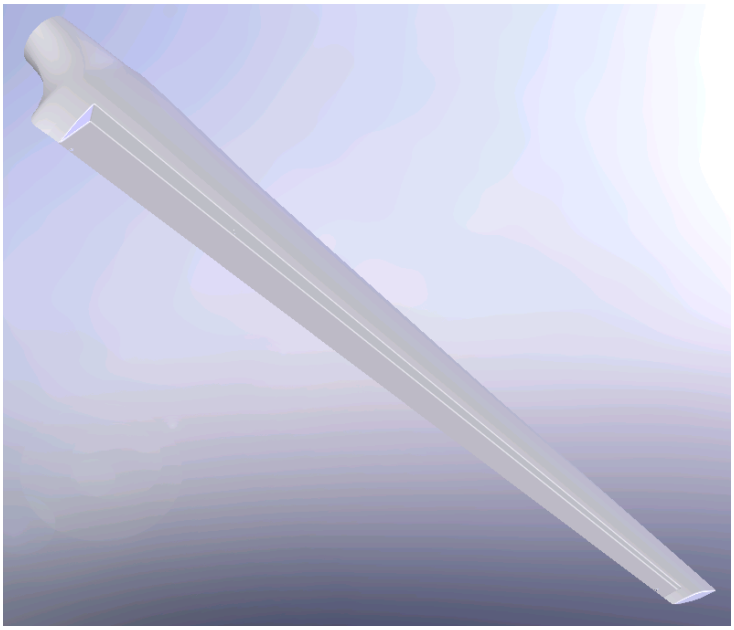

Figure 51. Wing with Material Removed for Gurney Flap

- Step Five: Once the material is removed a reinforcing shear web will have to be installed. This shear web will span from the top of the low pressure side to the inside of the high pressure side. This shear web will have to be epoxied into place.

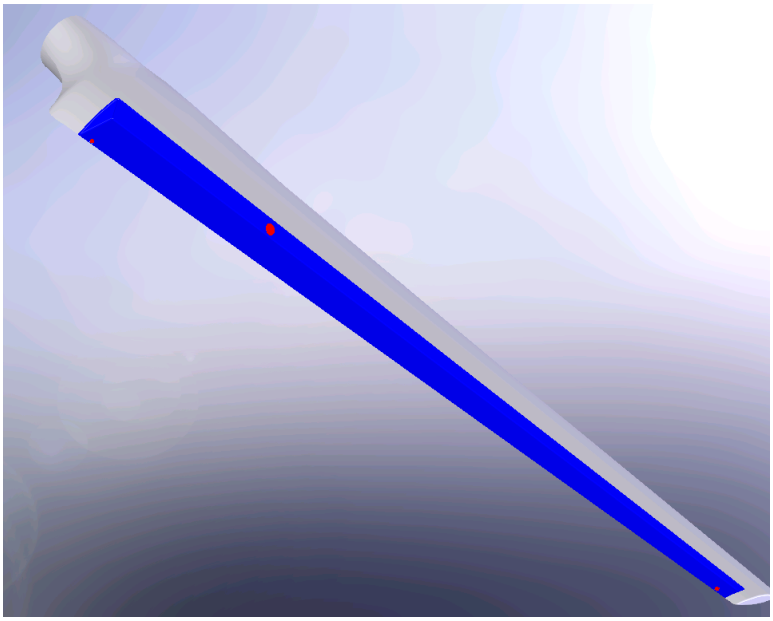

Figure 52. Shear web Epoxied Into place

- Step Six: The mounting points for the hardware will have to be installed. Using a predetermined pattern mark the locations of mounting points and drill through the material. A hole through the added shear web will have to be cut, this hole will have to line up with the rest of the mounting hardware within 1/8th of an inch.

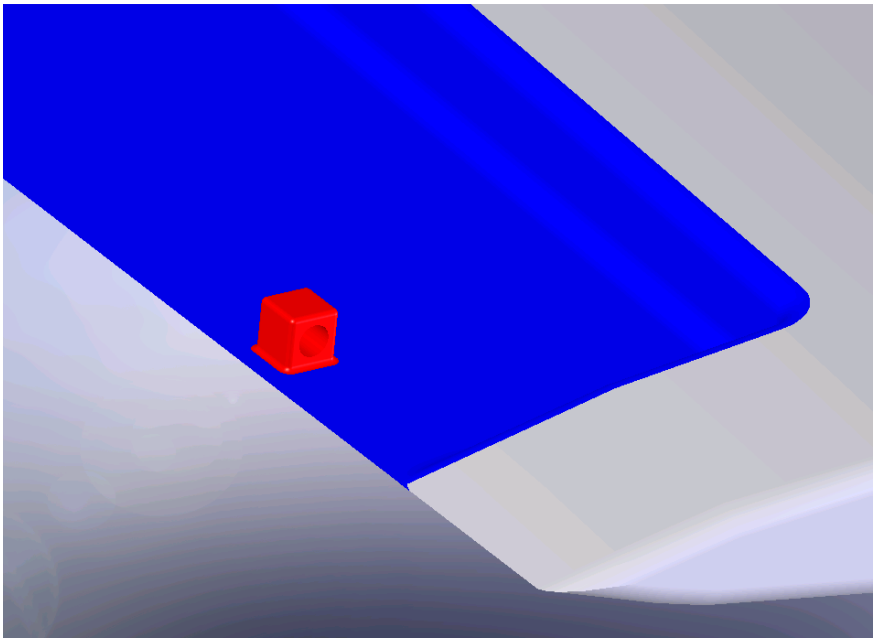

Figure 53. Mounting Points for Hardware

- Step Seven: The mounting points will have to be countersunk and backfilled in order to maintain the blades profile. The mounting points should be fit tightly and multiple checks should be made to ensure proper alignment and square in relation to the other mounting points.
- Step Eight: When the mounting points are secure and the shear web is cured the hardware can be installed. If manufacturing up to this point has been done with sufficient quality the hardware instillation should be a smooth operation. The electronic linear actuators, flap, and electrical lines should fit relatively easily within the design of the retrofitted blade.

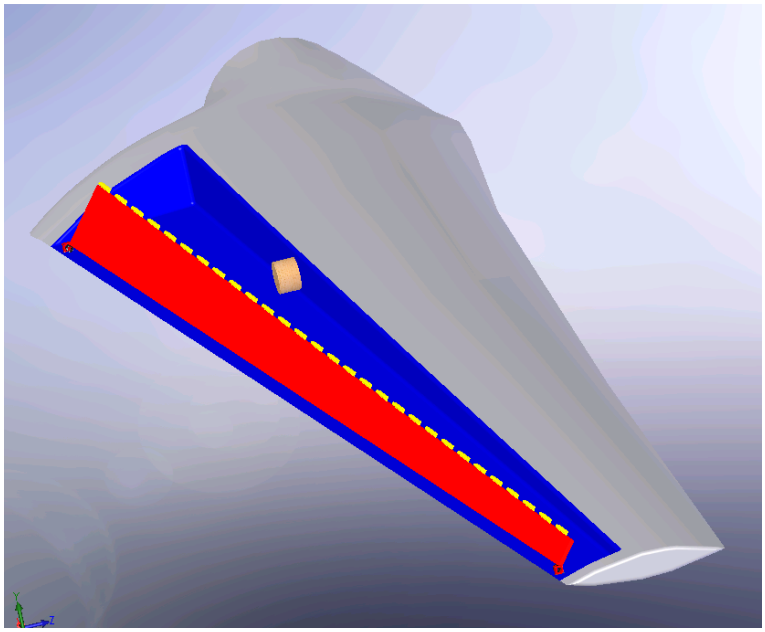

Figure 54. Instillation of Hardware into Blade

- Step Nine: Install the necessary relays and hardware into the rotor hub.
- Step Ten: Stab the blades back into the rotor hub and hook up the actuator's electrical lines in the blades to the control system in the rotor hub.
- Step Eleven: Test the system while still on the ground and make sure its functioning properly.
- Step Twelve: Fly the rotor hub/blades back into the air and onto the tower.
- Step Thirteen: Test the system while it is installed on the tower.

APPENDIX B

PARTS DRAWINGS OF FLAT PLATE TEST BED

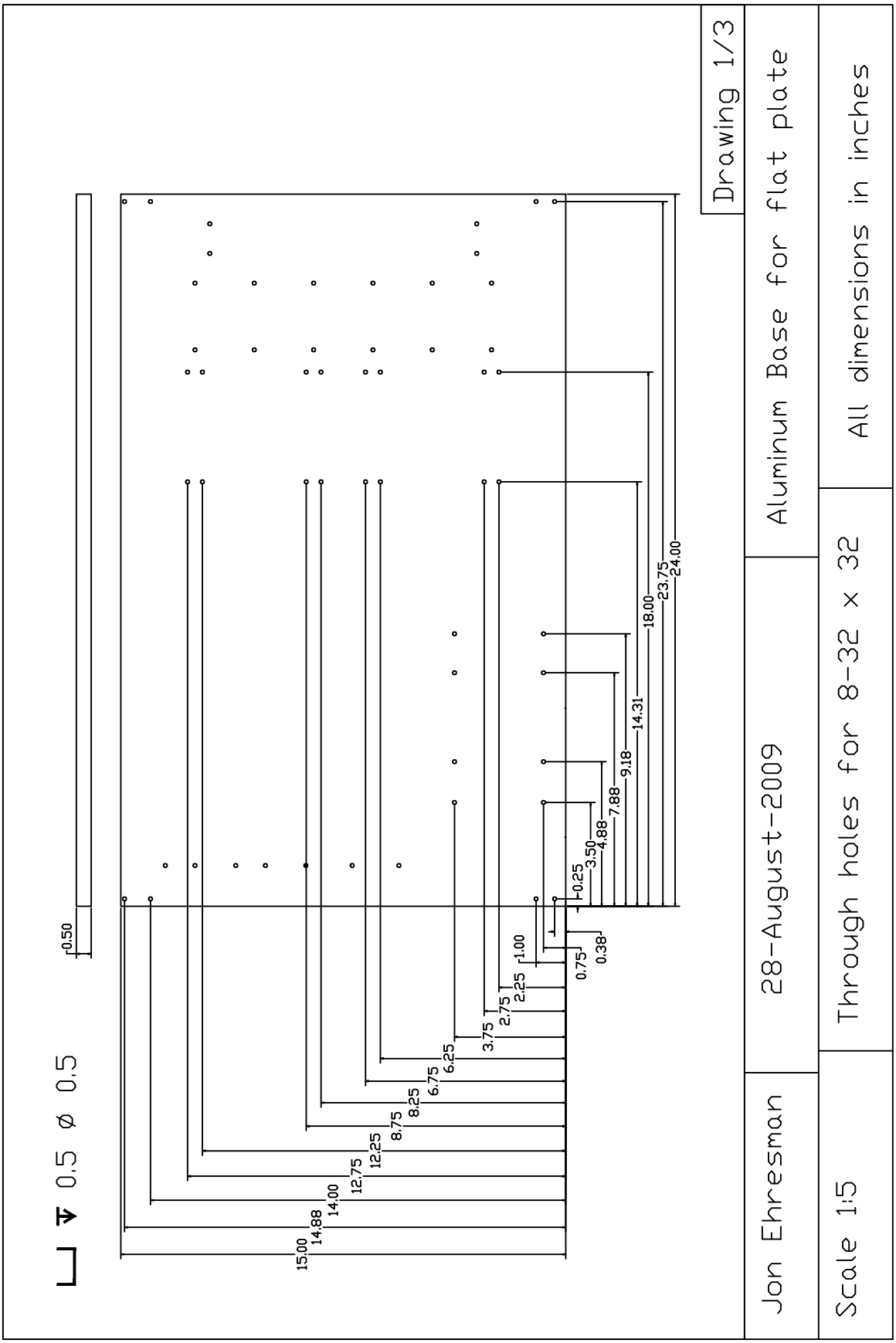
Drawing 1/3
Aluminum Base for flat plate
28-August-2009
Through holes for 8-32 x 32
All dimensions in inches
Jon Ehresman
Scale 1:5
0.5 ⌀ 0.5
0.50
0.25
0.38
0.75
1.00
2.25
2.75
3.50
3.75
4.88
6.25
6.75
7.88
8.25
8.75
9.18
12.25
12.75
14.00
14.31
14.88
15.00
18.00
23.75
24.00

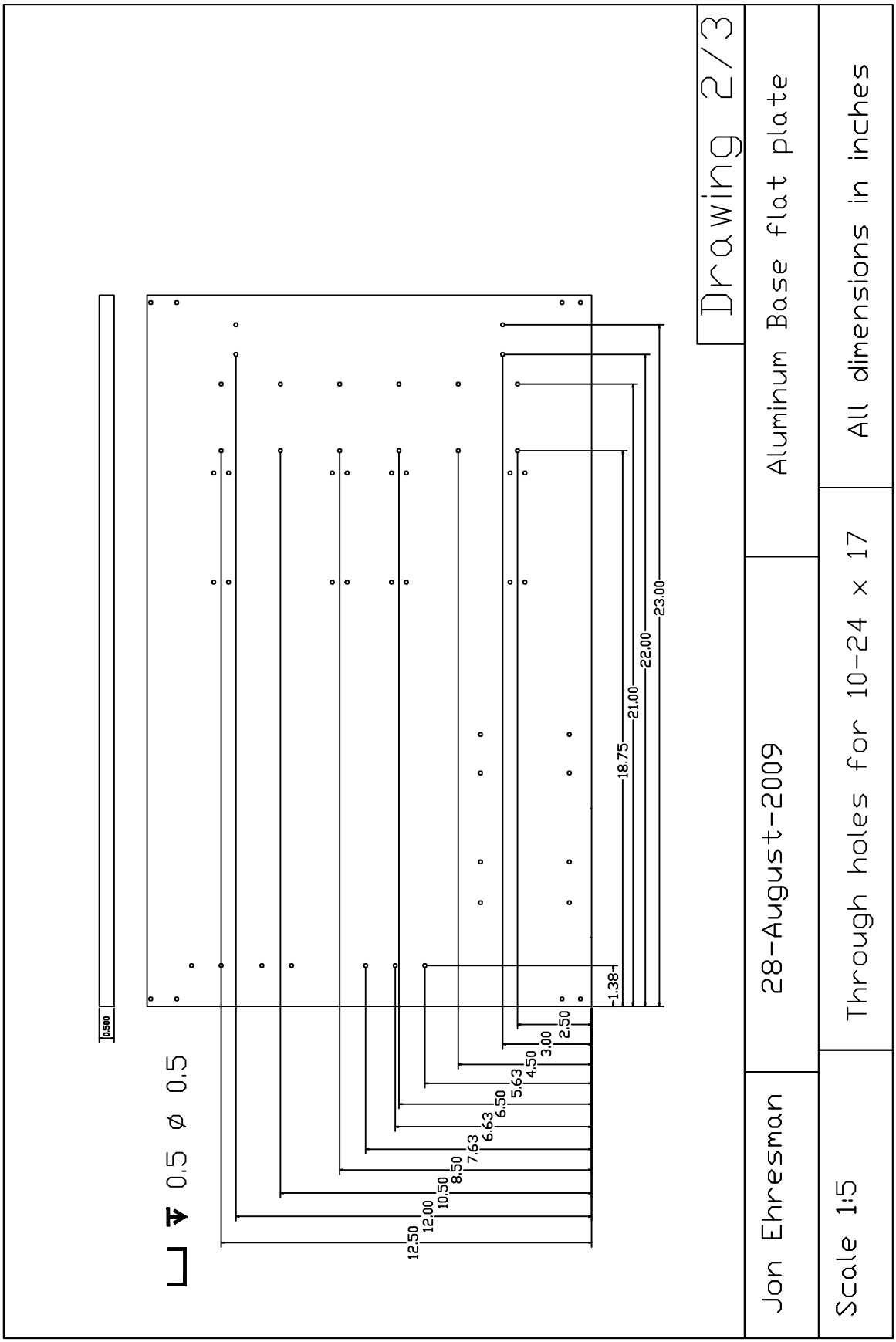
Drawing 2/3
Aluminum Base flat plate
All dimensions in inches
28-August-2009
Through holes for 10-24 x 17
Jon Ehresman
Scale 1:5
0.5 ⌀ 0.5
0.500
12.50
12.00
10.50
8.50
7.63
6.63
6.50
5.63
4.50
3.00
2.50
1.38
18.75
21.00
22.00
23.00

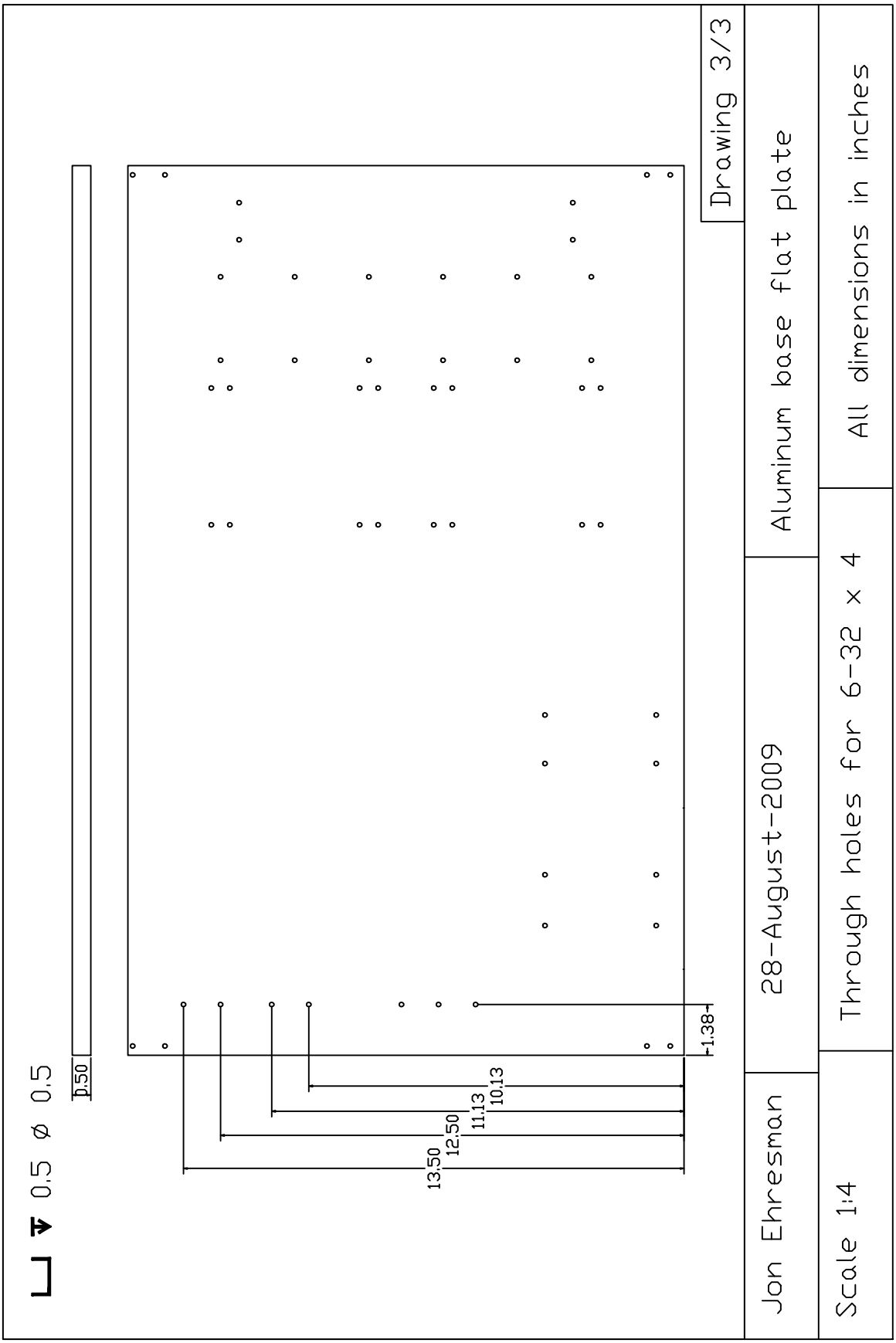
⌴ ↧ 0.5 ⌀ 0.5
0.50
13.50
12.50
11.13
10.13
1.38
Drawing 3/3
Aluminum base flat plate
28-August-2009
Jon Ehresman
Through holes for 6-32 x 4
All dimensions in inches
Scale 1:4

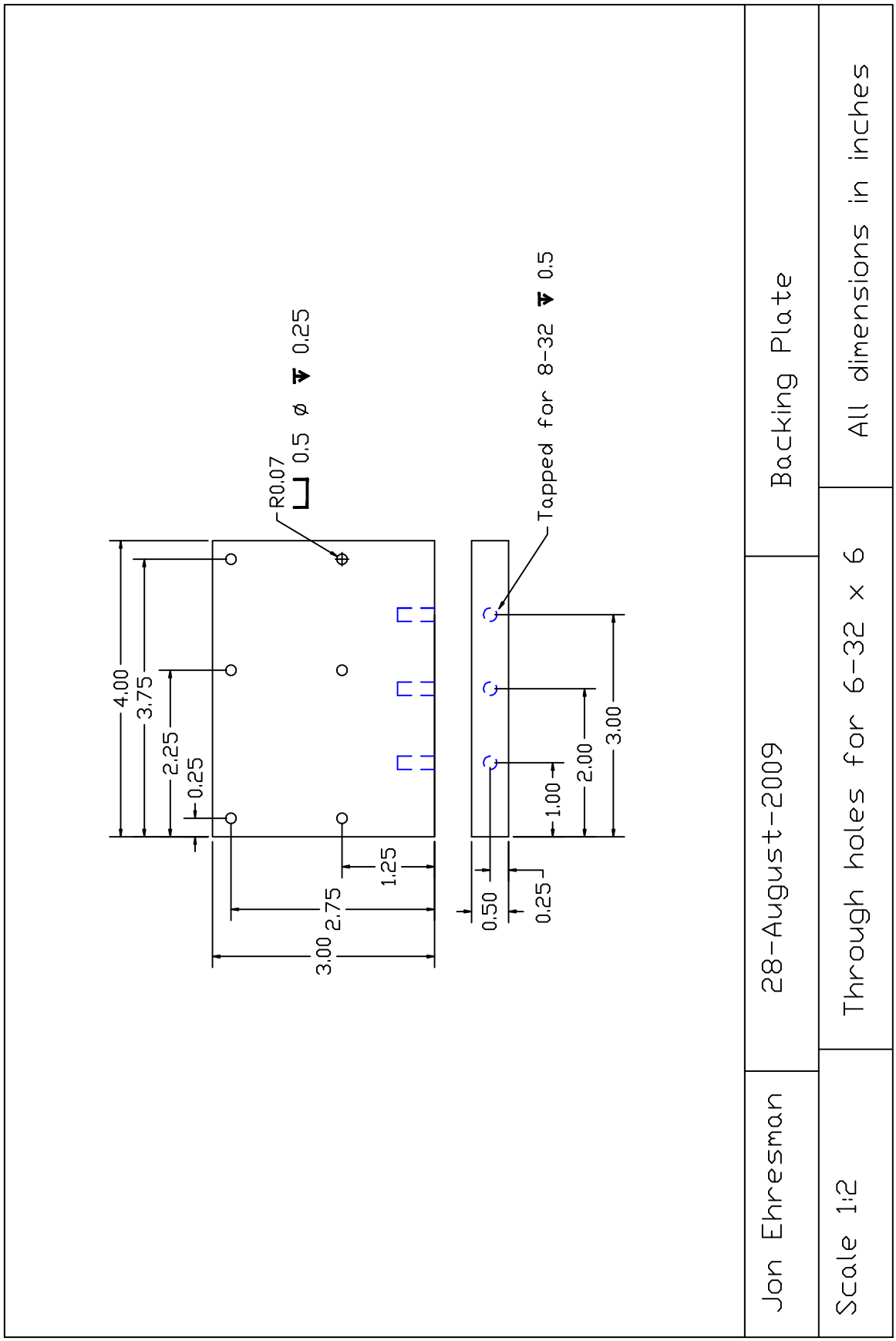
R0.07
0.5 Ø ⌖ 0.25
Tapped for 8-32 ⌖ 0.5
4.00
3.75
2.25
0.25
1.25
2.75
3.00
0.50
0.25
1.00
2.00
3.00
Jon Ehresman
28-August-2009
Backing Plate
Scale 1:2
Through holes for 6-32 x 6
All dimensions in inches

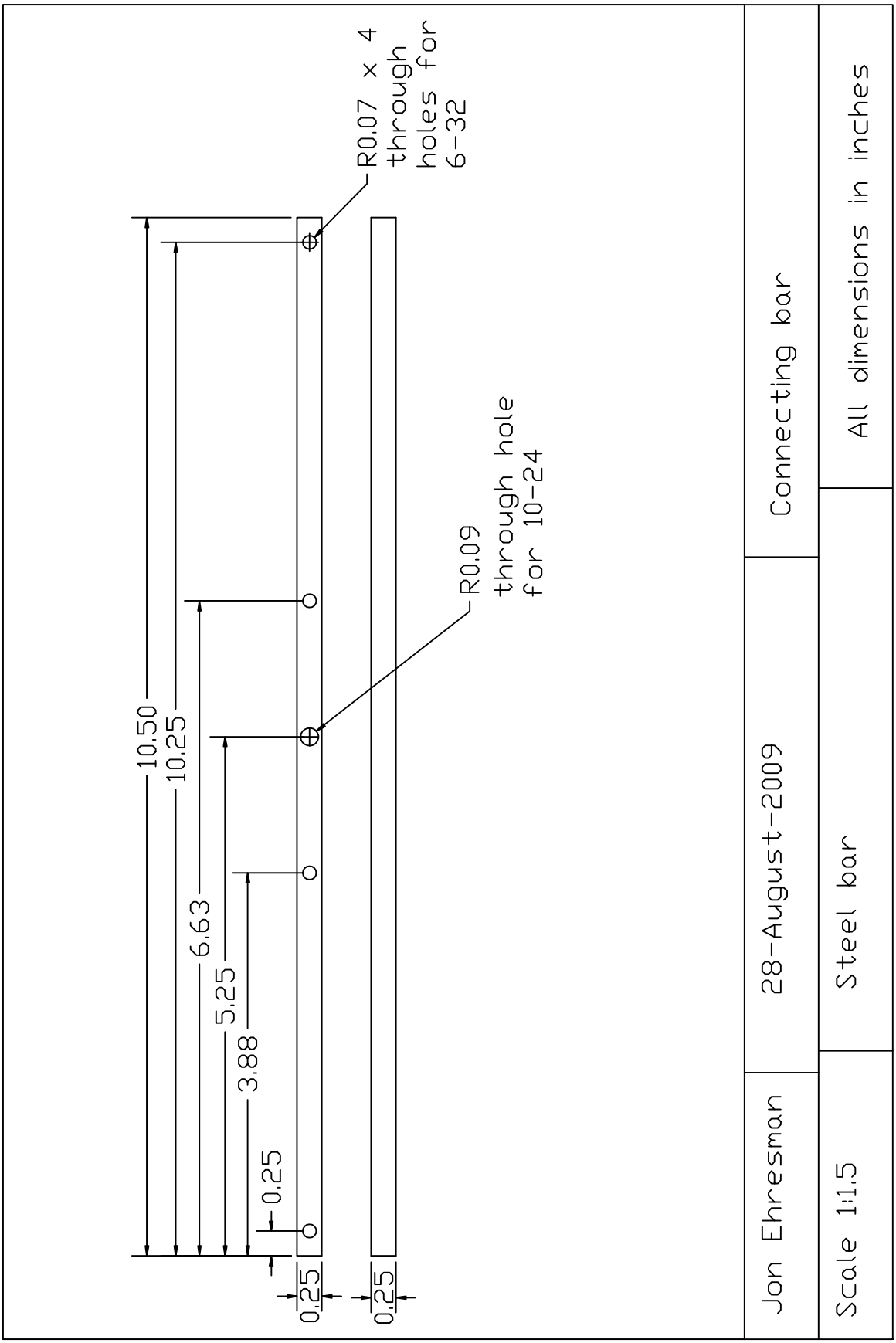
R0.07 x 4
through
holes for
6-32
R0.09
through hole
for 10-24
10.50
10.25
6.63
5.25
3.88
0.25
0.25
0.25
Connecting bar
28-August-2009
Steel bar
All dimensions in inches
Jon Ehresman
Scale 1:1.5

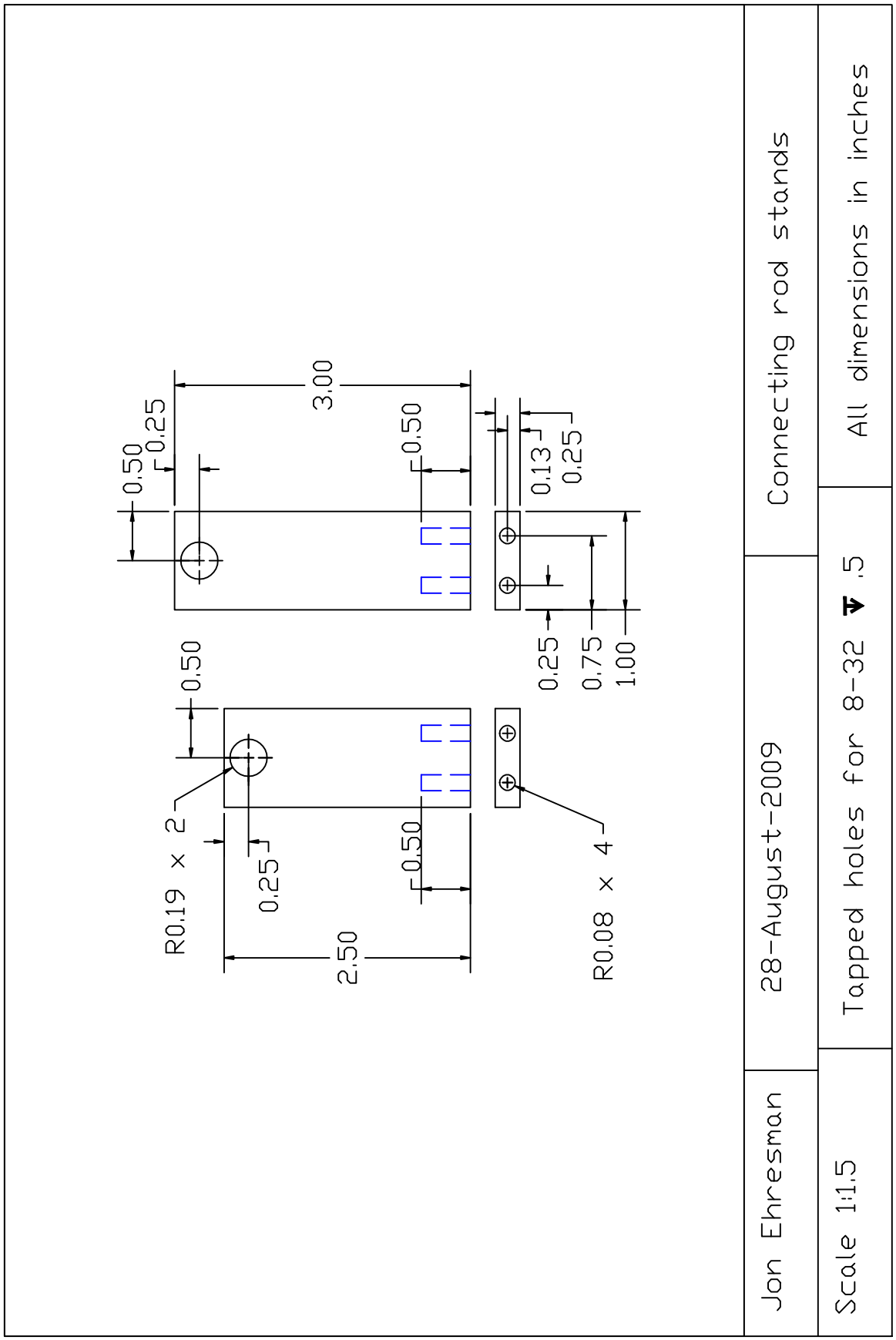
3.00
0.50
0.25
0.50
0.13
0.25
0.50
R0.19 x 2
0.25
0.50
2.50
0.25
0.75
1.00
R0.08 x 4
Connecting rod stands
28-August-2009
Jon Ehresman
Tapped holes for 8-32
All dimensions in inches
Scale 1:1.5

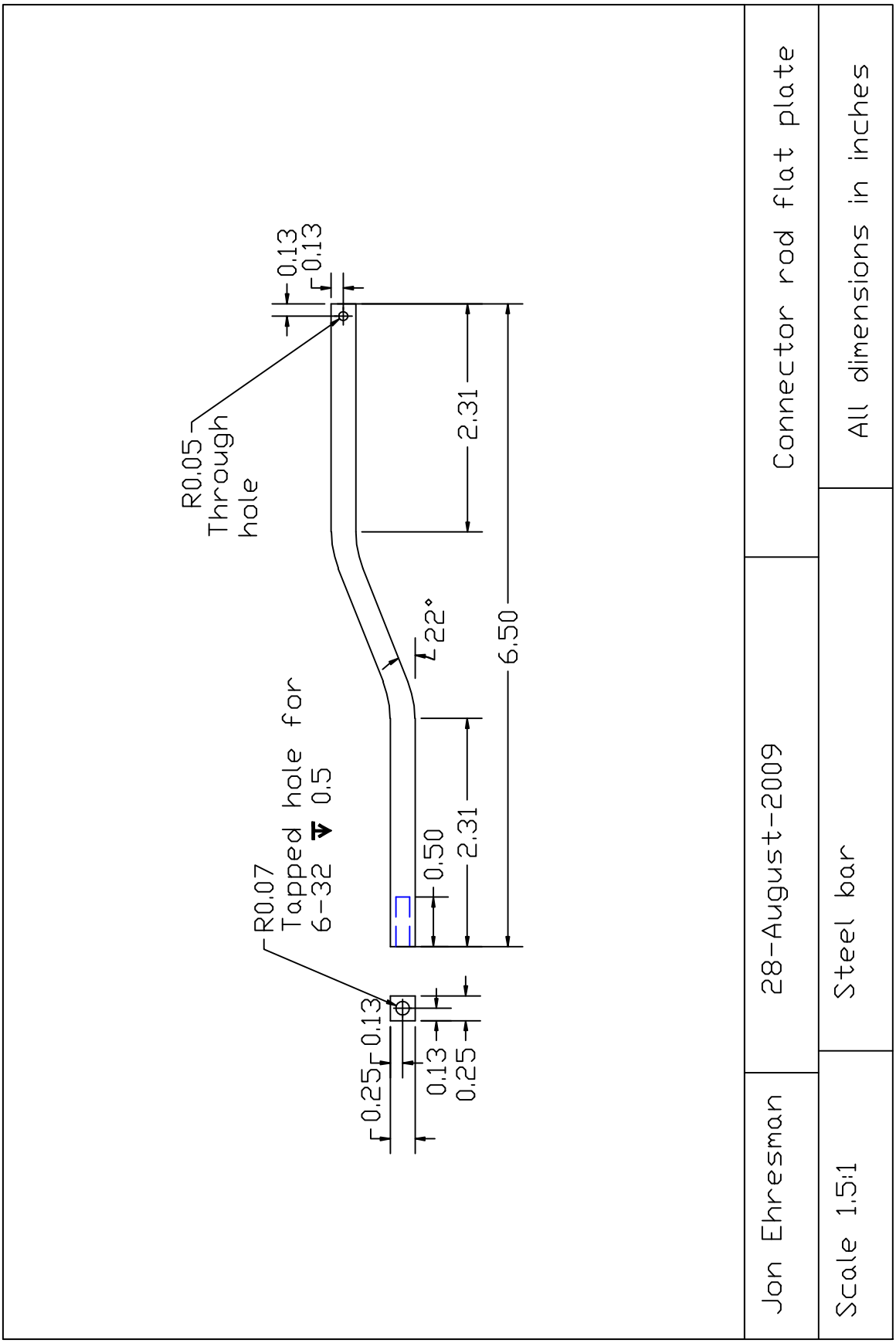
0.13
0.13
R0.05
Through
hole
2.31
22°
6.50
R0.07
Tapped hole for
6-32 ↧ 0.5
0.50
2.31
0.25
0.13
0.13
0.25
Jon Ehresman
28-August-2009
Connector rod flat plate
Scale 1.5:1
Steel bar
All dimensions in inches

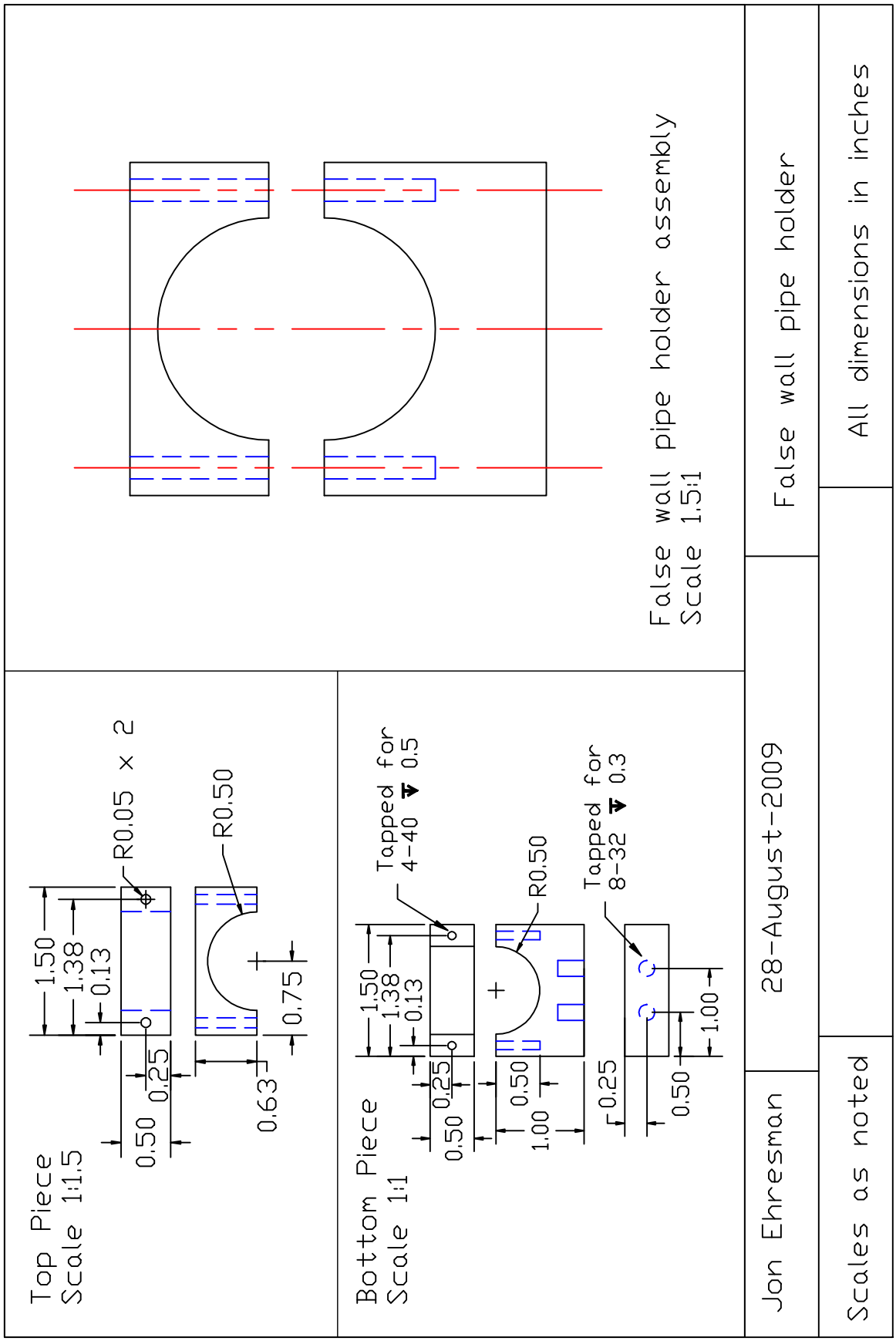
False wall pipe holder assembly
Scale 1.5:1
Top Piece
Scale 1:1.5
1.50
1.38
0.13
R0.05 x 2
R0.50
0.50
0.25
0.63
0.75
Bottom Piece
Scale 1:1
Tapped for
4-40 ↧ 0.5
Tapped for
8-32 ↧ 0.3
R0.50
1.50
1.38
0.13
0.50
0.25
0.50
1.00
0.25
0.50
1.00
Jon Ehresman
28-August-2009
False wall pipe holder
Scales as noted
All dimensions in inches

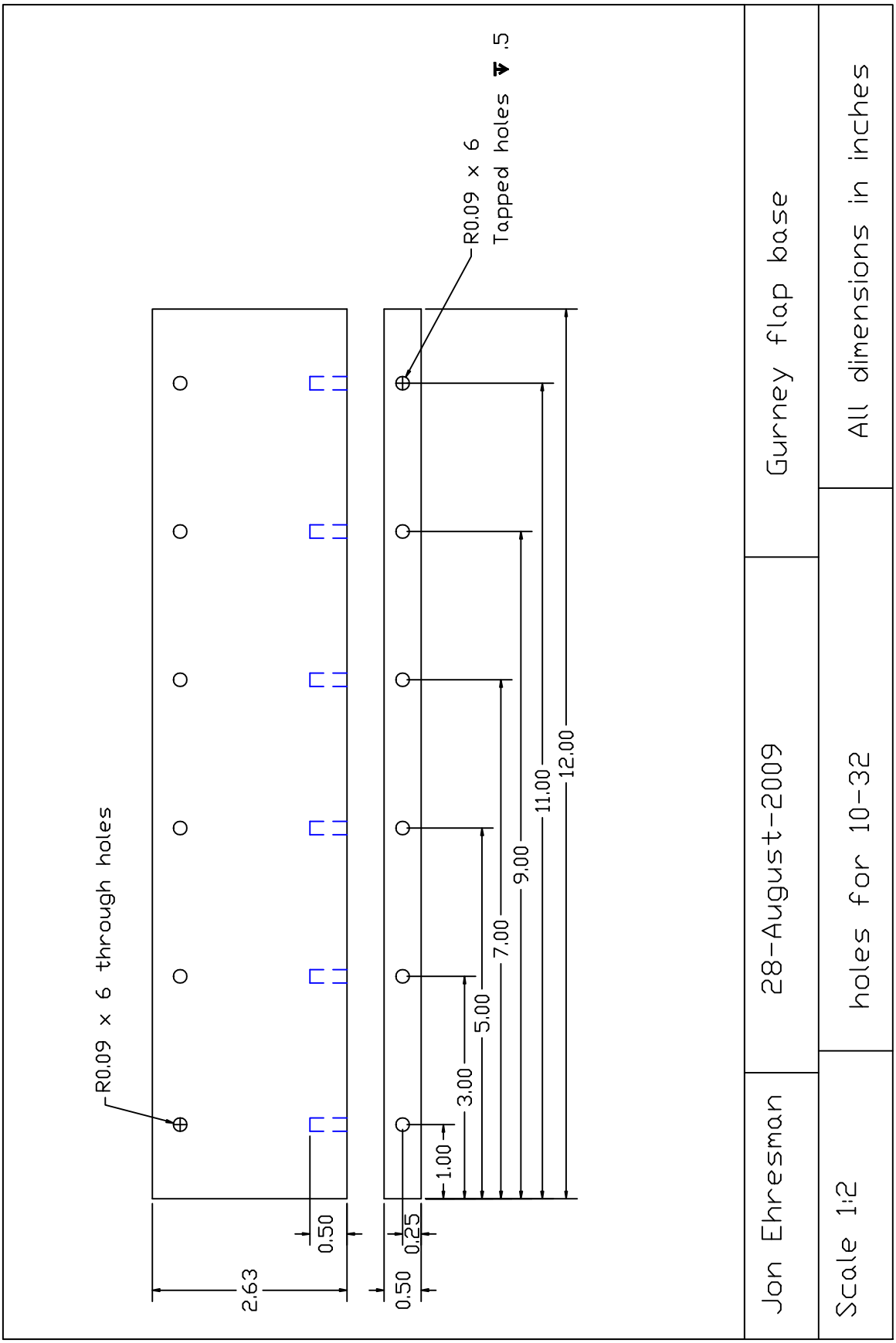
R0.09 x 6 through holes
R0.09 x 6
Tapped holes ↧.5
2.63
0.50
0.25
0.50
1.00
3.00
5.00
7.00
9.00
11.00
12.00
Gurney flap base
Jon Ehresman
28-August-2009
All dimensions in inches
Scale 1:2
holes for 10-32

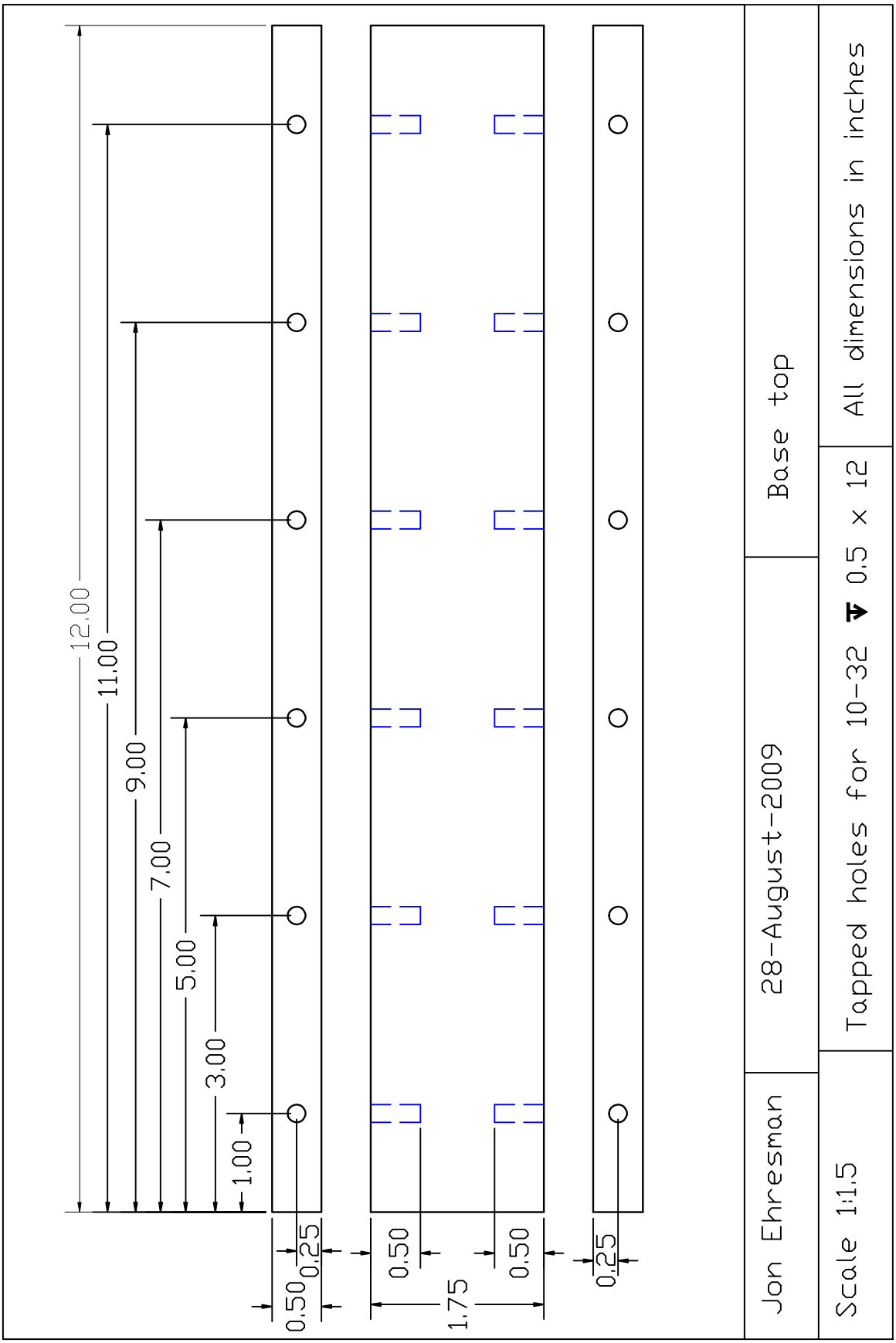
12.00
11.00
9.00
7.00
5.00
3.00
1.00
0.50
0.25
0.50
1.75
0.50
0.25
Jon Ehresman
28-August-2009
Base top
Scale 1:1.5
Tapped holes for 10-32 ↧ 0.5 x 12
All dimensions in inches

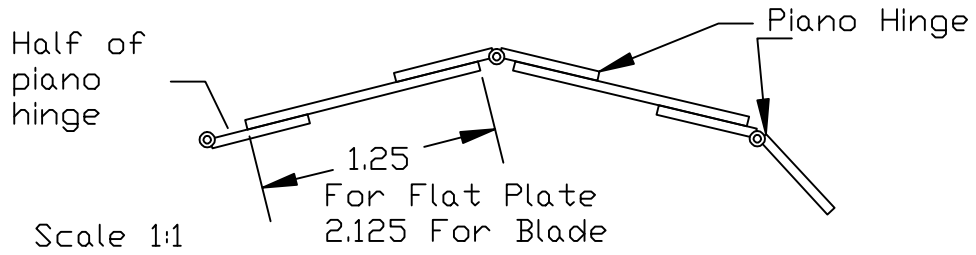

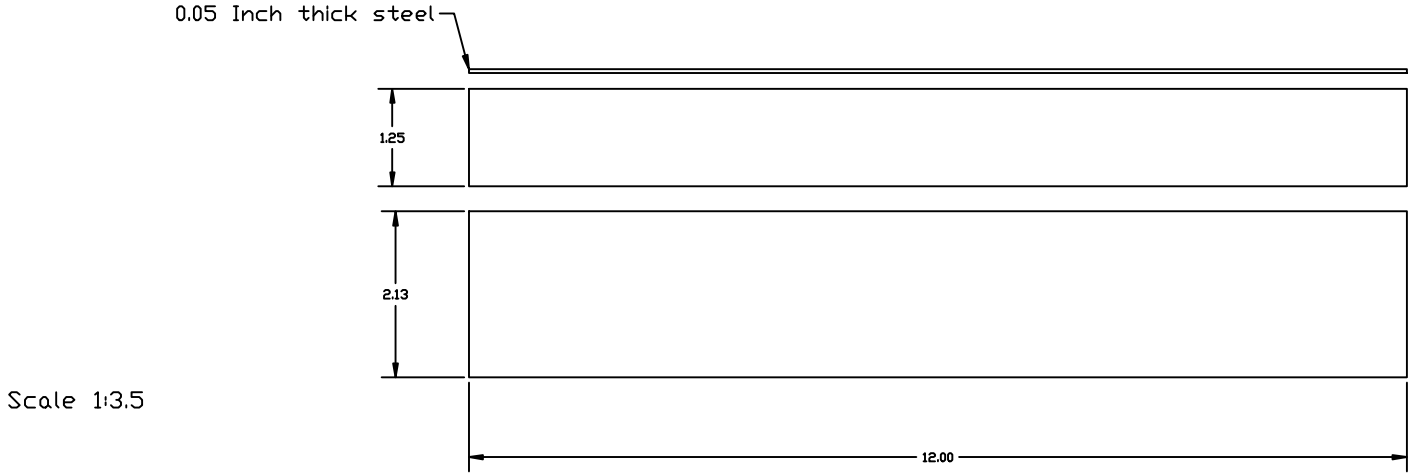

Jon Ehresman	28-August-2009	Gurney Flap for Flat plate and Blade
Scale as noted	Glue hinge to steel plate	All dimensions in inches

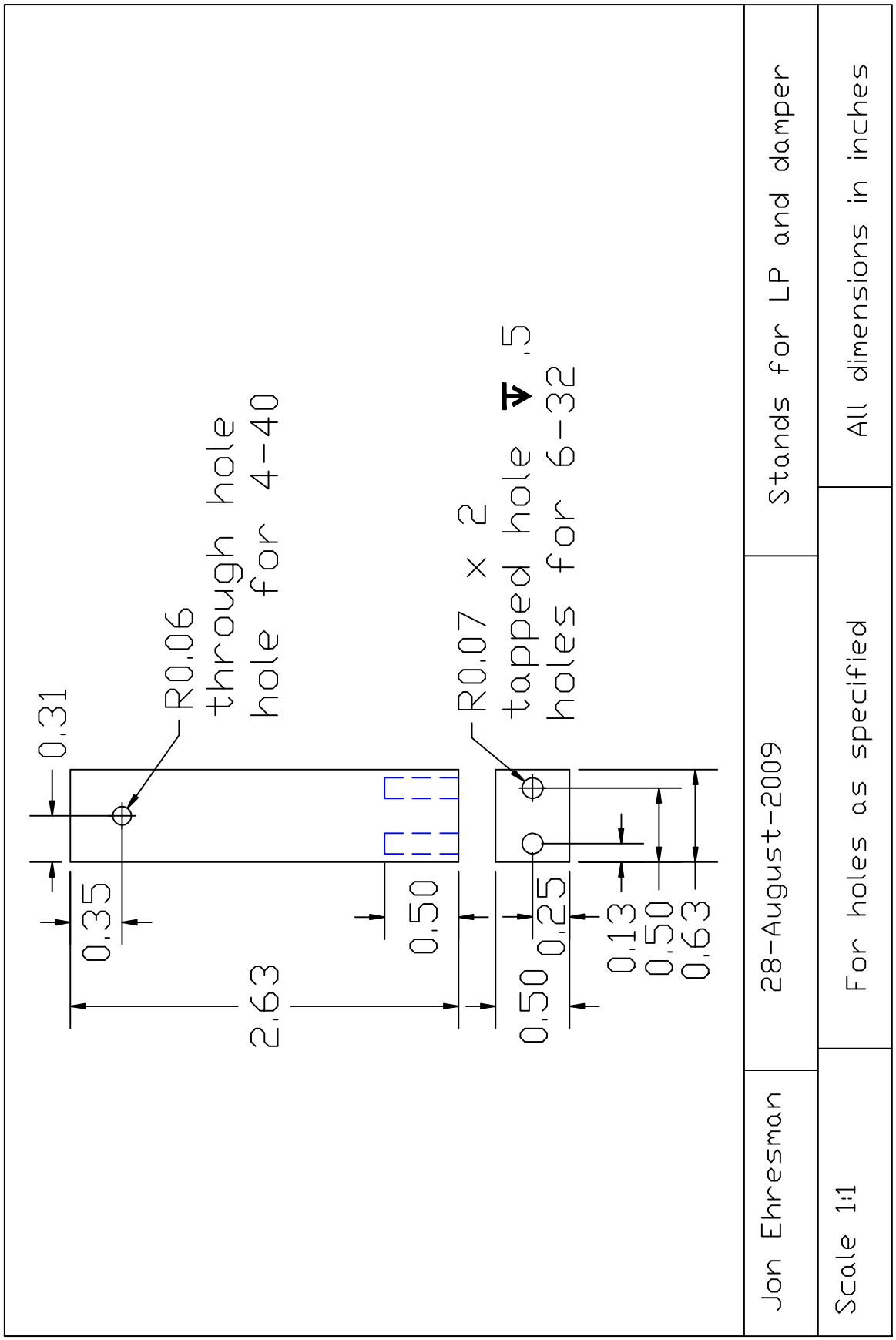
0.31
R0.06
through hole
hole for 4-40
R0.07 x 2
tapped hole
holes for 6-32
.5
0.35
2.63
0.50
0.50
0.25
0.13
0.50
0.63
Jon Ehresman
28-August-2009
Stands for LP and damper
Scale 1:1
For holes as specified
All dimensions in inches

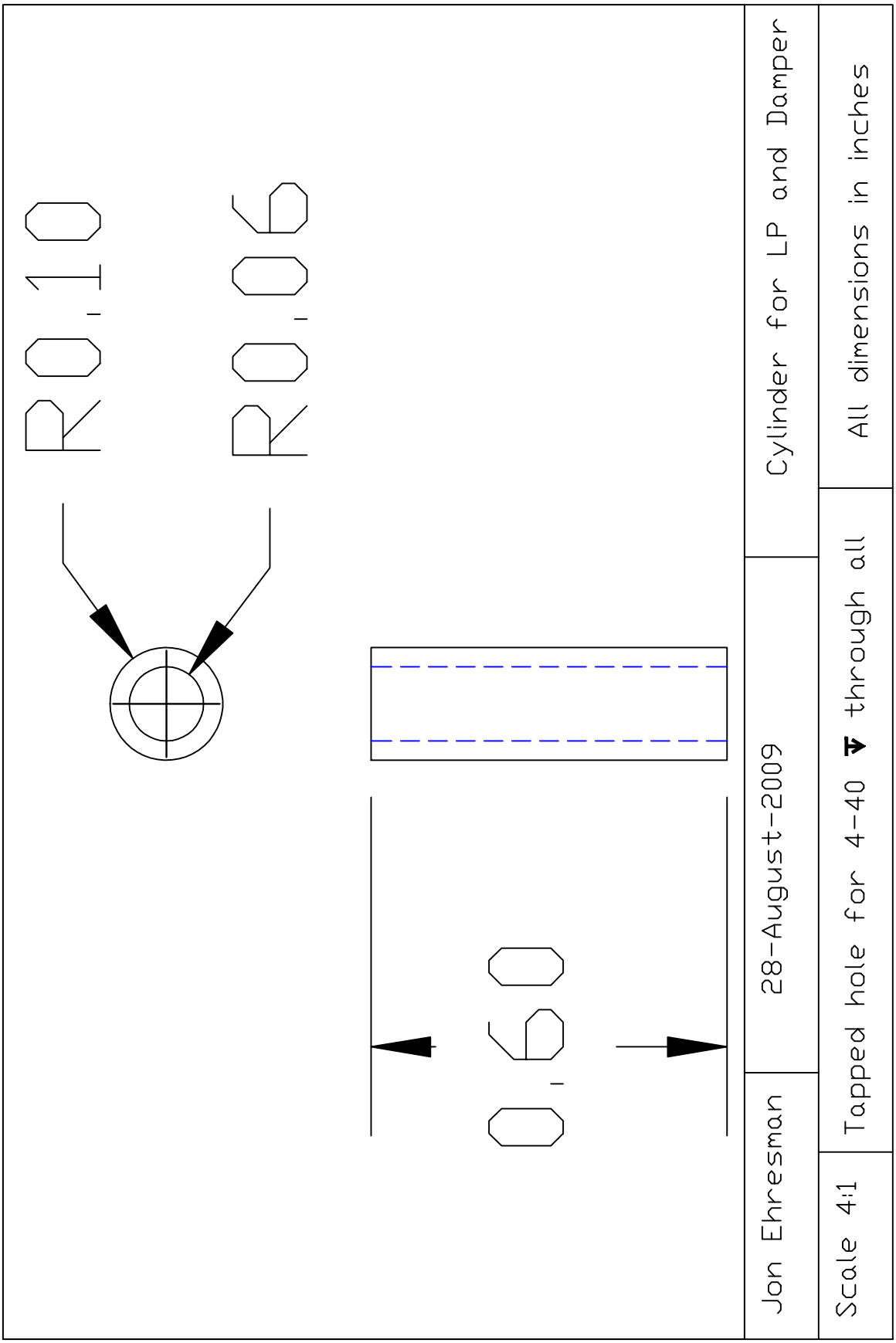
R0.10
R0.06
0.60
Jon Ehresman
28-August-2009
Cylinder for LP and Damper
Scale 4:1
Tapped hole for 4-40 ↧ through all
All dimensions in inches

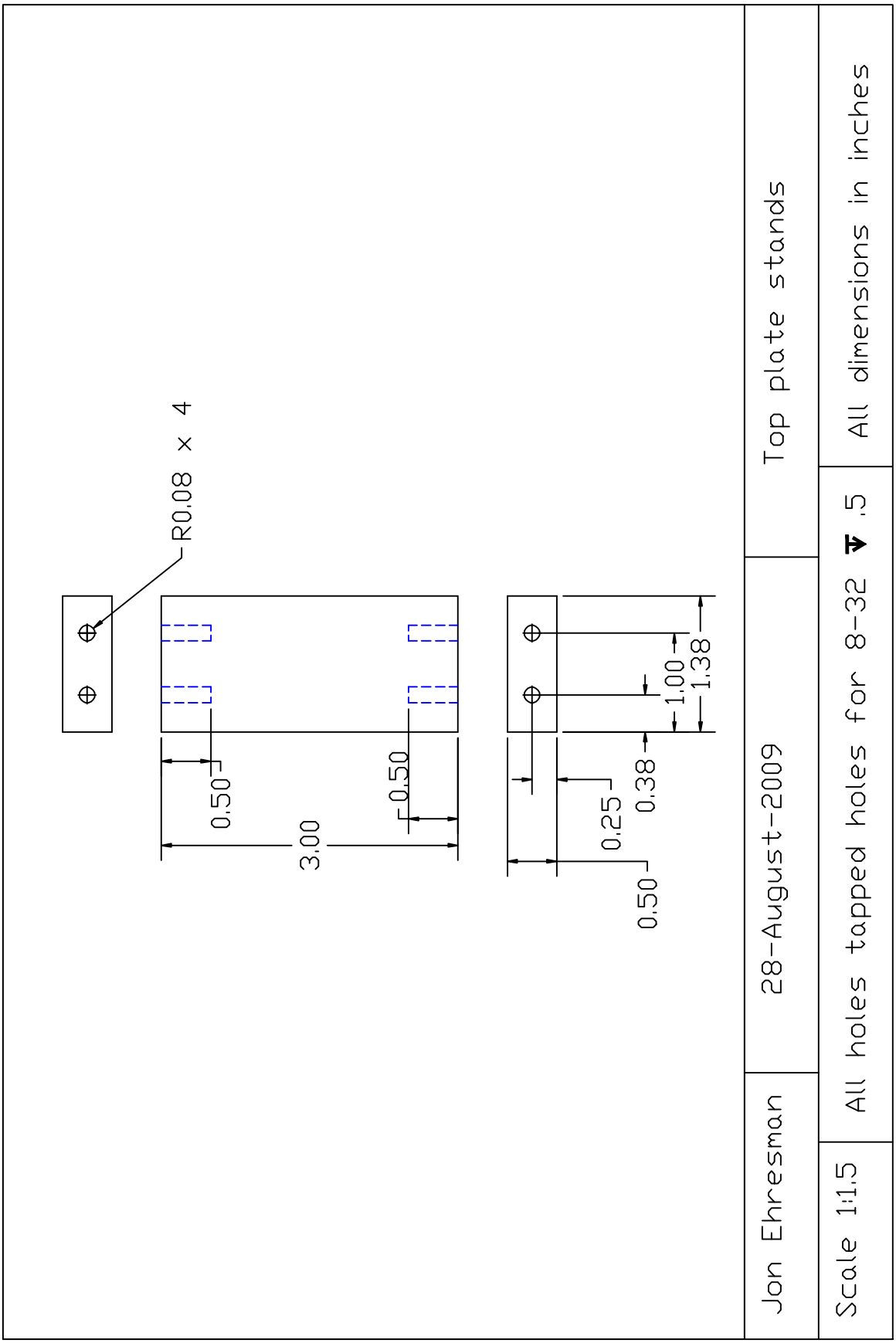
R0.08 x 4
0.50
3.00
0.50
0.25
0.38
0.50
1.00
1.38
Jon Ehresman
28-August-2009
Top plate stands
Scale 1:1.5
All holes tapped holes for 8-32 ↧ .5
All dimensions in inches

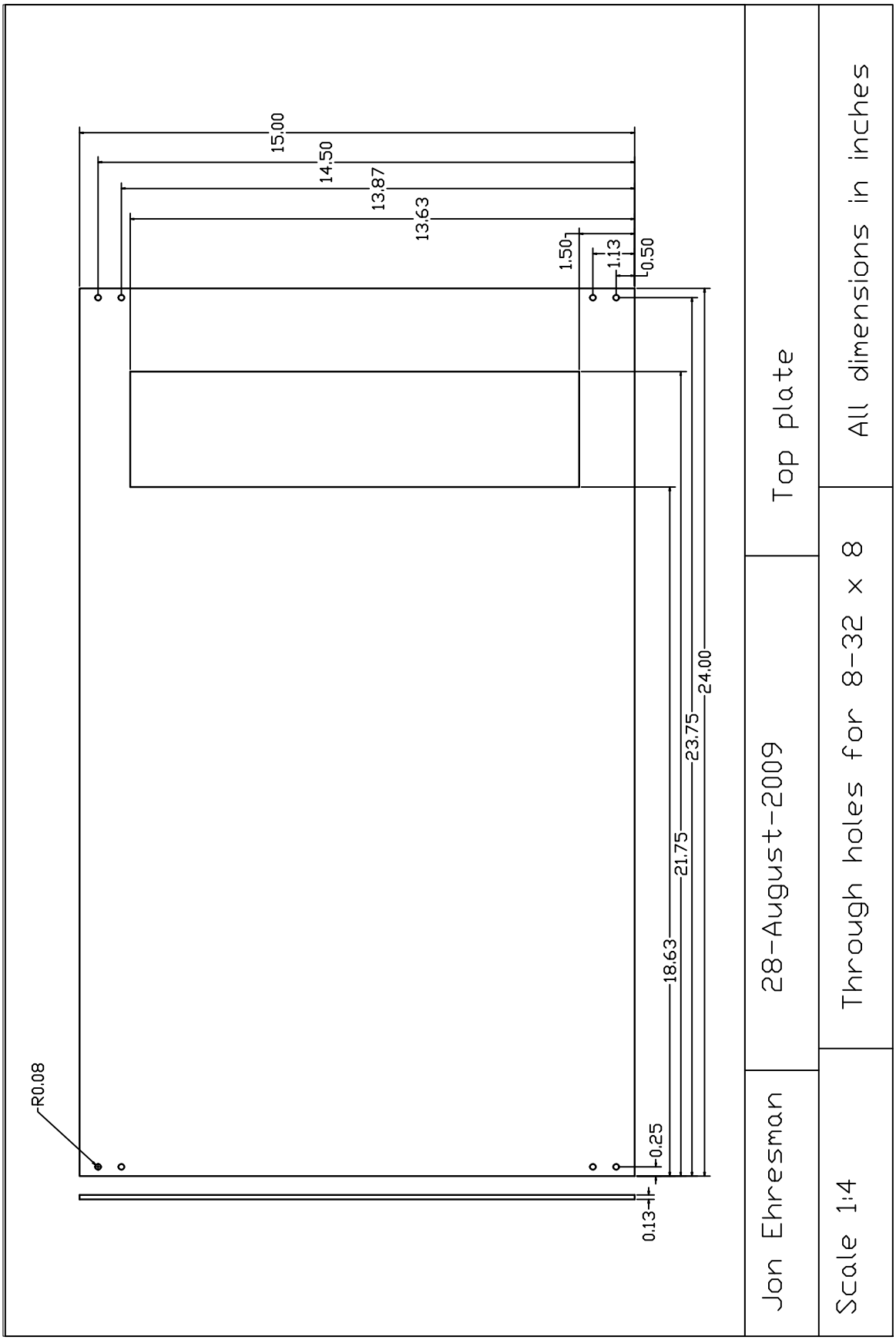
15.00
14.50
13.87
13.63
1.50
1.13
0.50
24.00
23.75
21.75
18.63
R0.08
0.25
0.13
Top plate
28-August-2009
Through holes for 8-32 x 8
All dimensions in inches
Jon Ehresman
Scale 1:4

APPENDIX C

PART DRAWINGS OF BLADE TEST BED

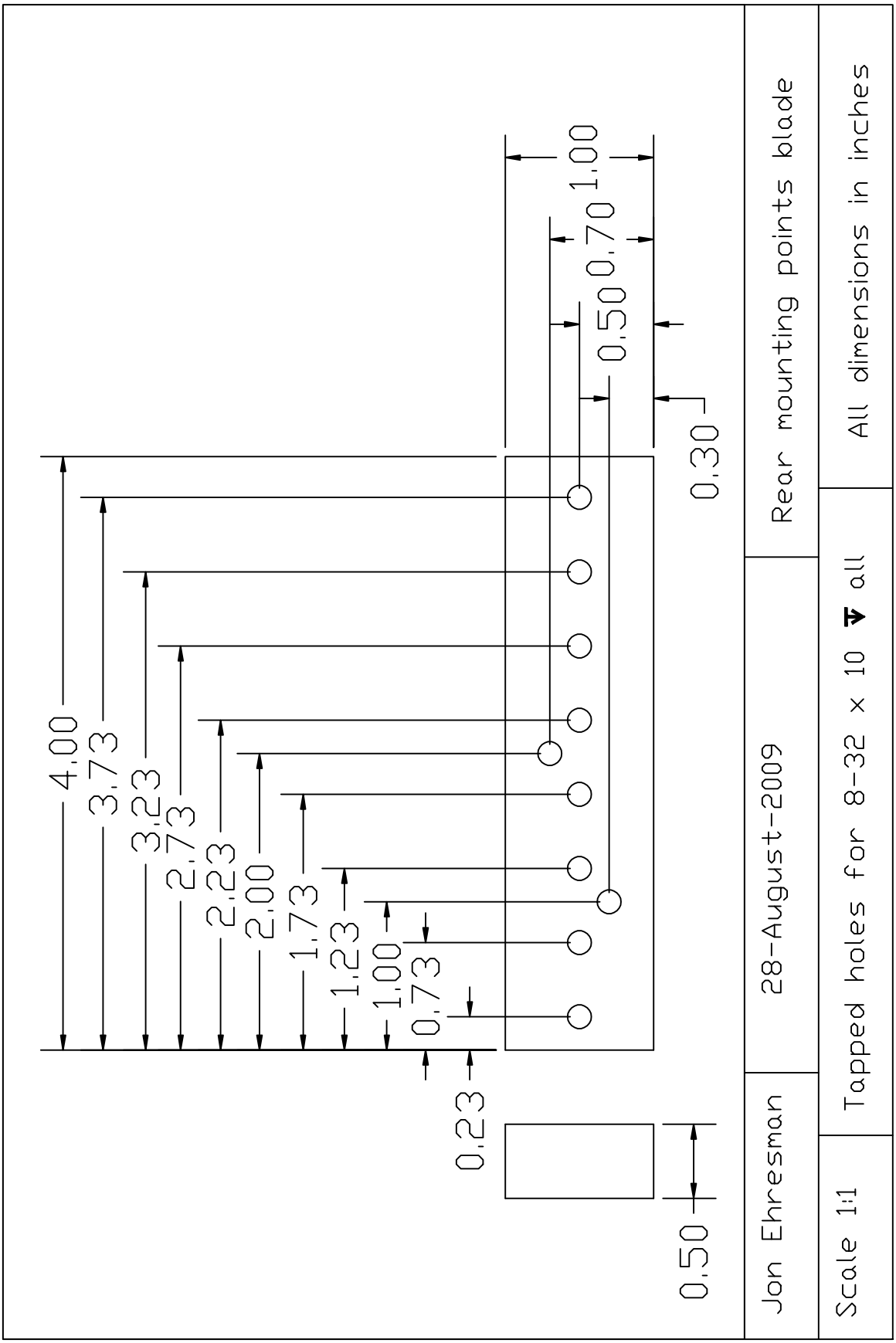
4.00
3.73
3.23
2.73
2.23
2.00
1.73
1.23
1.00
0.73
0.23
0.50
0.30
0.50
0.70
1.00
Rear mounting points blade
28-August-2009
Jon Ehresman
All dimensions in inches
Tapped holes for 8-32 x 10 ↧ all
Scale 1:1

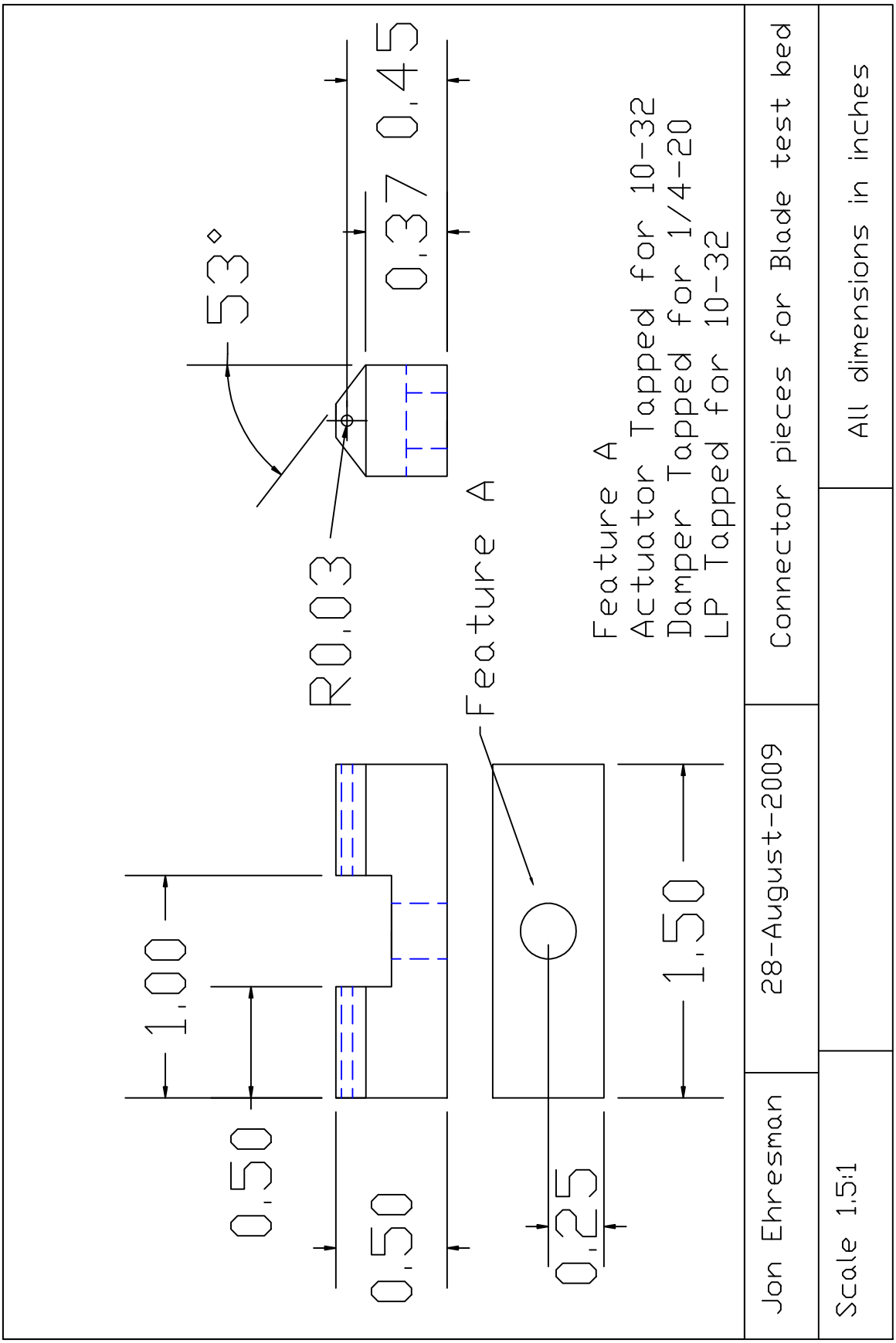
0.45
0.37
53°
R0.03
Feature A
1.00
0.50
0.50
0.25
1.50
Feature A
Actuator Tapped for 10-32
Damper Tapped for 1/4-20
LP Tapped for 10-32
Jon Ehresman
28-August-2009
Connector pieces for Blade test bed
Scale 1.5:1
All dimensions in inches

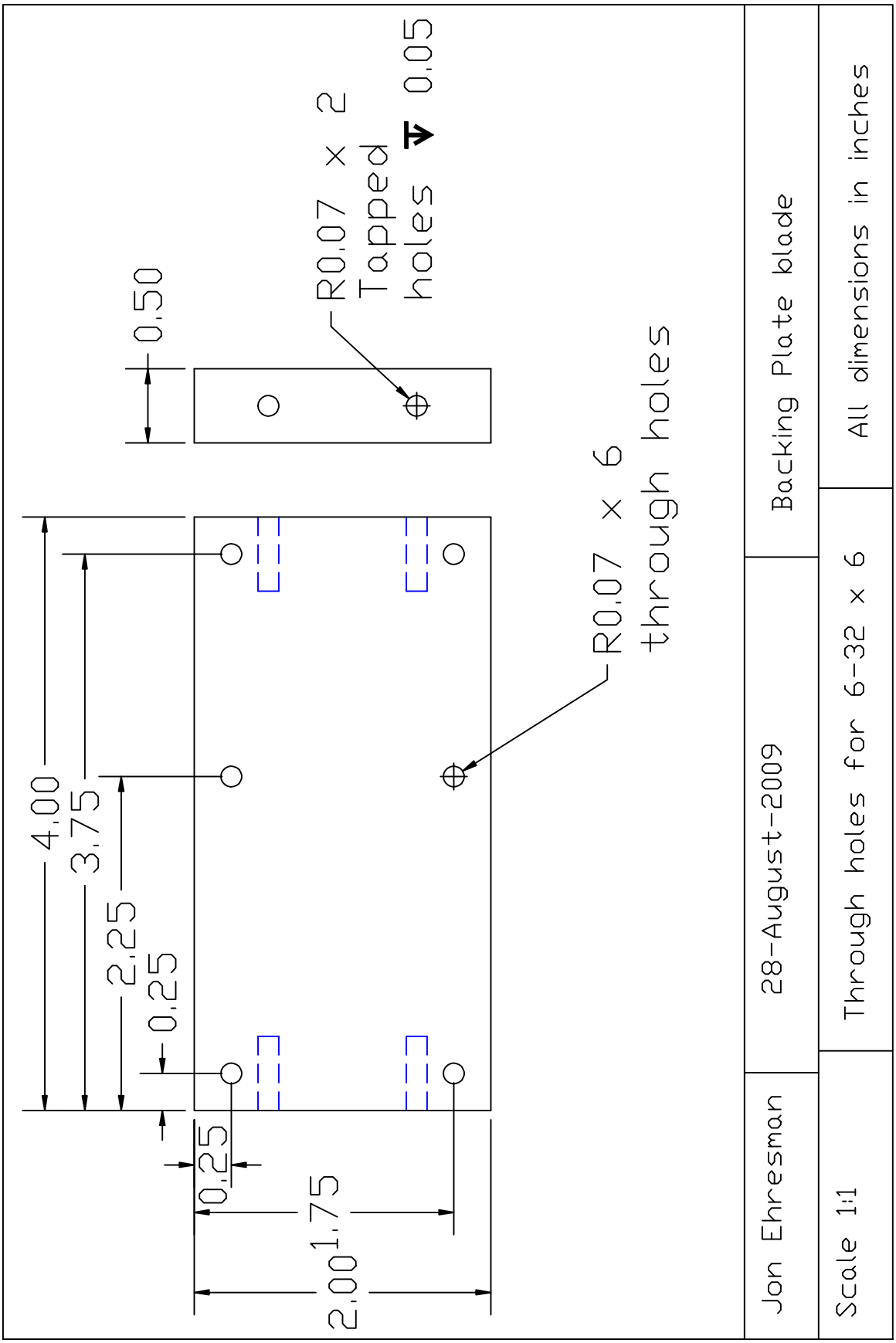
R0.07 x 2
Tapped
holes ↧ 0.05
0.50
R0.07 x 6
through holes
4.00
3.75
2.25
0.25
0.25
1.75
2.00
Backing Plate blade
28-August-2009
Jon Ehresman
Through holes for 6-32 x 6
Scale 1:1
All dimensions in inches

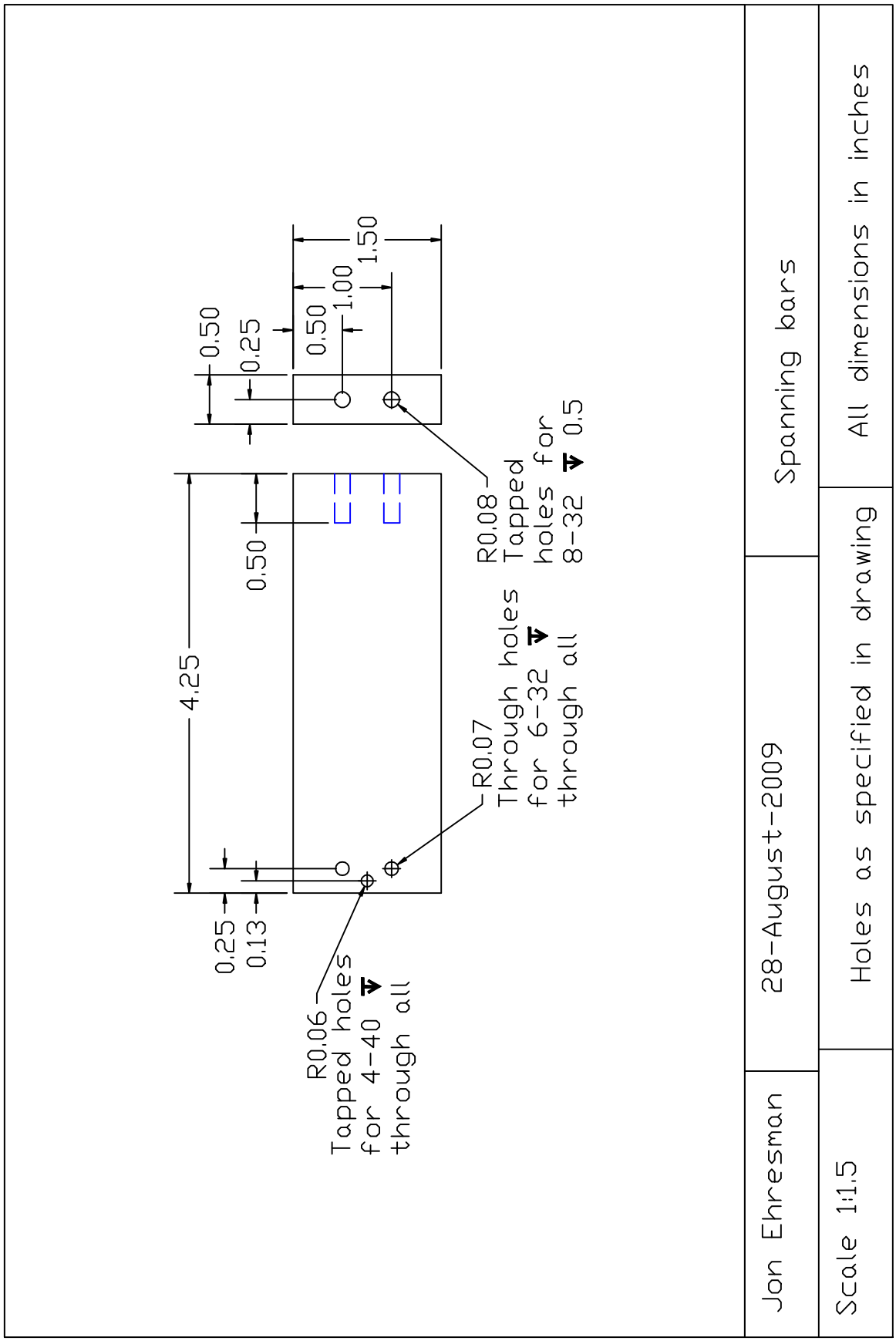
0.50
0.25
0.50
1.00
1.50
4.25
0.50
R0.08
Tapped
holes for
8-32 ↧ 0.5
R0.07
Through holes
for 6-32 ↧
through all
0.25
0.13
R0.06
Tapped holes
for 4-40 ↧
through all
Jon Ehresman
28-August-2009
Spanning bars
Scale 1:1.5
Holes as specified in drawing
All dimensions in inches

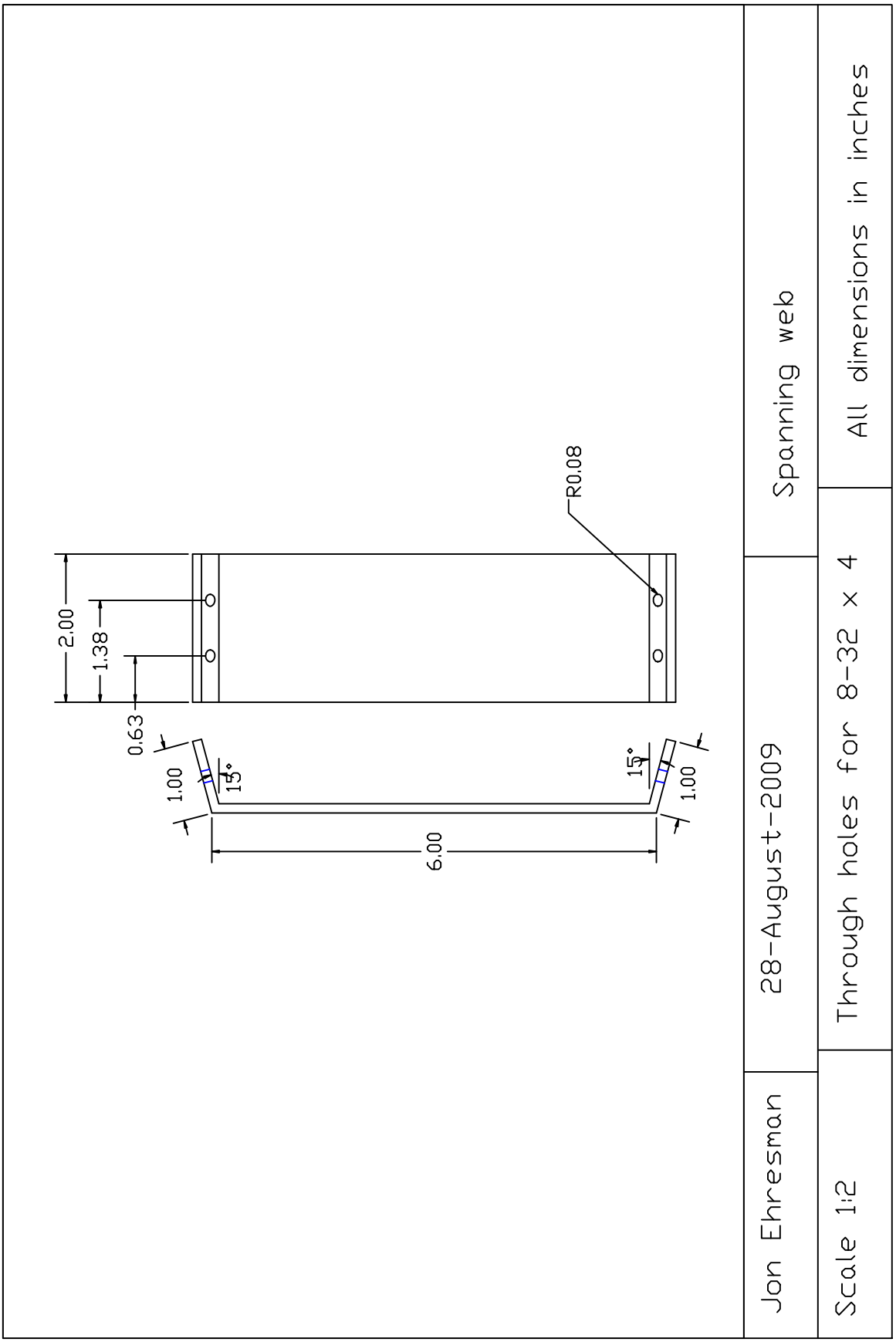
2.00
1.38
0.63
1.00
15°
15°
1.00
6.00
R0.08
Spanning web
28-August-2009
Through holes for 8-32 x 4
All dimensions in inches
Jon Ehresman
Scale 1:2